Characterization of the Transcriptional Regulator WhiB7 Establishes a Link between Metabolism and Intrinsic Antibiotic Resistance in Mycobacteria

by

Ján Burian

B. Sc., The University of Victoria, 2007

A THESIS SUBMITTED IN PARTIAL FULFILLMENT OF
THE REQUIREMENTS FOR THE DEGREE OF

DOCTOR OF PHILOSOPHY

in

THE FACULTY OF GRADUATE AND POSTDOCTORAL STUDIES
(Microbiology and Immunology)

THE UNIVERSITY OF BRITISH COLUMBIA
(Vancouver)

April 2015

Abstract

Mycobacterium tuberculosis (*Mtb*), the etiologic agent of tuberculosis, continues to be the world's deadliest human bacterial pathogen. Current treatments are notoriously limited, lengthy, and becoming increasingly ineffective due to drug-resistant mutant strains. WhiB7, a putative transcriptional regulator, is an essential component of intrinsic antibiotic resistance in *Mtb*. Unique to Actinobacteria, multiple paralogous WhiB-like proteins have diverse roles in physiology, but little is known about their mode of action or regulation. To investigate WhiB7, a combination of *in vitro* run-off, two-hybrid assays, protein pull-down experiments, and genetic approaches was used. WhiB7 was characterized as an auto-regulatory, redox-sensitive transcriptional activator, providing the first biochemical proof that a WhiB-like protein directly promotes transcription. WhiB7's antibiotic resistance function was dependent on three regions: an iron-sulfur cluster binding region likely required for stability; a middle region for binding to the vegetative sigma factor SigA; and a C-terminal DNA-binding region. Mutations disrupting any one of the regions led to an inability of WhiB7 to activate resistance. These experimental constraints were combined with protein modelling techniques to visualize the WhiB7:SigA:DNA complex which may serve as a platform for the design of inhibitors. Additionally, a GFP reporter was constructed to monitor *whiB7* induction, and was used to screen our custom library of almost 600 bioactive compounds including the majority of clinical antibiotics. Expression was induced by compounds having diverse structures and targets, which did not correlate with drug susceptibility of the *whiB7* mutant. Antibiotic-induced transcription was synergistically increased by the reductant dithiothreitol, an effect mirrored by a *whiB7*-dependent shift to a highly reduced intracellular condition reflected by the reduced:oxidized mycothiol ratio. Amino acid metabolism also contributed to WhiB7-mediated intrinsic resistance. To gain insights into whether other

genetic loci contribute to WhiB7-mediated antibiotic resistance, a transposon library of *Mycobacterium smegmatis* was screened for WhiB7-like drug susceptibility or resistance. These studies revealed a putative aspartate aminotransferase (*MSMEG_4060*) that contributed to *whiB7* repression and a pair of adjacent hypothetical genes (*MSMEG_3637/3638)* that contributed to *whiB7* induction. Continued characterization of WhiB7 may serve as a paradigm for other WhiB-like proteins and lead to novel and desperately needed therapies for tuberculosis.

.

Preface

A version of Chapter 2 (sections 2.2 and 2.4) has been published:

Burian, J., Yim, G., Hsing, M., Axerio-Cilies, P., Cherkasov, A., Spiegelman, G. B., and Thompson, C. J. (2013) The mycobacterial antibiotic resistance determinant WhiB7 acts as a transcriptional activator by binding the primary sigma factor SigA (RpoV), *Nucleic Acids Res 41*, 10062-10076.

I designed all research, performed all experiments with the noted exceptions, analyzed data, and wrote the manuscript; CJT supervised the research, data analysis, and wrote the manuscript; GY, supervised by GBS, performed transcriptional run off experiments, analyzed data and wrote the methods pertaining to RNAP purification and *in vitro* run-off. MH and PA, supervised by AC, modeled protein structures and wrote the methods for the modelling.

A version of Chapter 2 (section 2.1) and Chapter 3 has been published:

Burian, J., Ramon-Garcia, S., Sweet, G., Gomez-Velasco, A., Av-Gay, Y., and Thompson, C. J. (2012) The Mycobacterial Transcriptional Regulator *whiB7* Gene Links Redox Homeostasis and Intrinsic Antibiotic Resistance, *J Biol Chem 287*, 299-310.

I designed all research, performed all experiments with the noted exceptions, analyzed data, and wrote the manuscript; S.R.G. designed and performed the mycothiol studies, and analyzed data. G.S. assembled the Sweet library and analyzed data. A.G.V., supervised by Y.A, performed mycothiol studies. C.J.T supervised the designed research, analyzed data. J.B. wrote the manuscript then strengthened by C.J.T. and S.R.G. and G.S.

A version of Figure 21 has been published:

Burian, J., Ramon-Garcia, S., Howes, C. G., and Thompson, C. J. (2012) WhiB7, a transcriptional activator that coordinates physiology with intrinsic drug resistance in Mycobacterium tuberculosis, *Expert review of anti-infective therapy 10*, 1037-1047.

I wrote the manuscript under the direction of C.J.T. S.R.G. provided important concepts through stimulating discussion. Based on my results and direction C.G.H. assembled Figure 2 (i.e., Figure 21).

Chapter 4 is under preparation for publication. I, supervised by Dr. Thompson, designed, performed, analysed all the experiments and wrote the section. MiSeq high-throughput sequencing was performed in collaboration with Dr. Sunita Sinha and Jennifer Chiang from Dr. Corey Nislow's laboratory. Dr. Nislow provided helpful discussion in selection of the Nextera tagmentation. Dr. Sinha performed the MiSeq sequencing.

Table of Contents

List of Tables

List of Figures

List of Abbreviations

3-AT	3-amino-1,2,4-triazole
5' RACE	rapid amplification of 5' complementary DNA ends
5'-UTR	5'- untranslated region
OD_{600}	optical density at 600 nm
aa	amino acids
AIDS	acquired immune deficiency syndrome
bp	base pairs
CV	column volumes
DMTSS	direct mapping of transcriptional start sites
DTT	dithiothreitol
eGFP	enhanced green fluorescent protein
FeS	iron-sulfur
FMN	flavin mononucleotide
$FMNH_2$	reduced flavin mononucleotide
HGT	horizontal gene transfer
IPTG	isopropyl-β-D-thiogalactopyranoside
KO	knock-out
MIC	minimum inhibitory concentration
MSH	mycothiol
MSSM	mycothiol disulfide
Mtb	*Mycobacterium tuberculosis*
NAD^+	oxidized nicotinamide adenine dinucleotide
NADH	reduced nicotinamide adenine dinucleotide
NSM	non-selective screening media
O_2	oxygen
PCR	polymerase chain reaction
RT-qPCR	real-time quantitative polymerase chain reaction
RCHO	long carbon-chain aldehyde
RCOOH	long carbon-chain carboxylic acid
RNAP	holo-RNA polymerase
SEM	standard error of the mean
SDS-PAGE	sodium dodecyl sulfate-polyacrylamide gel electrophoresis
SSM	selective screening media
TB	tuberculosis
TSS	transcriptional start site
uORF	unannotated open reading frame
Wbl	WhiB-like

Acknowledgements

First and foremost I want to thank my parents Dr. Ján Burian and Maria Burianová. My accomplishments are a humble reflection of their support, guidance and love.

I am eternally thankful to my supervisor Dr. Charles J. Thompson for not only giving me the opportunity to join his group, but also for his incredible support, guidance and continued encouragement. I want to thank all the Thompson Lab members, past and present, and highlight Dr. Santiago Ramón-García, Dr. Gaye Sweet, Dr. Takeshi Murakami, and Carol Ng for their mentorship, kindness and friendship. Many thanks to my collaborators, highlighted throughout my thesis. Without their expertise, hard work, and commitment it would have been impossible to expand my scientific horizons. A big thank you to my committee comprised of Dr. Lindsay Eltis, Dr. Thomas Beatty, Dr. Erin Gaynor, and formerly Dr. George Spiegelman for their advice and guidance, and ensuring my training stayed on track. I also want to thank my undergraduate mentor Dr. William Kay, the opportunity to work in his laboratory during my undergraduate degree provided me with experience that has proved invaluable.

I want to thank the community 2nd floor (east wing) of the Life Sciences Centre. Be it procrastination in the Gaynor lab student office with Mark Pryjma, the all too truthful sarcasm of Dr. John Nomellini, coffee time with Dr. Julian Davies, brewing talk with Dr. John Smit or starting up random office parties, without you the rigors of graduate school would not have been as easy to endure. I also want to thank the Department of Microbiology and Immunology for establishing a world class graduate experience, with a special thank you to Kelsey Harmse and Darlene Birkenhead.

Lastly, I want to thank all my fellow Microballologists past and present, with special thanks to Keith Mewis, Michael Jones, Erik Nielson, Eric Brown, Scott Lambie, Jarvis Li, Rafael Saer, Craig Kerr, Sam Kheirandish, Cedric Brimacombe and Monte Doebel-Hickok. I will never forget the Tuesdays and beyond, and of course that we live in a microbial world.

To my friend Dr. Dmitry Apel. Your boundless curiosity and enthusiasm, unwavering dedication, tireless work ethic, and selflessness will continue to inspire me against whatever challenges the future brings.

1 Introduction

1.1 Actinobacteria

Actinobacteria are an ancient and diverse lineage of bacteria adapted to terrestrial and aquatic environments around the world with varied morphologies and genetic repertoires (*1*). They are gram positive bacteria with high G+C DNA (*2*), and a shared ~100 bp insertion within their 23S rRNA genes (*3*). Most contain mycothiol as their primary thiol reductant (*4*). Overall, almost all actinobacteria share a set of six unique proteins, two of which belong to the WhiB family (*5*). In mycobacteria, these correspond to WhiB1 and WhiB2.

The unique metabolic capabilities of actinobacteria have many beneficial applications. The wide-ranging catabolic capacity of rhodococci has great potential for industrial purposes including biotransformation and remediation of polluted environments (*6*). *Streptomyces* are the source of the majority of antibiotics as well as other useful secondary metabolites (*7*). The advent of rapid and cost-effective whole genome sequencing, together with the development of novel technologies, promises a resurgence in identification and application of additional unique compounds from *Streptomyces* (*8, 9*).

A group of actinobacteria, known as the mycolata, are unique in that their cell walls contain mycolic acids. The mycolata is comprised of the genera *Mycobacterium, Rhodococcus, Corynebacterium, Nocardia, Gordona, Dietzia,* and *Tsukamurella*. Several species are notable pathogens, such as *Corynebacterium diphtheria* (diphtheria), *Rhodococcus equi* (pneumonia in horses), *Nocardia asteroides* (opportunistic infection), and especially *Mycobacterium tuberculosis* (tuberculosis) and *Mycobacterium leprae* (leprosy). The very thick and hydrophobic mycolic acid-containing cell envelopes are an important factor for infection making the bacteria

highly resistant to a variety of stresses. Importantly, in the context of today's medical treatment, the cell envelope acts as an effective barrier for antibiotic penetration (*10*). Additionally, much research has been focused on the immunomodifying effects of mycolic acid-containing glycolipids, such as trehalose-6,6'-dimycolate (cord factor), not only as a way to understanding pathogenesis but also for their possible practical applications (*11*).

1.2 Mycobacterial diseases

Taxonomists recognize 85 different species of *Mycobacterium* (*12*). While many are saprophytic, inhabiting varied terrestrial and aquatic environments, several are prevalent human pathogens. *Mycobacterium tuberculosis (Mtb)*, the etiologic agent of tuberculosis (TB), is an ancient and highly successful pathogen. Over the last two hundred years, TB has claimed the lives of more than one billion people (*13*). In fact, even today, it remains the world's deadliest human bacterial pathogen. *Mtb* was identified by Robert Koch in 1882, a Nobel prize winning achievement, and was used as the template for his now famous 'Koch postulates,' the founding principles of medical microbiology (*14, 15*).

The progenitor of *Mtb* is thought to be as old as 3 million years and may have infected ancient hominid ancestors of *Homo sapiens* (*16*). Modern members of the *Mycobacterium tuberculosis* complex (*Mtb, M. bovis, M. africanum, M. microti, M. pinnipedii,* and *M. caprae*), the group of mycobacteria that can cause TB in various animals, evolved from a single ancestor about 20,000 years ago (*14, 16*). TB can be documented in Egypt 5,000 years ago, India 3,300 years ago, China 2,300 years ago and was studied by Hippocrates in ancient Greece (*14*).

In the mid-20th century the discovery of *p*-aminosalicylic acid (1943), streptomycin (1944), isoniazid (1952), and rifampicin (1966) began the modern era of TB treatment and it was

proposed that TB could be eradicated in 100 years (*14, 17, 18*). However, at the beginning of the 1990s it was estimated that one in three people continued to be infected with *Mtb* (*19*). In 1993 the World Health Organization (WHO) declared TB a global health emergency (the only disease to be declared so) and estimated almost 10 million new cases of TB a year (*20*).

Leprosy, also known as Hansen's disease, caused by infection with *Mycobacterium leprae,* or the lesser known *Mycobacterium lepromatosis,* continues to generate over two hundred thousand cases per year (*21*). Relative to *Mtb, M. leprae*'s intracellular lifestyle has allowed mutations that reduced its total genome size and the number of functional genes. Less than 50% of the *M. leprae* genome encodes functional genes (*22*). This massive reduction took place within the last 20 million years (*23*). The long history of *M. leprae* infection has led to unique adaptations to its human host. This has led to many unresolved challenges including the establishment of a culture medium allowing *in vitro* growth as well as developing a reliable animal model. The latter problem is highlighted by an excerpt from Scollard *et al.* (*24*), "an exhaustive yet incomplete list of animal species tested as models for leprosy begins with rabbits infected by Hansen and includes dogs, cats, pigeons, chickens, paddy birds, canaries, parrots, lovebirds, eels, tadpoles, frogs, toads, pigs, turtles, snakes (including rattlesnakes), goldfish, rainbow perch, various saltwater fish, rats, black mice, white mice, "dancing" mice, chipmunks, golden hamsters, albino hamsters, gerbils, a variety of nonhuman primates, and guinea pigs." In spite of the challenges to leprosy research, the disease is readily treatable with antibiotics, although resistance is on the rise (*25*).

Buruli-ulcer disease, caused by *Mycobacterium ulcerans*, is the third most prevalent mycobacterial disease in immunocompetent individuals, but a lack of study has left few therapeutic options outside of surgery (*26*). Furthermore, the spread of HIV has led to the rise of

opportunistic *Mycobacterium avium* infections in AIDS patients (*27*). As with most bacterial infections, the primary option to combat mycobacterial infections is antibiotic treatment. However, mycobacteria present a unique challenge due to their high intrinsic antibiotic resistance, which is the major obstacle for effective treatment options.

1.3 Intrinsic antibiotic resistance of *Mycobacterium tuberculosis*

Intrinsic resistance to any given drug may be determined by an interactive network including effector proteins, regulatory proteins, and inducers (*28*). Intrinsic resistance begins with antibiotic penetration of the cell envelope and the activation of resistance systems which include antibiotic efflux pumps, antibiotic degrading or modifying enzymes, and target modifying enzymes to combat the generated stress (Figure 1). The unique mycobacterial cell envelope has long been thought to be responsible for the antibiotic resistance of *Mtb,* but it alone, even though it plays a key role, is not enough to fully protect the bacillus (*17*). Sequencing of the *Mtb* H37Rv genome (*29*) identified many potential resistance determinants that act in synergy with the cell wall barrier (*30, 31*). The genome contains genes encoding drug-modifying enzymes, such as beta-lactamases and aminoglycoside transferases (*29*); efflux-pumps such as Tap (*Rv1258*) (*32*) and P55 (*Rv1410c)* (*33*); and target modifying enzymes like ErmE (*Rv3065*) (*34*). Mycobacteria also express MfpA, a pentapeptide repeat protein that mimics the structure of DNA to sequester fluoroquinolones (*30*).

The high level of intrinsic antibiotic resistance to a variety of chemotherapeutic agents is an enormous barrier to effective TB treatment, limiting therapy to just a handful of drugs. The standard regiment consists of four antibiotics (rifampicin, isoniazid, ethambutol, pyrazinamide) used in combination for a minimum of six months. Combination therapy is necessary to limit the

rise of acquired point mutations causing further antibiotic resistance (*35*). Unfortunately, antibiotic shortages, improper treatment, and patient non-compliance have led to multi drug- and extensively drug-resistant, MDR and XDR respectively, TB. In 2008, the World Health Organization estimated the global proportion of MDR-TB to be 4.6% of all TB cases and the XDR-TB proportion of MDR-TB cases to be 7% (*36*). The prevalence of TB, the emergence of drug resistant strains and the lack of effective treatment options has spurred the scientific community to look for new approaches to *Mtb* treatment.

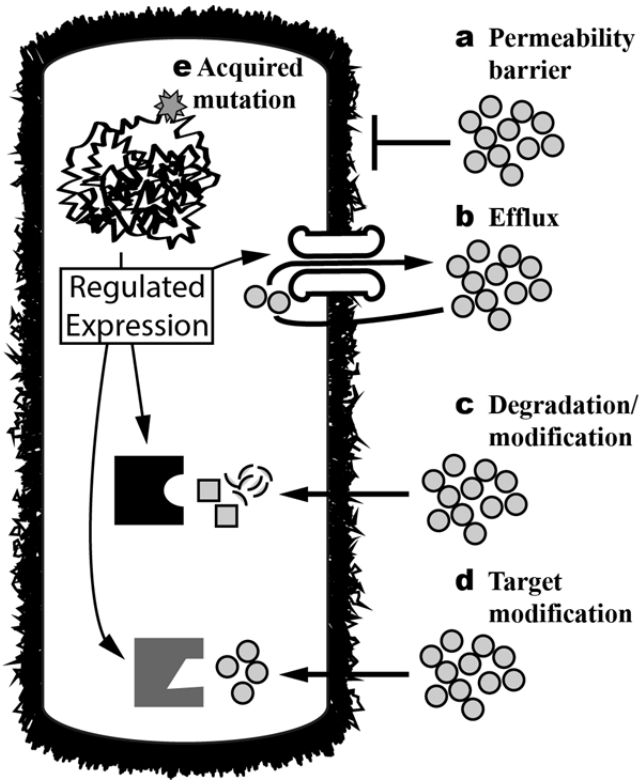

Figure 1. Modes of antibiotic resistance in mycobacteria. Intrinsic antibiotic resistance of mycobacteria begins with their (a) thick hydrophobic cell envelope which acts as an effective permeability barrier to limit the rate of antibiotic entry into the cells. Entry induces the expression of several different antibiotic resistance systems including (b) efflux pumps, (c) antibiotic-degrading or modifying enzymes, and (d) target-modifying enzymes. In addition to intrinsic resistance, mycobacteria can acquire resistance to antibiotics by (e) point mutations within their genome.

1.4 Overcoming antibiotic resistance

Studies of antibiotic activities have traditionally focused on their abilities to inhibit specific targets essential for bacterial growth including cell wall biosynthesis, transcription, translation,

and DNA replication, with the assumption that these are the direct causes of growth arrest or cell death (*37*). However, there is growing recognition that chromosomal genes serving physiological functions can have alternative roles as antibiotic resistance genes. Many antibiotics activate expression of a broad array of genes having no direct relationship to conventional drug resistance genes (*38-42*). For example: ribosome targeting antibiotics trigger heat or cold shock responses in *E. coli* (*43*); in *Salmonella enterica* serovar *Typhimurium,* antibiotic treatment generates large perturbations in cell metabolism by activating transcription of up to 5% of its genes (*38*); in *Streptomyces*, sub-MIC concentrations of the antibiotics erythromycin, pristinamycin, or thiostrepton, induce major changes in gene expression (*39, 40, 42*).

Gene disruption experiments or overexpression of genomic libraries in various bacteria, including *Escherichia coli* (*44*), *Pseudomonas aeruginosa* (*45, 46*), *Acinetobacter baylyi* (*47*) and *Mycobacterium* (*31, 48, 49*), consistently identify multiple genes that can contribute to resistance. Importantly, the redox poise of a cell may also play an important role, as the biosynthesis of H_2S has been shown to mitigate the toxic effects of oxidative stress and provide resistance to many structurally and functionally diverse antibiotics (*50*). Additionally, adaptive physiological changes may promote novel antibiotic tolerant states associated with bacterial communities like biofilms or stochastically adapted non-replicative persistor cells (*51, 52*). Lastly, while horizontal gene transfer (HGT) is a leading force for generating antibiotic resistance in many infectious diseases (*53*), the narrow, and otherwise sterile, niche *Mtb* typically occupies (i.e., granulomas within human lungs) eliminates the possibility of HGT to mediate further resistance (*54*). Therefore, subverting intrinsic antibiotic resistance in *Mtb,* and other mycobacterial pathogens, may lead to new treatment using previously ineffective antibiotics. The gene *whiB7*, the focus of my study, is a critical factor for the activation of known antibiotic

resistance genes, as well as metabolic genes with functions seemingly unrelated to antibiotic resistance, in mycobacteria (*55*).

1.5 WhiB-like proteins

The WhiB-family is found only in actinobacteria (*5, 56*). The '*whi*' terminology was coined by Hopwood *et al.* (*57*) to describe mutants of *Streptomyces coelicolor* maintaining a *white* mycelium rather than proceeding to generate grey spores. The work was advanced by Chater (*58*) who mapped nine genetic loci responsible for white mutations which he named *whiA-I*. Later, WhiB was recognized as a novel transcription factor-like protein not necessarily linked to sporulation, and likely playing an intimate role in actinobacterial cell division (*59, 60*). Sequencing of the *Mtb* H37Rv genome revealed four closely related *whiB* genes (labeled 1-4) (*29*). Further work established that *whiB*-like (*wbl*) genes are found across, and only in, actinobacteria, with seven *whiB* homologs (*whmA-G*) in *Mtb*, *M. bovis* BCG and the fast growing *M. smegmatis* (*56*). The majority of published work has not adopted the *whm* terminology maintaining the number annotation set out by Cole *et al.* (*29*) when reporting on *Mtb whiB* genes (ex. *whiB2 = whmD = whiB*). Confusingly, literature outside of mycobacteria has adopted the use of the *wbl* terminology (ex. *whiB7 = wblC*). The *whiB* gene from *S. coelicolor* has served as a prototype for the WhiB-family of putative transcriptional regulators. Actinobacteria (and at least one actinophage), including mycobacteria, all have multiple *whiB* paralogs in their genomes (*56, 60*). These WhiB paralogs also play important roles in functions unrelated to cell division, such as antibiotic biosynthesis and redox balance.

All Wbl proteins share three sequence motifs: four conserved cysteines, a G(V/I)WGG sequence (tryptophan-containing turn) unique to Wbls, and a C-terminal block of basic amino

acids. The cysteines coordinate an iron-sulfur (FeS) cluster (*61*), while the tryptophan-containing turn likely positions the C-terminus so that the positively charged amino acids can interact with DNA (*56, 59*). Despite the central importance of *whiB* genes, little is known about the signals that activate their transcription or the molecular mechanisms of their products. Most studies have focused on the seven WhiB homologs found in *Mtb* (*whiB1-7*).

1.6 WhiB family proteins in mycobacteria

Since *whiB* genes are found only in Actinobacteria, they are attractive targets of inhibition for the treatment of *Mtb* infections. In mycobacteria, WhiB proteins play vital roles in fundamental cell processes including cell division, redox homeostasis, virulence, and antibiotic resistance.

WhiB1 is an essential protein that is nitric oxide sensitive and can behave as a transcriptional repressor *in vitro* (*62*). The *whiB1* gene is regulated by a cAMP-binding protein (Rv3676) that promotes *whiB1* transcription at low concentrations of cAMP and inhibits transcription at high concentrations of cAMP (*63*). Interestingly, *Mtb* produces a burst of cAMP upon entry into macrophages that may promote survival within the antibacterial environment of phagosomes. Rv3676 also positively regulates *rpfA* (*64*), a resuscitation-promoting factor that serves to stimulate growth in stationary phase cultures of *Mtb* (*65*). These observations suggest that, in addition to its essential function during normal growth, WhiB1 may be co-regulated with genes involved in both survival and the reactivation of dormant *Mtb*.

WhiB2 is the ortholog of the *S. coelicolor* WhiB. It is also essential in *Mtb* and plays a role in cellular septation as well as regulating its own expression (*66-68*). Transcription of *whiB2* is increased as cultures enter stationary phase, and stimulated during nutrient starvation or after treatment with cell envelope inhibitors (*69*). Interestingly, the mycobacterial phage TM4 uses an

N-terminally truncated homolog of WhiB2 as a negative regulator of the host *whiB2* to prevent superinfection (*68*).

WhiB3 has an important role in *Mtb* pathogenesis (*70*). It activates the production of virulence lipids that serve as a redox sink during infection (*71*). It has redox-sensitive DNA-binding activity and may sense intracellular redox to modulate metabolism (*71, 72*). A screen of potential WhiB3 binding sites suggests that it activates transcription of genes involved in fatty acid metabolism and stress responses (*73*). It is also highly upregulated in late stationary phase and upon acidic stress (*69*).

Little is known about *whiB4, whiB5* and *whiB6*, but they may also be important for *Mtb* virulence. WhiB4 contributes to pathogenesis and dissemination by modulating the redox balance of the cell (*74*), while WhiB5 is important for immunomodulation and reactivation (*75*). All are expressed throughout growth, with *whiB5* down-regulated during late stationary phase, and repressed in response to membrane stress (*69*). Additionally, *whiB4* may be within a regulon under the control of a sigma factor (SigF) that reacts to various stress inducers (*76*). Lastly, *whiB6* is highly upregulated upon membrane stress (SDS and ethanol treatment, and heat shock) (*69*) and may play a role in the activation of the ESX-1 secretion system important for pathogenesis and macrophage escape (*77*).

WhiB7 is of particular interest as it provides resistance to several structural classes of antibiotics (*55*). In addition to antibiotic treatment, *whiB7* is also up-regulated by certain physiological stresses including iron starvation, heat shock and entry intro stationary phase (*69*). *whiB7* may also play a role in virulence as it is one of a handful of genes (including *whiB3*) that is globally up-regulated in the *Mtb* complex within resting or activated murine macrophages (*55, 78*) as well as in the lungs of infected mice (*79*). Temporal analysis of the *Mtb* transcriptome

during macrophage infection shows that *whiB7* is one of the first genes expressed after entry into this hostile environment (*80*).

1.7 Iron-sulfur cluster-containing transcriptional regulators

FeS clusters are prosthetic groups that play key structural and functional roles in a vast array of proteins. These clusters occur in a variety of structures and redox states, contributing to their broad functional versatility (*81*). These functions include electron transfer, catalysis, disulfide reduction, sulfur donation, iron storage and transcriptional regulation (*81*). The two most common types of clusters are the planar [2Fe-2S] and the cubane [4Fe-4S]. Proteins loaded with FeS clusters are in a holo form, while those lacking FeS clusters are referred to as apo proteins. Both the holo and apo proteins can adopt multiple redox states. For example, [2Fe-2S] clusters can exist in the oxidized, $[2Fe\text{-}2S]^{2+}$, or reduced, $[2Fe\text{-}2S]^{1+}$, state. Similarly, [2Fe-2S] and [4Fe-4S] clusters are generally coordinated by four cysteines which form disulphide links when the apo protein is oxidized, or exist as thiols when reduced.

FeS proteins can activate or repress transcription by several different mechanisms (*82*). For example, SoxR contains a [2Fe-2S] cluster and represses *soxS* in the $[2Fe\text{-}2S]^{1+}$ state. In response to oxidative stress, the cluster is oxidized to $[2Fe\text{-}2S]^{2+}$, and SoxR activates *soxS* expression (*83*). A second example is provided by FNR, which acts as a master regulator in *E. coli*'s adaptation to anaerobic growth. In the absence of O_2, FNR contains a [4Fe-4S] cluster and activates a regulon of more than 100 genes (*84*). Under aerobic conditions, O_2 rapidly converts the cluster to a [2Fe-2S] form, inactivating FNR (*85*). Finally, IscR regulates genes encoding FeS cluster production. When loaded with a [2Fe-2S] cluster, IscR represses the operon. In the absence of FeS clusters, IscR is in the inactive apo form (*86*). This regulatory logic generates a

positive feedback loop for FeS cluster assemble to maintain homeostatic levels. Together, these examples demonstrate the diverse ways in which FeS cluster chemistry can regulate transcriptional activity.

1.8 Wbl transcriptional regulation and other proposed activities

Mtb Wbl proteins (WhiB1-7) heterologously expressed in *E. coli* and purified under anaerobic conditions all contain a [2Fe-2S] cluster and are redox sensitive (*61*). Oxidation leads to a loss of the FeS clusters and the formation of two intramolecular disulfide bonds between pairs of the four conserved cysteines. Alternatively, a *S. coelicolor* paralog (WhiD) purified from *E. coli* also contained a [2Fe-2S] cluster, but anaerobic reconstitution led to the coordination of an [4Fe-4S] cluster (*87*). As expected, oxidation of reconstituted WhiD caused a rapid conversion to a [2Fe-2S] form, followed by a relatively slow release of the [2Fe-2S] cluster and generation of the apo protein. Importantly, the [4Fe-4S] and [2Fe-2S] clusters can be distinguished by absorption spectroscopy as shown by the time course of WhiD oxidation (Figure S1) (*87*). The exact forms of FeS clusters that occur in *Mtb* Wbl proteins *in vivo* are debatable, but alterations in DNA-binding affinity based on redox changes are described below.

Recent studies have shown that WhiB1 (*62*), WhiB2 (*68*) and WhiB3 (*71*) bind DNA with different affinities in a redox-sensitive manner. The oxidized apo forms of WhiB1, WhiB2, WhiB3, and WhiB4 bind DNA more tightly than their respective holo-proteins (*62, 68, 71, 74*). While these studies support the idea that Wbls are redox-sensitive transcriptional regulators, due to the narrow scope of activity (DNA-binding), observed in both holo and apo forms, firm conclusions on the redox state of functional Wbls *in vivo* cannot be drawn. Additionally, only

apo WhiB1 was shown to directly influence transcription, having a negative effect on transcription of the *groEL2* promoter *in vitro* (*88*).

Regardless of their precise redox states, WhiB2 (*89*), WhiB3 (*71, 73*), WhiB5 (*75*), and WhiB7 (*55*) are hypothesized to be transcriptional activators based on microarray analyses, mutant phenotypes, and other indirect evidence. WhiB3, the best characterized member of the family, binds DNA (*71*) as well as the primary mycobacterial sigma factor, SigA (*70*).

Sigma factors are proteins that direct RNA polymerase to specific promoters and promote initiation of RNA synthesis. SigA is the primary sigma factor (σ^{70} homolog) in *Mtb*. Its sequence can be split into four regions from the N- to C-terminus (*90*). Briefly, Region 1 prevents SigA:DNA binding when SigA is not associated with RNA polymerase, Region 2 binds the -10 promoter element, Region 4 binds the -35 promoter element, and Region 3 is a linker between Regions 2 and 4. For WhiB3:SigA binding experiments, Steyn *et al.* (*70*) used a 160-residue C-terminal fragment (residues 369-528) of SigA, referred to as $SigA_{C160}$. $SigA_{C160}$ spans several SigA structural regions including the terminus of Region 2, as well as Region 3 and Region 4. Importantly, WhiB3 and $SigA_{C160}$ did not interact when arginine 515, located at the C-terminus of Region 4, was substituted with histidine. This suggests that like many other transcriptional regulators (*91*), WhiB3 targets Region 4 of SigA. This has functional implications as sigma factor-binding transcriptional factors likely interact with DNA sequences that are either overlapping or immediately adjacent to the -35 promoter element (*92*). The hypothesis that WhiB3 is a direct transcriptional regulator is further supported by the observation that *Mtb* strains lacking *whiB3* or containing the SigA R515H mutation show a similar decrease in virulence (*71, 72, 93*). However, direct Wbl-mediated activation of transcription continues to be debated as a second thioredoxin-like function has been suggested for Wbls.

Studies by the Agrawal group have suggested that WhiB1 (*94*), WhiB3 (*95*), and WhiB4 (*96*) function as thioredoxins. Furthermore, the group has shown that all *Mtb* WhiB proteins, with the exception of WhiB2, have insulin reductase activity in the presence of the reducer dithiothreitol (DTT) (*61*). However the relevance of a redox reaction between a reducer and iron-sulfur depleted proteins on an artificial substrate *in vitro* may not translate to significant *in vivo* activity. They proposed that the evolution of so many WhiB-type thioredoxins is an adaptation for substrate specificity, but argued against their possible roles as transcription factors. Additionally the group has proposed a chaperone-like function for WhiB2, inferred from the observation that it prevents aggregation of several model protein substrates (*97*). WhiB2's cysteines are dispensable for its chaperone activity *in vitro*, but are required to complement the *whiB2* mutation *in vivo* (*67*). As *whiB2* is an essential gene, it seems unlikely its chaperone activity, if present *in vivo*, is WhiB2's primary function. Clearly, more analysis is required to understand the complex molecular functions of this interesting family of proteins.

1.9 Mycothiol

Mycothiol is the main small molecule thiol in most actinobacteria, playing a critical role in maintaining a reducing environment within the cytoplasm (*4*). Mycothiol plays a comparable role to that of glutathione in gram-negative bacteria. Interestingly, mycothiol is significantly more resistant to heavy-metal-ion catalyzed auto-oxidation than glutathione (*98*). Mycothiol acts as an electron donor when it is in its reduced monomeric state (MSH). Oxidation of mycothiol leads to a disulphide-bridged dimer (MSSM). Mycothiol is maintained in its reduced state by MSH disulfide reductase (*99*).

The co-occurrence of mycothiol and Wbls, exclusively in actinobacteria, has led to the suggestion that they may interact (*56*). Wbls might function as 'mycoredoxins' by direct mycothiol reduction to perhaps facilitate their proposed thioredoxin roles (*100*). However, not all actinobacteria contain mycothiol suggesting that Wbls can perform other non-mycothiol related function(s) (*101*). For example, mycothiol-deficient *M. smegmatis* is viable, suggesting the essential roles of WhiB1 and WhiB2 are not disrupted (*102*).

In *Mtb*, mycothiol is essential for growth (*103*). Lowering mycothiol content in *Mtb* leads to decreased virulence, an increase in susceptibility to rifampicin, but an increase in isoniazid resistance (*103, 104*). Due to its important roles in stress resistance and growth, biosynthesis of mycothiol is an attractive drug target for TB treatment. In other actinobacteria such as *M. smegmatis* (*102*), *R. jostii* RHA1 (*105*), and *Corynebacterium glutamicum* (*106*), mycothiol-deficient strains show high susceptibility to oxidative stress as well as broad antibiotic susceptibility. The broad resistances provided by mycothiol indicate that it functions within multiple detoxification pathways. Curiously, all mycothiol deficient mutants share an increased susceptibility to macrolides. The pleiotropic antibiotic susceptibility has led to the hypothesis that mycothiol may be linked with WhiB7 (*101*).

1.10 WhiB7

WhiB7 is a multi-drug resistant determinant in *Streptomyces lividans,* performing a similar function in *Mtb, M. bovis* BCG, *M. smegmatis,* and *Rhodococcus jostii* RHA1 (*55, 107*). Microarray data suggest it is a transcriptional activator and identified its putative regulon (*55*). WhiB7, like all other Wbls described above, contains four conserved cysteines that bind a redox-sensitive FeS cluster and a characteristic tryptophan-containing turn. Like other Wbl proteins,

WhiB7 has basic amino acid residues at its C-terminus that are likely needed for DNA-binding. In the case of WhiB7, the residues match the consensus sequence for an AT-hook, a motif known to bind the minor groove of AT-rich DNA (*55, 108*). By analogy to other WhiB proteins, the three conserved regions (Figure 2) are likely required for activity (*59, 67*).

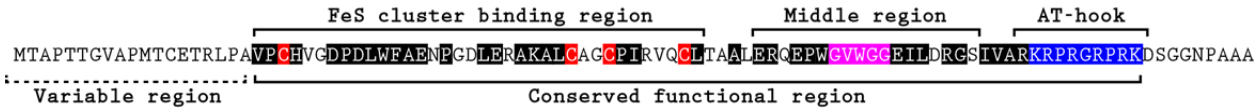

Figure 2. Amino acid sequence of *M. smegmatis* WhiB7 highlighting conserved residues and features. *M. smegmatis* WhiB7 was compared with homologs from *Mtb*, *R. jostii* RHA1 and *S. coelicolor*. Conserved or chemically similar residues shared across the homologs are highlighted black. The Wbl-specific motifs are coloured with the four conserved FeS cluster-binding cysteines in red, the tryptophan turn in pink, and the AT-hook motif in blue.

The observation that constitutive expression of *whiB7* activates its own transcription suggests autoregulation (*55*). Together, the AT hook motif and microarray data support the hypothesis that WhiB7 is a DNA-binding transcriptional activator. Understanding how WhiB7 senses antibiotic-induced signals to activate intrinsic resistance genes may allow more effective uses of drug combinations (*109*) or novel WhiB7 inhibitors for treatment of mycobacterial diseases including tuberculosis.

1.11 WhiB7 regulon

Microarray data identified a putative regulon including known antibiotic resistance genes and suggested WhiB7 is autoregulatory (*55*). The regulon contains *eis (Rv2416c), tap (Rv1258c), erm (Rv1988)*, as well as other genes with functions seemingly unrelated to antibiotic resistance.

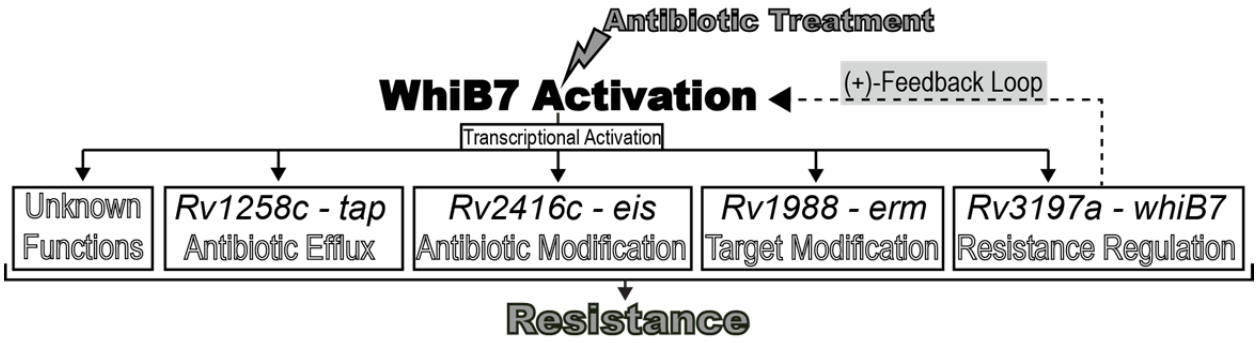

Figure 3. General pathway of WhiB7 mediated resistance. Microarray studies provide this hypothetical pathway. Antibiotic treatment leads to an activation of WhiB7 expression which is required for the transcriptional activation of several known antibiotic resistance genes as well as genes seemingly unrelated to antibiotic resistance. Importantly, this includes transcriptional activation of *whiB7* generating a positive feedback loop and amplified up-regulation of the system leading to resistance.

Eis, named for 'enhanced intracellular survival', promotes mycobacterial survival within macrophages (*110*). It does this by acetylating the host protein DUSP16/MKP-7, which suppresses the immune response (*111*). Surprisingly, Eis also provides antibiotic resistance by acetylating aminoglycosides (*111, 112*). Transcriptional start sites have been mapped downstream of SigA-like promoter sequences in two studies. One study identified a promoter by cloning the *Mtb eis* locus in *M. smegmatis* on a high copy number plasmid (*113*), and the other identified a different start site, more likely to be its native promoter, in studies of *Mtb* H37Rv and kanamycin resistant *Mtb* clinical strains (*114*). The latter showed that overexpression of *eis* resulting from mutations within its promoter led to kanamycin resistance. Interestingly, the levels of SigA are correlated with an increase in *eis* activation (*115*). The authors suggest that there are "yet unidentified transcriptional activators (that) contribute to *eis* expression", which I hypothesize is WhiB7.

Tap is an efflux pump primarily associated with tetracycline resistance but also provides resistance/ tolerance to a spectrum of other antibiotics (*32, 116, 117*). For example, it is

responsible for macrophage-induced rifampicin tolerance (*118*). Tap is required for long term viability in liquid cultures, implying that it serves to detoxify the cytoplasm upon entry into stationary phase (*117*). There is growing recognition that over-expression of efflux pumps with physiological functions contributes to multi-drug resistance not only in mycobacteria but other pathogens (*28, 119*). Louw *et al.* (*120*) showed that rifampicin induced multiple efflux pumps, including *tap*, in rifampicin-resistant *Mtb,* providing cross-resistance to the fluoroquinolone ofloxacin.

Erm is a ribosomal methyltransferase providing resistance to macrolides (*121*). Importantly, pre-incubating *M. smegmatis* with sub-inhibitory concentrations of macrolides significantly increases macrolide resistance in an *erm(38)* dependent manner (*122*).

In addition to known resistance genes, several chaperones, including *groES* (*Rv3418c*) and *groEL2* (*Rv0440*), may be induced by WhiB7 (*55*). Interestingly, *groEL2* is repressed by WhiB1 (*88*). Furthermore, outside of stress response genes, WhiB7 also may induce genes linked to cell metabolism such as *Rv1257c,* a possible glycolate oxidase whose transcription is linked to *tap* (*Rv1258c*), and *aspC* (*Rv0337c*), a probable aspartate aminotransferase. How these may contribute to antibiotic resistance remains elusive (*55*).

1.12 Research hypothesis and rationale

To date, the debate about Wbl function and mechanism of action remains unsettled. My hypothesis is that WhiB7 is a transcriptional activator that responds to a fundamental change in cell metabolism resulting from a common, downstream effect of antibiotics, which induce or mimic physiological stress signals. The change in cell metabolism depends on a yet uncharacterized pathway leading to *whiB7* activation in competition with an alternate pathway

preventing *whiB7* activation under non-inducing conditions. As WhiB7 is a protein conserved throughout the *Mycobacterium* genus, understanding its regulation and function, along with the functions of its downstream targets in intrinsic antibiotic resistance, may result in new treatment options to diseases caused by mycobacteria. The thesis aims to address three main questions.

1. Is WhiB7 a transcriptional activator?

Analysis of the WhiB7 protein sequence suggests it is a transcriptional regulator. Various genetic (ex. *whiB7*-reporter systems and complementation assays) and molecular biology (ex. two-hybrid assays, *in vitro* transcription assays and protein pulldown) approaches were used to dissect how WhiB7's three regions (Figure 2) combine to increase transcription at a subset of promoters.

2. What is the *whiB7* induction signal?

A *whiB7*-reporter was used to generate a comprehensive list of biologically active compounds that induce transcription. The identified molecules were analysed for a common activity or structure that leads to *whiB7* induction. Unique activators led to an investigation of redox and amino acid metabolism as sources of the *whiB7* induction signal.

3. Are there other contributors to the WhiB7-resistance pathway?

To identify other genetic elements that contribute to *whiB7* regulation or WhiB7 function, a transposon library was generated and exposed to several WhiB7-specific antibiotics. Genome-wide screening for loci with decreased transposon insertion frequencies after antibiotic selection identified candidate genes that may contribute to WhiB7 expression or function.

2 WhiB7 is a redox-sensitive transcriptional activator

2.1 Information about collaborators

Andrea Basler and Jeffery Hu initially cloned pMS689GFP and pTB674lux, respectively. I thank Dr. Julian Davies for providing pAmilux and Dr. William Jacobs for providing pMV361.hyg. I thank Andrea Basler and Dr. Gaye Sweet for sharing their 5' RACE transcription start site mapping results. I am most thankful for a fruitful collaboration with Dr. Grace Yim, under the supervision of Dr. Spiegelman. I assisted Dr. Yim with purification of the RNAP. Dr. Yim then performed and analysed the *in vitro* transcription run-off. I thank Dr. Michael Hsing and Dr. Peter Axerio-Cilies, under the supervision of Dr. Artem Cherkasov, for generating the *de novo* structural model of WhiB7:SigA interaction. Finally, I thank Dr. Thomas Beatty for access to the spectrophotometer, and Dr. Rafael Saer for technical assistance.

2.2 Introduction

Identification of promoters that drive the expression of genes of interest provides insight into their regulation. Once a start site is mapped, the -10 and -35 promoter elements can be examined to suggest the sigma factor that targets the promoter and the surrounding sequence can be examined for motifs that may be targeted by transcriptional regulators. Because WhiB7 is likely autoregulatory, and plays a critical role in transcriptional activation of an array of target genes, studies of the *whiB7* promoter may provide insights into mechanisms and regulation of intrinsic resistance.

Identification of a minimal functional promoter, followed by construction of a promoter-reporter fusion, are used as tools to investigate transcription *in vivo* (*123*). As WhiB7 is

hypothesized to be autoregulatory and its gene is up-regulated to a variety of stresses, a *whiB7* promoter-reporter fusion may provide a system to:

1) investigate WhiB7-mediated transcriptional activation and identify the essential sequence motifs of the antibiotic-inducible *whiB7* promoter

2) screen compounds (ex. antibiotics) to identify a common structure or target for *whiB7* induction

For reporters to be effective tools, they need to meet several criteria. First, the reporter must generate a reproducible signal in response to the transcriptional activator. Second, their expression should not be detrimental to cell growth. Third, the assay should be simple. Two widely used reporters are bacterial luciferase (*124*) and green fluorescent protein (*125*).

Bacterial luciferase produces light and is encoded by five genes, *luxABCDE* (Figure 4). The *luxAB* genes encode a two-component flavin-dependent monooxygenase that produces light by using O_2 to oxidize RCHO (*126*) (Figure 4b). In mycobacteria, *Vibrio harveyi luxAB* has been used as a reporter for viability (*127*) and promoter activity (*128*). Importantly, due to the rapid decay of the Lux system in *Mtb, V. harveyi* luciferase can be used to monitor temporal gene expression (*129*). However, the activity of the Lux system is subject to changes in the levels of reduced FMN and the RCHO. On the other hand, the green fluorescent protein has become an indispensable tool to monitor gene expression (*130*). One of the most widely used enhanced forms, eGFP, is superior to wild type in both brightness and stability (*125, 131*). Relative to LuxABCDE, eGFP is simpler and smaller, requiring a single protein to convert 488 nm excitation to a 509 nm emission signal (Figure 4c). Fluorophore maturation in eGFP requires the cyclization of three adjacent amino acid residues and is sensitive to reduction (*132*).

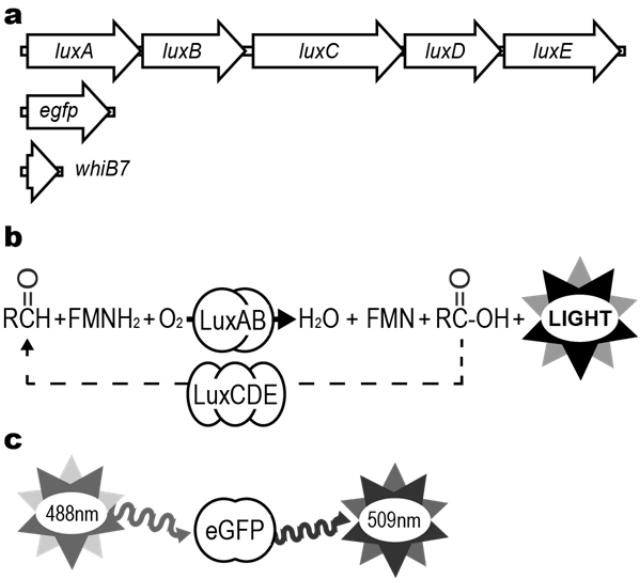

Figure 4. Comparison of the *luxABCDE* and *egfp* reporters. (a) Genetic organization and size of the *luxABCDE* (5664 bp) and *egfp* (720 bp) reporters relative to *M. smegmatis whiB7* (300 bp). **(b)** Light generation reaction catalyzed by LuxABCDE. **(c)** eGFP emits 509 nm light after excitation at 488 nm.

The *luxABCDE* reporter was fused to the *whiB7* promoter region from *Mtb*, while *egfp* was fused to the *M. smegmatis* region. The abilities of the reporters to detect *whiB7* induction were then monitored in *M. smegmatis*. RT-qPCR confirmed that *whiB7* transcription was activated in *M. smegmatis* by erythromycin (an inducer of *whiB7* in *Mtb* (*55*)), but not isoniazid. Therefore treatment with erythromycin served as a positive control for *whiB7* induction, and isoniazid as a negative control.

2.3 Construction of a suitable reporter system for monitoring *whiB7* transcription

2.3.1 Performance of the *lux* reporter

Since the *whiB7* promoter was not yet mapped, the strategy devised for constructing the *luxABCDE* reporter included a fusion of the entire intergenic region between *whiB7* and the upstream gene (*uvrD2*). The *Mtb* H37Rv DNA fragment contained nucleotides -2 to -674 upstream of the annotated start codon of *whiB7* (*Rv3197a*), which included the last 245 bp of *uvrD2*. The integrative reporter vector constructed, pTB674lux, was then transformed into *M. smegmatis* wild type as well as the *whiB7* KO strain. Of note, a multi-copy vector was also constructed but no transformants could be isolated implying, at higher copies, the Lux system may be lethal to *M smegmatis*. This was reasonable as the plasmid carries genes specifying a potentially toxic product, a RCHO required for the luminescence reaction (Figure 4b). *M. smegmatis*/ pTB674lux produced light in response to erythromycin, but not isoniazid, with maximum intensity after about 180 minutes (Figure 5a). This demonstrated that pTB674lux could indeed monitor *whiB7* expression and, because the *Mtb* promoter region was used, suggested that regulatory motifs and the transcriptional regulators controlling *whiB7* expression are conserved between *M. smegmatis* and *Mtb*. Conversely, *M. smegmatis whiB7* KO/ pTB674lux showed no luminescence in treated or untreated controls (data not shown). This was puzzling as some background luminescence was expected due to basal expression of the *whiB7* promoter. As the Lux system was dependent on cell metabolism, I hypothesized that WhiB7 could be contributing to the light cycling reaction.

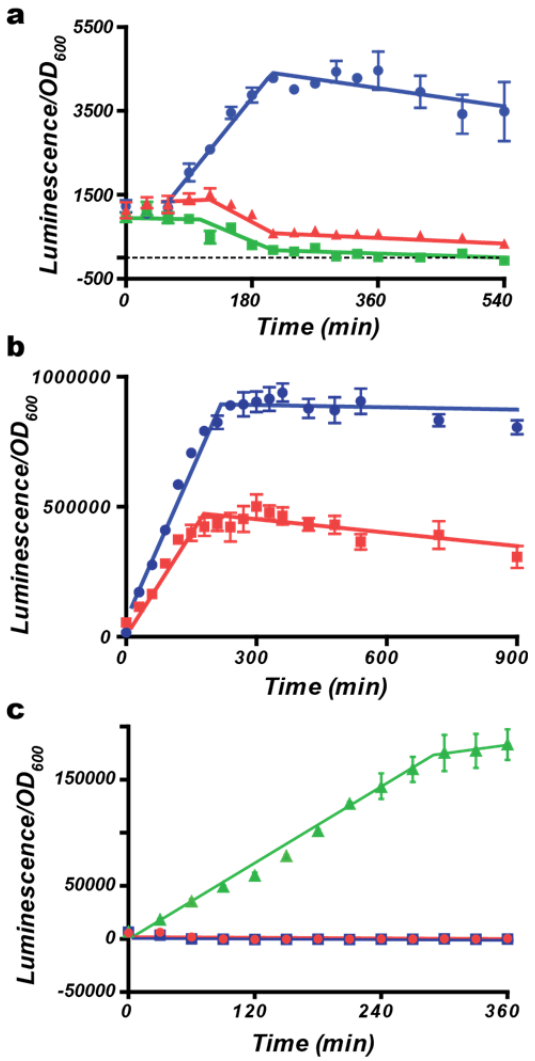

Figure 5. Analyses of LuxABCDE as a reporter of *whiB7* promoter activity. (a) Exponentially growing cultures of *M. smegmatis* containing the pTB7lux reporter were treated with 1 µM erythromycin (blue circles), 50 µM isoniazid (green squares), or left untreated (red triangles) and the luminesce measured over time. **(b)** Signal output from cultures containing the *luxABCDE* constitutively expressing pLUXon plasmid in *M. smegmatis* wild type (blue cirles) and *whiB7* KO (red squares). **(c)** Luminescence of 0 (green triangles), 2.2 (blue squares) and 11 µM (red circles) Bay 11-7085 treated pLUXon in *M. smegmatis*. All samples were prepared in triplicate. Values plotted are the mean ± SEM. Lines are drawn to illustrate the trend. Results are representative of multiple transformants.

To test whether LuxABCDE activity might be dependent on *whiB7*, *whiB7* was constitutively expressed using the *Mtb* HSP60 promoter (pLUXon). Luminescence of pLUXon was monitored in *M. smegmatis* wild type and *whiB7* KO strains. Luminescence output by pLUXon was at a much lower level in the *whiB7* KO strain than wild type (Figure 5b). This surprising observation revealed that optimal light production by the LuxABCDE protein complex was somehow directly influenced by WhiB7-dependent physiological signals. In addition, a limited screen of our antimicrobial compounds, using pTB674lux, revealed that at

least one drug, the IκB-α phosphorylation inhibitor BAY 11-7085 (*133*), quenched bioluminescence. BAY 11-7085 arrested light production from both pTB674lux (data not shown) and pLUXon (Figure 5c) in *M. smegmatis* at concentrations below its minimum inhibitory concentration (MIC). Together, these results showed that the LuxABCDE reporter was dependent on WhiB7 and that some compounds can have direct or indirect inhibitory effects on its activity. While these observations may lead to future insights into the role of *whiB7* or antibiotics on mycobacterial physiology, it was clear that pTB674lux is not a suitable reporter of *whiB7* promoter activity.

2.3.2 Performance of the *gfp* reporter

To monitor the promoter controlling the *M. smegmatis whiB7* gene, the multi-copy plasmid pMS689GFP was constructed. For pMS689GFP, the first 9 base pairs of *whiB7* and the 689 nucleotide upstream region was fused to *egfp*. This region corresponds to the entire 513 bp intergenic region and the last 176 bp of the nearest upstream gene, *uvrD2*. To determine whether this region contained the *whiB7* promoter, erythromycin or isoniazid were added to cultures of *M. smegmatis*/ pMS689GFP (Figure 6a). Erythromycin, but not isoniazid, induced fluorescence in these cultures to a maximum level after about 300 minutes confirming that pMS689GFP contained the antibiotic inducible *whiB7* promoter and that expression of eGFP could monitor its transcriptional activation. Furthermore, the levels of erythromycin-induced pMS689GFP fluorescence were much lower in the *whiB7* KO background (Figure 6b). This effect could be complemented by providing *whiB7 in trans,* using an integrative vector driving its expression from the constitutive HSP60 promoter (p361com.apra; Figure 6c). This provides evidence that WhiB7 is indeed autoregulatory and plays an essential role in activating its own promoter.

To ensure that WhiB7 did not have an effect on eGFP fluorescence, a constitutively expressed version (pGFPon) was constructed similar to pLUXon. Unlike pLUXon, pGFPon generated indistinguishable levels of fluorescence in *M. smegmatis* wild type and *whiB7* KO strains (Figure 6d). Overall, these results show that, although the level of response is lower relative to pTB674lux, pMS689GFP is the superior reporter system for monitoring *whiB7* transcription *in vivo*.

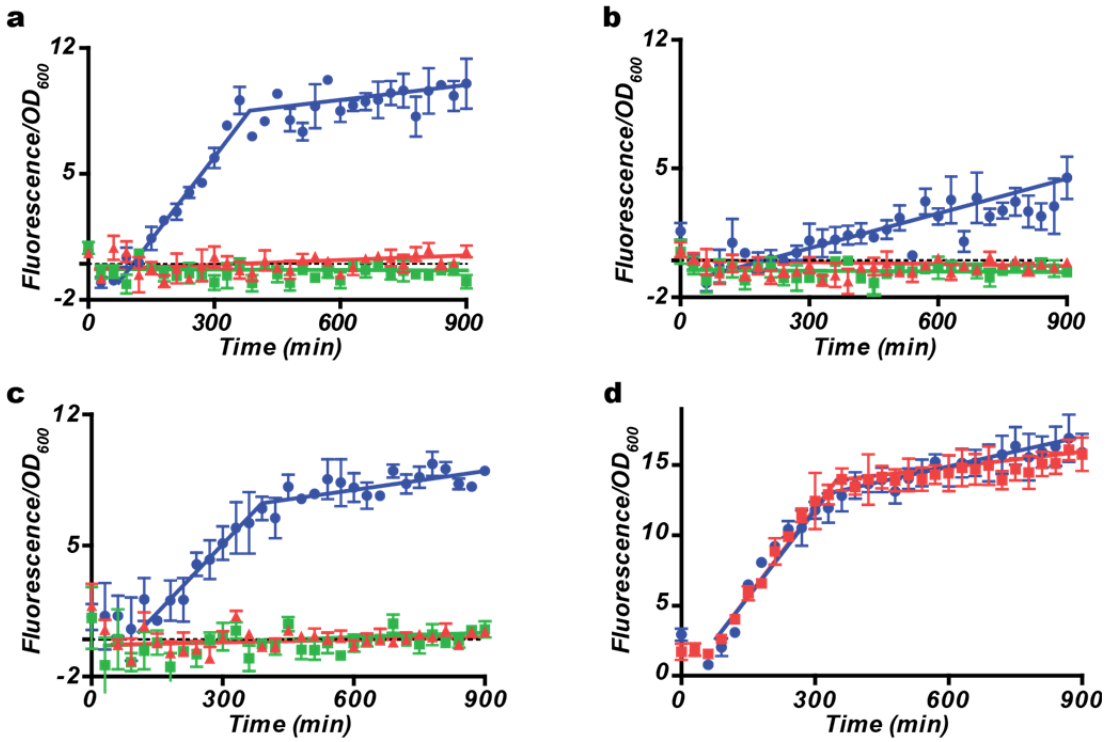

Figure 6. Analyses of eGFP as a reporter of *whiB7* promoter activity. (a) Exponentially growing *M. smegmatis*/ pMS689GFP was treated with 1 μM erythromycin (blue circles), 50 μM isoniazid (red triangles), or untreated (green square). **(b)** The erythromycin-induced fluorescence of pMS689GFP was decreased in the *whiB7* KO, **(c)** a defect that was restored by providing *whiB7 in trans* (strain *whiB7* KOC). **(d)** Signal output from cultures containing pGFPon in *M. smegmatis* wild type (blue circles) and *whiB7* KO (red squares). Values plotted are the mean ± SEM of triplicate samples. Lines are drawn to illustrate trends. Results are representative of multiple transformants.

2.4 The *whiB7* promoter

2.4.1 Identification of the *whiB7* promoter

There have been several attempts by members of our laboratory, including Andrea Basler and Gaye Sweet, to map the *whiB7* transcriptional start site (TSS) using the widely applied Rapid Amplification of 5' complementary DNA ends (5' RACE) method (*134*). 5' RACE utilizes an oligonucleotide that is complementary to the gene of interest as a primer for cDNA synthesis from an mRNA template. The 3' end of the cDNA product is then tagged by a homopolynucleotide tail, which is used as a non-specific primer along with a second primer specific for the gene to amplify, clone and sequence the 5' mRNA nucleotides. The 5' RACE method identified the TSS at a nucleotide located 106 bp upstream of *whiB7* (data not shown). An independent method, monitoring for a PCR product using cDNA synthesized from total mRNA as template and primers located farther and farther upstream of *whiB7*, indicated that the TSS was located between nucleotides 99 and 113 bp upstream of *whiB7* supporting the 5' RACE results. To determine whether the promoter was present in this region, the *whiB7* 689 nucleotide upstream region of pMS689GFP was shortened to 125, 167, 191, 227, 274 or 387 bp (data not shown). Surprisingly, none of the constructs elicited background fluorescence under non-inducing conditions or antibiotic inducible fluorescence similar to pMS689GFP. This implied that the region did not contain the *whiB7* promoter.

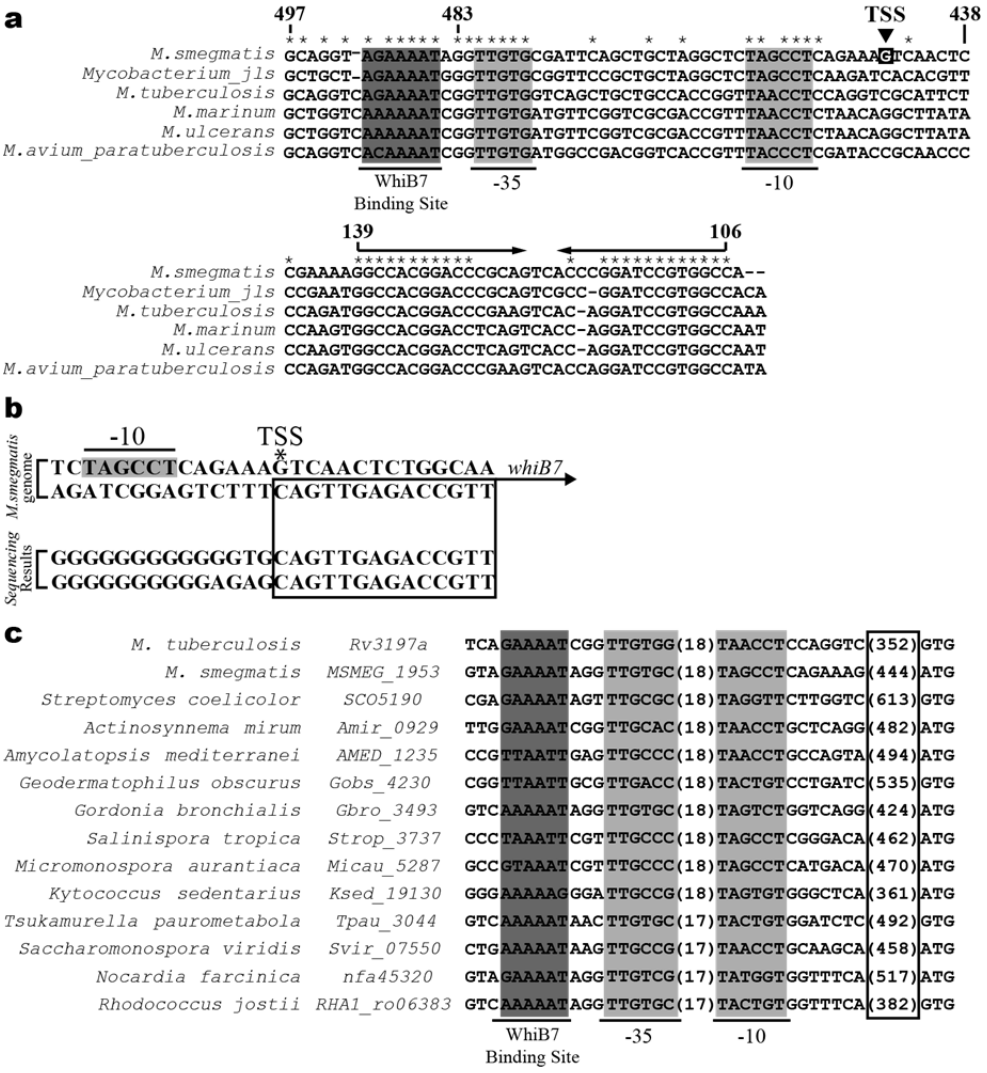

Figure 7. Sites and sequences defining the antibiotic inducible *whiB7* promoter. (a) (top) Alignment of a 60 bp region 438 to 497 nucleotides upstream of *M. smegmatis whiB7* with sequences from five different *Mycobacterium* species. Conserved nucleotides are designated by the star (*), the mapped transcriptional start site is highlighted by the black box, the -10 and -35 region are highlighted light grey and the putative WhiB7 binding site is highlighted dark grey (bottom). Alignment of a 43 bp region showing a conserved palindrome (arrows) from 103 bp to 139 bp upstream of *M. smegmatis whiB7*. **(b)** Directed mapping of transcription start site sequences of two independent clones (bottom) aligned to the *M. smegmatis* genome sequence (top). The matching sequence is boxed, the transcriptional start site is marked TSS and the -10 site is highlighted grey. **(c)** An alignment of the identified *whiB7* promoter motif across 13 genera of Actinobacteria. The variable distance from the start codon is boxed, the -10 and -35 region are highlighted light grey, and the putative WhiB7 AT-rich binding site is highlighted dark grey.

Due to the conserved nature of *whiB7* function in mycobacteria and other actinobacteria (*55, 107*), I reasoned that its regulation should be conserved as well. This was supported by the fact that the *Mtb whiB7* promoter functioned as expected in a heterologous host, *M. smegmatis* (Figure 5). To look for conserved sequences that may play a role in *whiB7* regulation, the upstream region of multiple mycobacterial *whiB7* orthologs was aligned to the 689 nucleotide *M. smegmatis* sequence known to contain the antibiotic-inducible promoter (Section 2.2.2). The multiple sequence alignment identified three areas of conservation. In a 5' to 3' direction; the first was the last 176 bp of the proximal gene *uvrD2* (not shown), the second was a region that resembled a promoter roughly 440 bp upstream of *whiB7* (Figure 7a; top), and the third was a large palindrome 106 to 139 upstream of *whiB7* (Figure 7b; bottom). Based on the large palindrome, it was likely that its secondary structure terminated cDNA synthesis and therefore the TSSs mapped by the aforementioned 5' RACE and RT-PCR were indeed incorrect as suggested by the shortened reporters. Since the region between nucleotides 438 and 497 bp contained conserved nucleotides that resembled -10 and -35 promoter elements, it was reasoned that this may be the *whiB7* promoter. Importantly, the region also contained a conserved AT-rich sequence upstream of the -35 site which could serve as a target for the WhiB7 AT-hook. Due to the palindrome a modified 5' RACE protocol was employed to confirm this region as the *whiB7* promoter.

The Directed Mapping of Transcriptional Start Sites (DMTSS) method (*135*) offers significant improvements to 5' RACE. Instead of generating a single cDNA product using a specific primer, DMTSS uses a random hexamer primer to generate full length cDNA from all RNA fragments (Figure 8). Therefore, RNA beyond the palindrome would be targeted and synthesized.

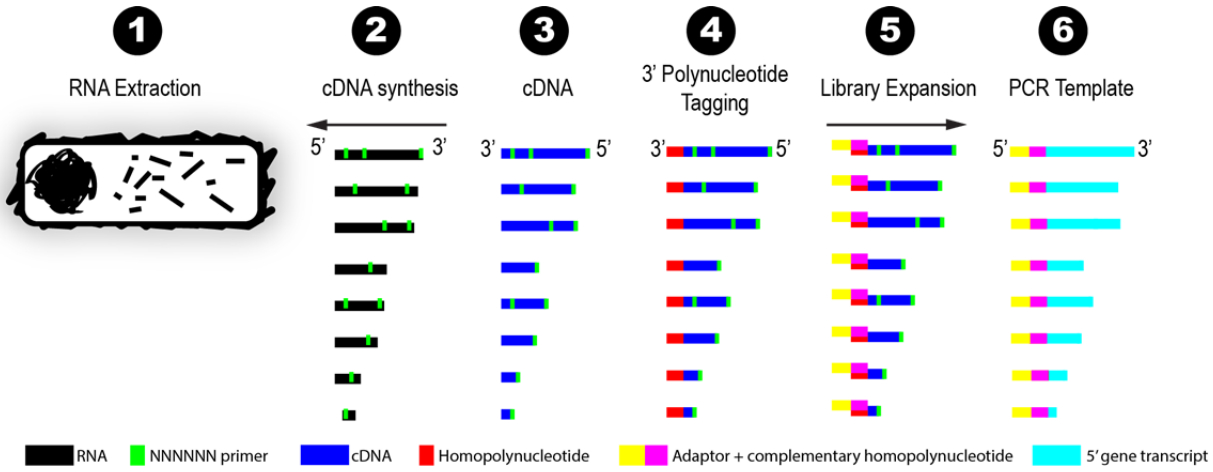

Figure 8. Outline of the Directed Mapping of Transcriptional Start Sites (DMTSS) method. Extracted RNA (1) is converted to cDNA using a random hexamer primer (2). This promotes the synthesis of full length cDNA from all RNA fragments (3). The cDNA is tagged with a homopolynucleotide tail (4) and then 'linearly expanded' by a primer complementary to the tail with an added 5' adaptor sequence (5). TSSs can then be probed using a primer complementary to the adaptor (yellow) and the gene of interest (6).

DMTSS was developed to probe *Escherichia coli* TSSs and therefore I designed a custom adaptor sequence for use in mycobacteria. To identify the *whiB7* TSS, a primer targeting a region upstream of the palindrome was used. Results showed the *M. smegmatis whiB7* TSS was the 445th nucleotide upstream of *whiB7* (Figure 7b). As *whiB7* is conserved in many Actinobacteria, analysis of *whiB7* orthologous loci in 12 different genera, selected from the KEGG database (http://www.genome.jp/kegg), were analyzed for a similar promoter. All the genera screened contained the identified promoter consensus sequence at various distances upstream of *whiB7* orthologs (Figure 7c). The identified *Mtb whiB7* promoter matched the results from a subsequently published genome-wide TSS mapping experiment (*136*). In all cases, there is a 5 bp AT-rich sequence three bases upstream of a conserved -35 promoter element, TTGNNN, and a

conserved -10 promoter element, TANNNT. This strongly suggests that *whiB7* regulation is conserved across Actinobacteria.

2.4.2 *whiB7* promoter confirmation by truncations of the *gfp* reporter

To demonstrate that the identified sequence was the antibiotic inducible *whiB7* promoter, pMS689GFP was modified and the response analyzed *in vivo.* The 689 bp region used to construct the promoter-reporter fusion was shortened to 497 (pMS497GFP), 483 (pMS483GFP), or 438 (pMS438GFP) nucleotides. As expected, removal of the entire conserved region (Figure 7a; pMS438GFP) resulted in no observed fluorescence in untreated or erythromycin treated *M. smegmatis* cultures (Figure 9a), confirming the region 483 to 497 bp contained the *whiB7* promoter. Restoration of the promoter (pMS497GFP) restored antibiotic inducible fluorescence of the reporter system (Figure 9b). This trend was observed with a broad range of *whiB7* activators including retapamulin, tilmicosin, doxycycline, linezolid, A23187 and acivicin (data not shown). A significantly reduced fluorescence response was observed with pMS483GFP, which contained the promoter but lacked the conserved AT-rich sequence (Figure 9b). This decreased fluorescence mirrored results seen with the pMS689GFP reporter in the *whiB7* KO strain (Figure 6), providing evidence that the conserved AT-rich sequence was required for WhiB7-mediated transcriptional activation. Importantly, a similar AT-rich sequence was also present three bases upstream of the -35 promoter element of the gene *eis* (*114*), which belongs to the WhiB7 regulon (Figure 9c). Additionally, the genes *tap* and *erm*, also within the putative WhiB7 regulon, were found to have the proposed promoter motif (Figure 9c). Together, these results suggest that WhiB7 binds the AT-rich sequence, likely through its C-terminal AT-hook, to promote transcription.

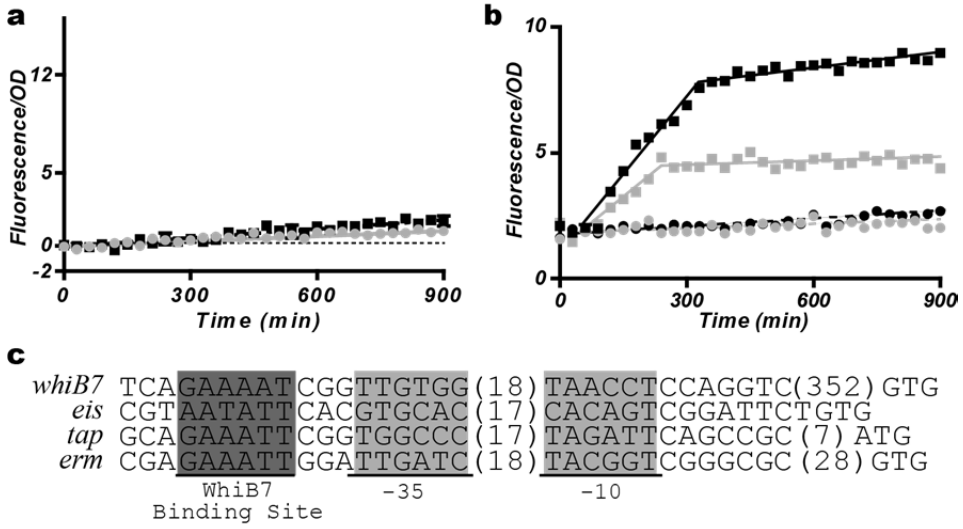

Figure 9. Sub-cloning in the GFP reporter vector localizes the *whiB7* promoter. (a) A fragment extending 438 bp upstream of *whiB7* (pMS438GFP) lacking the *whiB7* promoter was transcriptionally fused to the GFP reporter and either untreated (black squares) or treated with 1 μM erythromycin (grey circles) in *M. smegmatis*. **(b)** Fluorescence of shortened *whiB7*-promoter regions, pMS497GFP (black; full *whiB7* promoter) and pMS483GFP (grey; *whiB7* promoter lacking the AT-rich sequence), in *M. smegmatis* either untreated (circles) or treated with 1 μM erythromycin (squares). **(c)** The putative WhiB7 binding site and promoter motif is present upstream of several *Mtb* H37Rv genes within the WhiB7 regulon. The -10 and -35 region are highlighted light grey and the putative WhiB7 AT-rich binding site is highlighted dark grey. Values plotted are the mean ± SEM of triplicate samples. Lines illustrate the trend. Results are representative of multiple transformants.

2.5 Mode of WhiB7 mediated transcriptional activation

2.5.1 Binding of WhiB7 to SigA

Transcriptional activators that bind nucleotide sequences overlapping or adjacent to -35 promoter elements generally increase the affinity or stabilize sigma factor binding to the promoter, thereby stimulating transcription (*92*). The *whiB7* promoter matched the consensus sequence of SigA targeted promoters (*137*). A conserved AT-rich sequence, to which WhiB7 may bind, was located immediately upstream of the -35 promoter element (Figure 9). To determine whether

WhiB7 binds SigA, I cloned the a C-terminal fragment of *M. smegmatis* SigA (170 amino acid residues, 297-466), which was 99.6% identical to *Mtb* SigA (amino acids 359-528), referred to as $SigA_{C170}$. The fragment was slightly longer than $SigA_{C160}$ used to establish WhiB3:SigA interaction. An *E. coli* two-hybrid system (BacterioMatch II), as well as co-expression/pull-down experiments, were then used to test for protein-protein interaction between *M. smegmatis* WhiB7 and $SigA_{C170}$.

Two-hybrid systems are designed to monitor interactions between two proteins based on their abilities to localize RNA polymerase to a promoter upstream of a reporter gene. In the BacterioMatch II system, this results in higher expression of a histidine biosynthetic enzyme (HIS3) that can be monitored in a histidine auxotrophic reporter strain of *E. coli* grown on selective screening media (SSM) in the presence of 3-amino-1,2,4-triazole (3-AT), a HIS3 inhibitor (Figure 10a). The strength of the interaction determines the level of RNAP recruitment and therefore determines growth, which was measured as plating efficiency. To ensure that WhiB7 DNA-binding activity did not interfere with targeted localization to the reporter gene, the WhiB7 used as bait was truncated to remove the C-terminal AT-hook (WhiB7ΔC19; pBTW7ΔC19). Indeed, the use of WhiB7ΔC19 as bait and $SigA_{C170}$ (pTRG170) as target allowed growth on SSM (Figure 10b). This provided the first evidence of WhiB7:SigA interaction. WhiB7ΔC19:$SigA_{C170}$ interaction was prevented by the R515H mutation (Figure 10b) corresponding to the experiments done with WhiB3:$SigA_{C160}$. Importantly, expression of neither bait nor target protein alone promoted growth on SSM (Figure 11), and all strains grew normally on non-selective screening media (NSM) lacking histidine without the HIS3 inhibitor (Figure 10b).

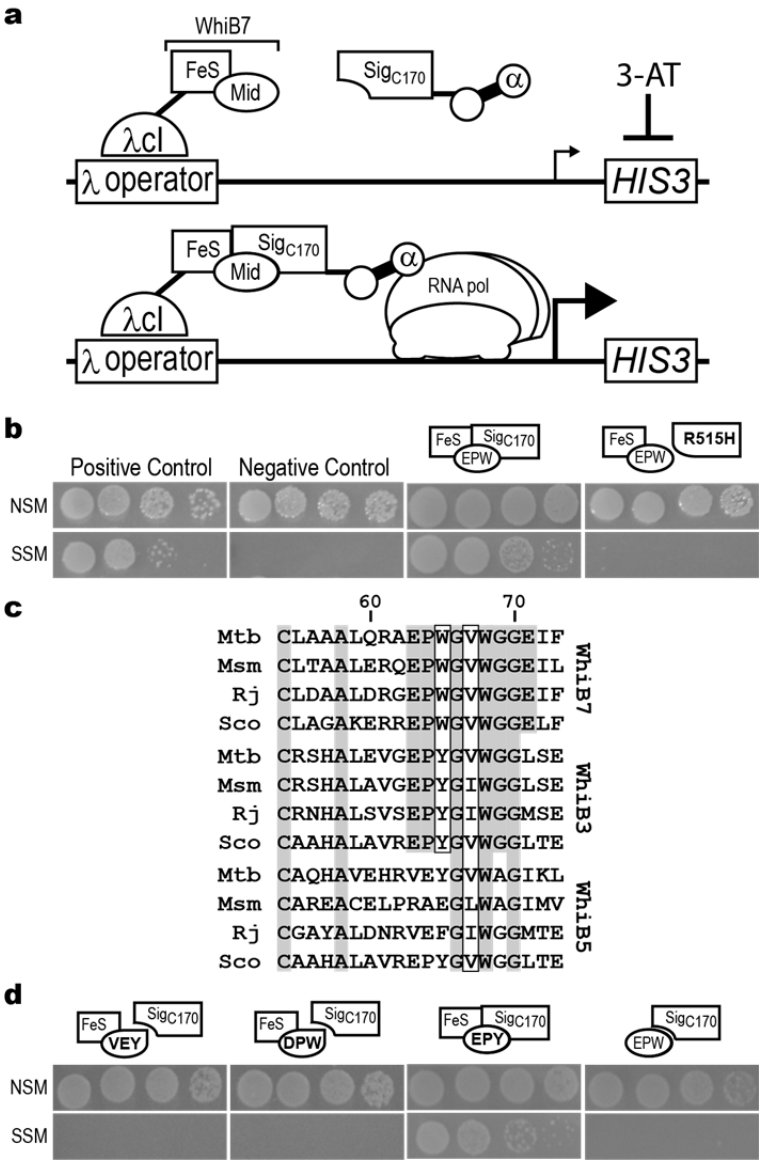

Figure 10. The binding of WhiB7ΔC19 to the C-terminus of SigA and its R515H mutant. (a) Schematic description of the BacterioMatch II two-hybrid system. A bait protein fusion (*M. smegmatis* WhiB7 + λcI) is targeted to a weak promoter expressing *HIS3* by λcI/ λ-operator interaction. 3-AT inhibits HIS3 activity resulting in histidine auxotrophy. Inhibition is overcome if the target protein fusion (*M. smegmatis* SigA + α) interacts with the bait protein. **(b)** Spotted dilutions (10^{-1}-10^{-4}) of reporter co-transformants on non-selective media (NSM) and SSM, to test protein interaction. Protein-protein interaction is indicated by growth on SSM. Bait and target vectors without inserts served as a negative control. The positive control was provided by Stratagene. Combinations of bait and target proteins tested are illustrated. WhiB7 is represented in two parts: the FeS cluster-binding region (aa 1-54; the box labelled 'FeS') and the middle region (aa 55-80; the oval labelled 'EPW'). The WhiB7 construct was partnered with a C-terminal fragment of SigA '$SigA_{C170}$', or its R515H mutant, 'R515H', as indicated. Results are representative of at least three independent co-transformants. **(c)** Peptide sequences of WhiB7 (top), WhiB3

(middle) and WhiB5 (bottom) spanning a region from the fourth cysteine to three residues downstream of the tryptophan-containing turn from *Mtb* (Mtb), *M. smegmatis* (Msm), *R. jostii* RHA1 (Rjo), and *S. coelicolor* (Sco). Conserved residues are highlighted grey and the chemically similar residues are boxed. **(d)** Similarly to 'b', $SigA_{C170}$ was partnered with various WhiB7 bait mutants or a truncated construct. Mutations in the middle region are bolded in the oval: EPY = W65Y, VEY = E63V P64E W65Y, DPW = E63D.

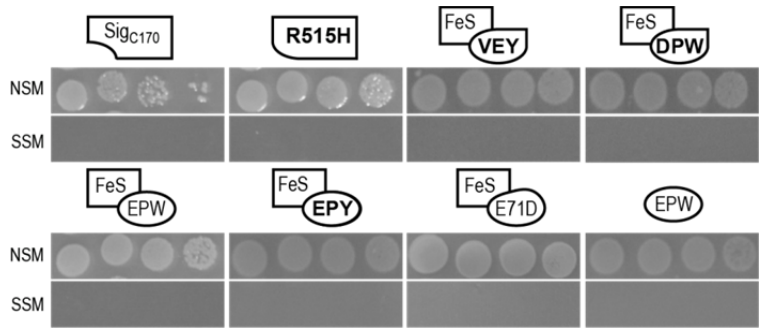

Figure 11. Bait or target constructs expressed with an empty partner. BacterioMatch II two-hybrid assay results for bait and target constructs paired with an empty partner vector. Bait and target illustrations presented are the same as in Figure 10.

To confirm WhiB7:SigA binding, *in vitro* pull-down experiments were done using full length WhiB7 fused to a 10xHis-tag (N-terminal) and $SigA_{C170}$ fused to a StrepII-tag (N-terminal). Proteins were co-expressed in *E. coli* (Figure 12a; lysate supernatant) and the soluble cytoplasmic fraction was passed through a Ni-NTA column that bound 10xHis-WhiB7. Elution from the column with imidazole co-purified $SigA_{C170}$ along with WhiB7 (Figure 12a; NiNTA elution). The eluate was then passed through a StrepTactin column that bound strepII-tagged $SigA_{C170}$. Elution from StrepTactin (using desthiobiotin) once again co-purified $SigA_{C170}$ along with WhiB7 (Figure 12a; StrepTactin elution), demonstrating that WhiB7 and SigA formed stable and soluble complexes. The fact that $SigA_{C170}$ was not purified on the Ni-NTA column in the absence of WhiB7 (Figure 13) demonstrated specificity. The UV spectrum of the purified WhiB7:$SigA_{C170}$ complex, which eluted as a brown/yellow solution, contained broad shoulders

centred at 325 nm and 425 nm indicating the presence of [2Fe-2S] WhiB7 (Figure 12b; see Figure S1 for comparison). This result was also consistent with anaerobically purified WhiB7 from *Streptomyces lividans*, which also coordinated [2Fe-2S] clusters (*107*). The amount of [2Fe-2S] cluster content was estimated using the molar extinction coefficient of 8000 $M^{-1}cm^{-1}$ at 400 nm (*138*) while the WhiB7:SigA protein complex amount was estimated by the calculated extinction coefficient of 27200 $M^{-1}cm^{-1}$ at 280 nm. [2Fe-2S] cluster content was calculated to be 0.96 (± 0.03) clusters per WhiB7:SigA complex. These data strongly suggest that SigA-bound WhiB7 contained a [2Fe-2S] cluster.

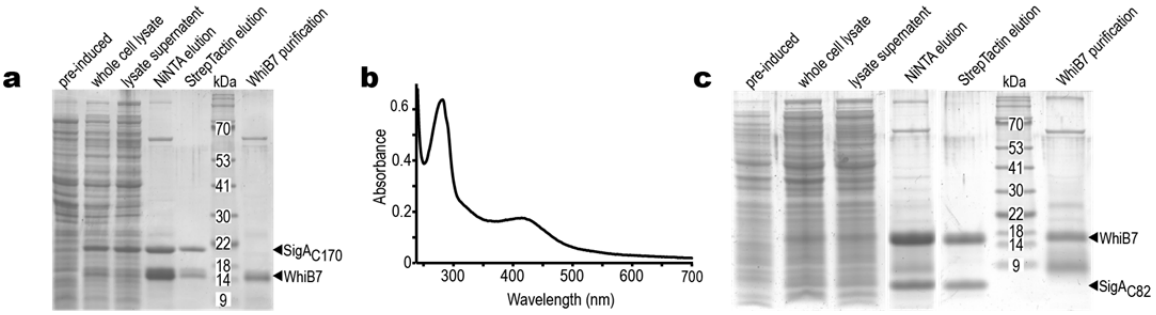

Figure 12. WhiB7 forms a stable and soluble complex with Region 4 of SigA in *E. coli*. (a) A C-terminal fragment of SigA ($SigA_{C170}$) was co-expressed with WhiB7 (whole cell lysate). Soluble proteins (lysate supernatant) were passed through Ni-NTA resin allowing purification of His tagged-WhiB7 and its binding partner, SigA (NiNTA elution). The Ni-NTA eluate was then passed through StrepTactin resin to bind strepII-tagged SigA resulting in co-purification of WhiB7 (StrepTacin elution). Fractions were separated by SDS-PAGE and proteins stained by GelCode. Protein molecular masses are estimated from standards with indicated masses (kDa). WhiB7 purification is the WhiB7 preparation used for *in vitro* run-off experiments. **(b)** Absorption of the StrepTactin eluate over a range of wavelengths. **(c)** Region 4 of SigA ($SigA_{C82}$) was co-expressed with WhiB7 (whole cell lysate). Soluble proteins (lysate supernatant) were passed through Ni-NTA resin allowing purification of His tagged-WhiB7 and its binding partner $SigA_{C82}$ (NiNTA elution). The Ni-NTA eluate was then passed through StrepTactin resin to bind StrepII -tagged $SigA_{C82}$ resulting in co-purification of WhiB7 (StrepTacin elution). WhiB7 purification is the WhiB7 preparation used for *in vitro* run-off experiments (note, a degraded form of WhiB7 was present in the preparation). Protein content was analysed as in 'a'.

The $SigA_{C170}$ fragment used in these experiments extended from the end of Region 2 through Regions 3 and 4. Since the R515H mutation that prevented WhiB7:SigA binding was located at the end of Region 4, I investigated whether Region 2 and 3 in $SigA_{C170}$ were dispensable for interaction with WhiB7. To map the WhiB7 binding site more precisely, a vector expressing the C-terminal 82 amino acids of SigA including only Region 4 ($SigA_{C82}$; pR4B7) was constructed. As was found with the $SigA_{C170}$ fragment, WhiB7 co-purified with $SigA_{C82}$ (Figure 12c). This indicates that the WhiB7 binding site is localized in Region 4 of SigA.

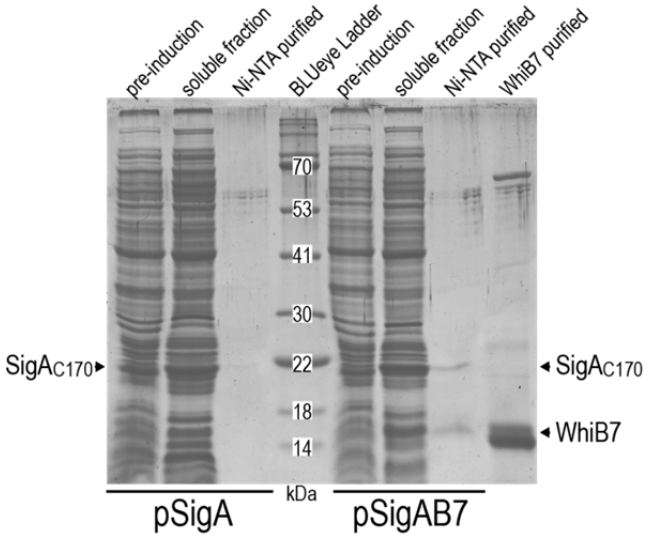

Figure 13. Batch co-purification of SigA by WhiB7 pull-down. A C-terminal fragment of SigA ($SigA_{C170}$) was expressed with (pSigAB7) and without (pSigA) WhiB7. Soluble proteins (soluble fraction) were passed through Ni-NTA resin and the retained protein eluted (Ni-NTA purified). The expected sizes are 20.9 kDa for SigA and 13.3 kDa for WhiB7. 10xHis-WhiB7 contains a very high proportion of positive amino acid residues (27/ 122) and was therefore expected to appear larger with SDS-PAGE separation. Pull-down of WhiB7 by Ni-NTA co-purified SigA (Ni-NTA purified pSigAB7). SigA expressed alone (pSigA) could not be purified by Ni-NTA. The WhiB7 purification used for *in vitro* run-off experiments is provided as a positive WhiB7 control (WhiB7 purification). The sizes of the ladder (BLUeye Ladder) are indicated (kDa).

WhiB7 has three regions predicted by its amino acid sequence: an FeS cluster binding region, a middle region, and an AT-hook (Figure 2). The C-terminal AT-hook was not required

for SigA binding (Figure 10). This indicated that the residue(s) responsible for SigA interaction were within the FeS cluster binding region and/or the middle region. Predictions of conserved Wbl structural features by Soliveri *et al.* (*56*) suggest that a loop between the FeS cluster binding region and the tryptophan-containing turn, within the middle region of Figure 2, "is a prime candidate for an interaction with another conserved cellular component (perhaps RNA polymerase, bound adjacent to a Wbl protein at a promoter)". Since WhiB3 interacts with SigA (*70*), but WhiB5 does not (*75*), I compared the WhiB7, WhiB3 and WhiB5 loop sequences from several genera, including *Mycobacterium, Streptomyces* and *Rhodococcus*. Both WhiB7 and WhiB3 contain a similar triplet sequence, EPW and EPY, in all species while WhiB5 had various dissimilar sequences (Figure 10c). Numerous transcriptional regulators are known to bind Region 4 of SigA, with interactions typically occurring between basic SigA amino acids (i.e., arginine or lysine) and acidic amino acids (i.e., glutamate or aspartate) in the activator protein (*91*). Therefore, the alignment suggested that the conserved anionic glutamate in WhiB7 (E63) and WhiB3 might interact with cationic arginine (R515) of SigA. The WhiB7 bait for the BacterioMatch system, WhiB7 (EPW), was therefore mutated to contain sequences mimicking WhiB3 (EPY), or WhiB5 (VEY). One other construct was made in which the glutamate was mutated to a chemically similar residue aspartate (DPW). Neither WhiB7 bait in which EPW was mutated to the WhiB5 sequence (pBTW7vey) nor the construct containing the glutamate to aspartate substitution (pBTW7d) interacted with SigA strongly enough to promote growth on SSM, while mutation to the WhiB3 sequence (pBTW7epy) retained activity (Figure 10d). This suggested that the glutamate (E63) was essential for SigA interaction, and that WhiB7 and WhiB3 may bind SigA in the same manner. A fragment of WhiB7 containing the EPW motif, spanning the middle region (Figure 2; WhiB7 aa 55-80), was also tested for SigA binding

(pBTW7mid) and was inactive (Figure 10d). Since WhiB7 bound to SigA appears to contain a [2Fe2S] cluster (Figure 12b), the result suggests that the presence of an FeS cluster may be critical for WhiB7:SigA binding.

Mutations of the conserved cysteines to alanines in WhiB1 or WhiBTM4 eliminate FeS cluster binding (*68, 139*). Additionally, at least two cysteine to alanine mutants of WhiB2 are inactive *in vivo* (*67*). Therefore, to investigate whether the FeS cluster contributed to WhiB7 binding of SigA, the 3rd cysteine (pBTW748) and both the 2nd and 3rd cysteines (pBTW74548; the CXXC motif), were mutated to alanines (Figure 2) and tested using the BacterioMatch system. Neither construct promoted growth under selective conditions indicating that the complex between SigA and WhiB7 was absent (Figure 14a). To further investigate these results using pull-down experiments, mutant genes were cloned into the expression vector used to co-express WhiB7 and SigA. Surprisingly, neither mutant protein was stably expressed either alone (Figure 14b) or with SigA (Figure 14c). These results suggested that, unlike WhiB1, loading of the FeS cluster appears to be essential for WhiB7 stability in *E. coli*. To ensure that the other mutants analyzed using the BacterioMatch system (Figure 10) were stable, each was expressed alone and could be purified at comparable levels to wild type WhiB7 (Figure 15). This demonstrated that WhiB7 instability was a unique function of the cysteine to alanine mutations, presumably due to loss of FeS cluster binding or perhaps improper folding of the apo protein.

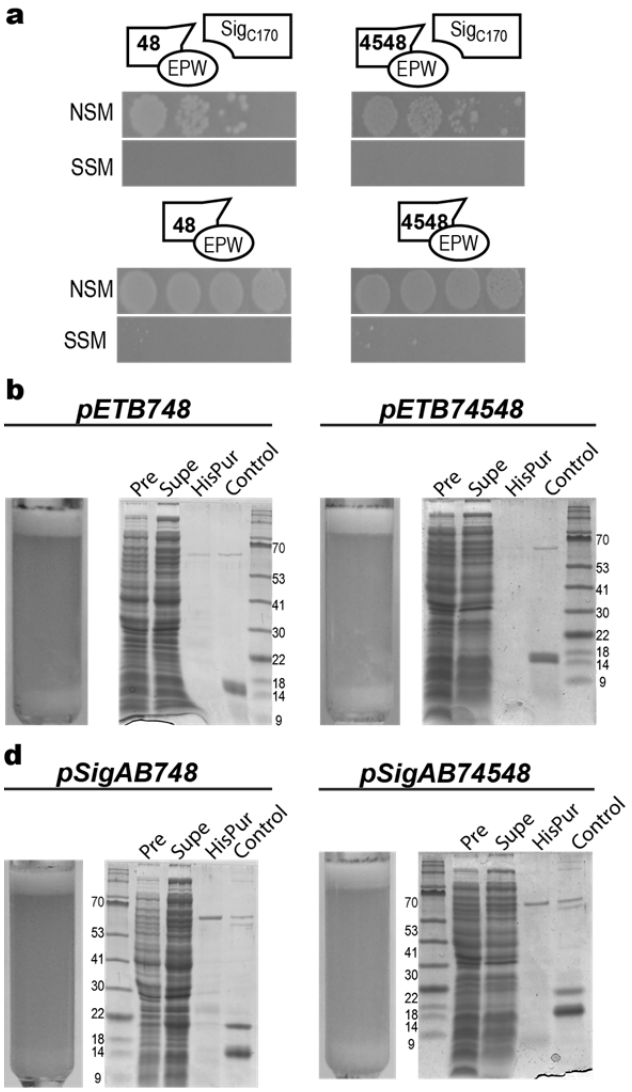

Figure 14. WhiB7s C48A and C45A C48A were unstable and interactions with SigA could not be monitored. **(a)** BacterioMatch two-hybrid results for cysteine mutants C48A (48) and C45A C48A (4548) in combination with $SigA_{C170}$ (top) or alone (bottom). No growth on selective screening medium (SSM) indicates no interaction. WhiB7 is represented in two parts: the cysteine iron binding box 'FeS' (aa 1-54) with the mutations indicated and the glycine rich tryptophan turn region oval 'mid' (aa 55-80). **(b)** Overexpression and purification of WhiB7 C48A (pETB748) and WhiB7 C45A C48A (pETB74548). The washed Ni-NTA resin was shown to remain light blue indicating that no FeS cluster containing protein was retained. A tricine SDS-PAGE gel shows the protein profiles of the purification steps including whole cell pre-induced (Pre), soluble protein post-induction (Supe), Ni-NTA purified fraction (HisPur), and a purified WhiB7 control (Control). The approximate kDA of the ladder bands is indicated. **(c)** Co-expression and purification of WhiB7 C48A (pSigAB748) and WhiB7 C45A C48A (p CDR42B74548) with a C-terminal fragment of SigA containing Region 4. The washed Ni-NTA resin was shown to remain light blue indicating that no FeS cluster containing protein was retained. A tricine SDS-PAGE gel shows the protein profiles of the purification steps including whole cell pre-induced (Pre), soluble protein post-induction (Supe), Ni-NTA purified

fraction (HisPur), and a purified WhiB7 or WhiB7:$SigA_{C170}$ complex control (Control). The approximate kDA of the ladder bands is indicated.

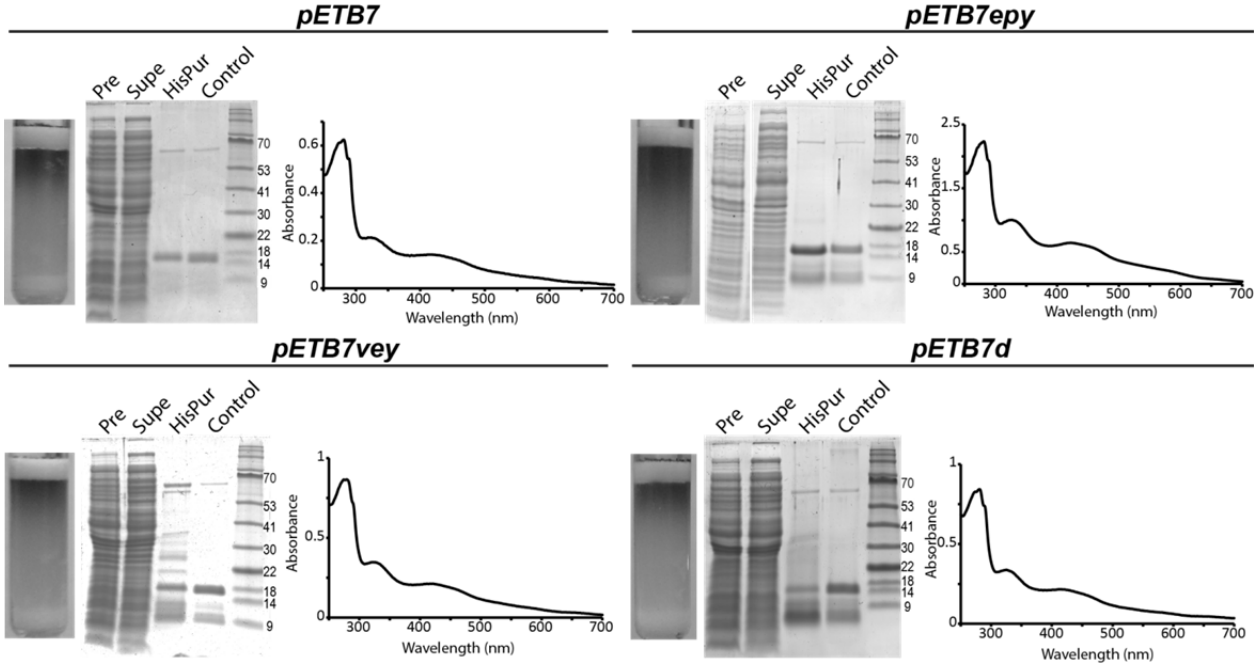

Figure 15. Expression and absorption spectra of non-cysteine WhiB7 mutants. Overexpression and purification of WhiB7 (pETB7), WhiB7 W65Y (pETB7epy), WhiB7 E63V P64E W65Y (pETB7vey), and WhiB7 E63D (pETB7d). A tricine SDS-PAGE gel shows the protein profiles of the purification steps including whole cell pre-induced (Pre), soluble protein post-induction (Supe), Ni-NTA purified fraction (HisPur), and a purified WhiB7 control (Control). The approximate kDa of the ladder bands is indicated. Purification in all cases resulted in a purified protein matching WhiB7. WhiB7 E63V P64E W65Y may be prone to multimerization. The absorption spectra of each eluate is shown.

2.5.2 WhiB7 promotes transcription *in vitro*

The *whiB7* promoter contains a conserved AT-rich sequence that may serve as a WhiB7 binding site. To test whether WhiB7 directly catalyzed transcription of its promoter, WhiB7 was purified for transcriptional run-off assays. WhiB7 contains an FeS cluster that is sensitive to air, but can be significantly stabilized by a reductant (*61*). 10xHis-WhiB7 was purified at 4 ºC under aerobic conditions using a Ni-NTA column. It eluted as a brown solution, characteristic of proteins

binding an FeS cluster. The electronic absorption spectrum contained broad bands centred at 325 nm and 425 nm, similar to the WhiB7:$SigA_{C170}$ spectrum (Figure 12b), which indicated the presence of a [2Fe-2S] cluster. Since the purification of WhiB7 was done aerobically, the eluate was expected to contain both apo- and holo- WhiB7 in various redox states. To stabilize FeS clusters, purified WhiB7 was supplemented with DTT and flash frozen.

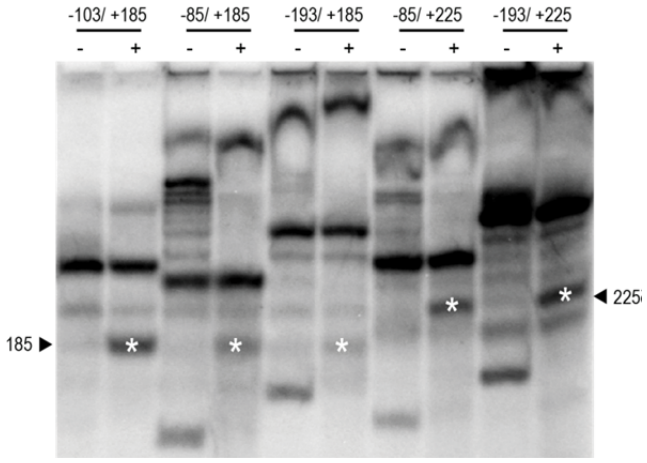

Figure 16. WhiB7 catalyzed run-off transcription from the predicted start site of the *whiB7* promoter. The size of the upstream (denoted by '-') and downstream (denoted by '+') lengths relative to the transcriptional start site (+1) of the templates are indicated. WhiB7, at a fixed concentration (3 μM), was added (+) or withheld (-). The products corresponding to the expected size of the *whiB7* promoter transcript (185 or 225 bp) are highlighted by white stars. The other prominent bands represent non-specific transcripts.

Holo-RNA polymerase (RNAP), loaded with a mixture of sigma factors, was isolated from exponentially growing *M. smegmatis.* Initially, control experiments using truncations of adjacent upstream and downstream regions of the *whiB7* promoter relative to the identified TSS were performed. Addition of purified WhiB7 to these reactions generated a product corresponding to the size of the region downstream of the mapped TSS, but no changes observed in variations of the upstream region (Figure 16). This demonstrated that WhiB7 stimulated transcription of the

identified promoter from the expected TSS. RNAP activity was then assayed using the *whiB7* and HSP60 promoters (Figure 17a) in the presence of increasing concentrations of WhiB7. Transcriptional run-off products were analyzed after separation on denaturing polyacrylamide gels (Figure 17b). WhiB7 catalyzed up to a fourfold increase in transcription of its own promoter in a concentration-dependent manner and had no significant effect on transcription from the HSP60 (Figure 17c). There was a relatively small increase of HSP60 activity when lower concentrations of WhiB7 were added. Although a minor direct effect cannot be ruled out, the fact that higher concentrations did not promote larger transcription increases from the HSP60 promoter indicated that this activity was insignificant. My studies suggested that the conserved cysteines, and therefore, by proxy, binding of an FeS cluster, were likely to be important for WhiB7 stability (Figure 14). As the purified WhiB7 contained bound FeS cluster, transcriptional run-off experiments were carried out to determine whether this was required for its activity. In studies of other holo WhiB proteins, diamide is known to release their FeS clusters generating oxidized apo proteins with intramolecular disulphide bonds between the conserved cysteines (*61, 62, 71*). WhiB7, treated with diamide, did not activate transcription (Figure 17d). The observation that diamide did not inhibit transcription from the WhiB7-independent HSP60 promoter demonstrated specificity as the loss of function was not due to oxidation of other components in the run-off reaction mix. Lastly, the AT-rich sequence upstream of the *whiB7* promoter was suggested to be required for WhiB7 mediated transcriptional activation *in vivo* (Section 2.3.2). When this AT-rich sequence was deleted, *in vitro* transcription was no longer promoted by WhiB7, confirming its requirement for WhiB7-dependent transcription activation (Figure 17e). Together, these results show that WhiB7 is a redox-sensitive transcriptional activator targeting the conserved AT-rich sequence upstream of the *whiB7* promoter.

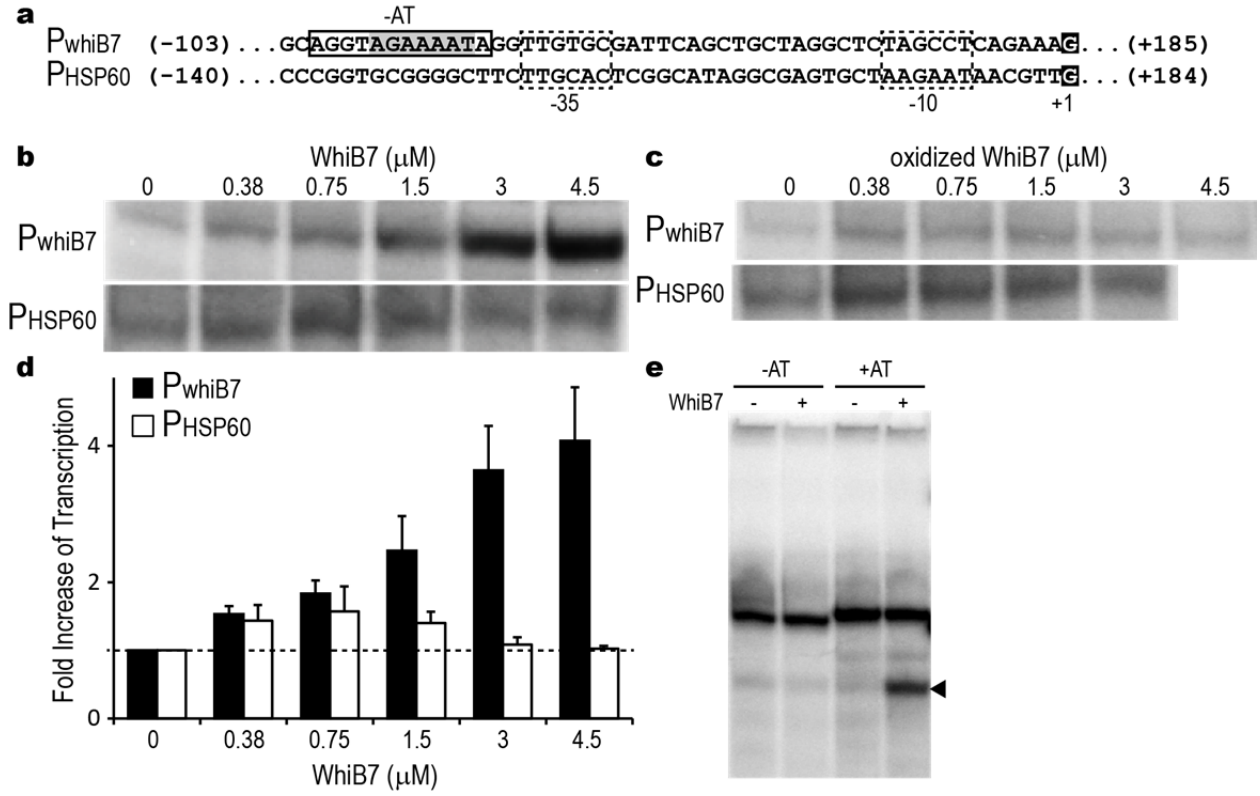

Figure 17. ***In vitro*** **run-off analysis investigates WhiB7-mediated transcriptional activation. (a)** Sequence of the *whiB7* (P_{whiB7}) and HSP60 (P_{HSP60}) promoters. The potential AT-rich WhiB7 binding site is highlighted in grey and the region deleted for experiments in 'e' is boxed. The -10 and -35 promoter elements are boxed within dashed lines and the transcriptional start site is highlighted as white text on a black background. **(b)** Transcriptional products from the *whiB7* (P_{whiB7}) and HSP60 (P_{HSP60}) promoters with the addition of an increasing amount of WhiB7 (0 – 4.5 μM). **(c)** Quantification of transcriptional activity observed in '**b**', as fold increase versus no WhiB7 of the *whiB7* (black) and HSP60 (white) promoters. Transcripts from three reactions were quantified and averaged. Error bars represent standard deviation. **(d)** Transcriptional products from the *whiB7* (P_{whiB7}) and HSP60 (P_{HSP60}) promoters with the addition of an increasing amount of oxidized WhiB7 (0 – 4.5 μM). **(e)** Transcriptional product (arrow) of the *whiB7* promoter with (right) and without (left) the conserved at AT-rich sequence (see '**a**'). Reactions were carried out in the presence (+; 3.0 μM) or absence (-) of WhiB7. The other prominent bands represent non-specific end-to-end transcripts.

2.5.3 Potential targets for WhiB7 inhibition *in vivo*

Having established the requirement of the AT-rich sequence upstream of the promoter for WhiB7-catalyzed transcription (Figure 17), experiments were carried out to investigate the role of the WhiB7 C-terminal AT-hook in targeting this sequence *in vivo*. A C-terminally truncated protein lacking the AT-hook was tested for its ability to complement the *M. smegmatis whiB7* KO strain. Resistance to representative members of several structural classes of antibiotics within the *whiB7* sensitivity spectrum were screened, including an aminoglycoside (spectinomycin), a tetracycline (tetracycline) and macrolides (clarithromycin and roxithromycin). The *whiB7* KO strain was more sensitive to spectinomycin (8-16 fold), tetracycline (8-fold), clarithromycin (>32 -fold) and roxithromycin (>32-fold) (Table 1). Constitutive expression of full length WhiB7 (pFB7), but not a C-terminally truncated, AT-hook lacking WhiB7ΔC19 (pFB7AT), restored antibiotic resistance in the *M. smegmatis whiB7* KO to wild type levels, demonstrating that the AT-hook was required for activation of resistance systems *in vivo* (Table 1). Interestingly, expression of WhiB7ΔC19 in the parental background consistently lowered its antibiotic resistance twofold (relative to the vector control and pFB7), suggesting that the WhiB7ΔC19 may compete with functional WhiB7 protein for SigA binding (Table 1) to sequester it in an inactive form. In addition, an N- and C-terminally truncated WhiB7 (WhiB7ΔN19C6; pB7fun), which corresponded to the conserved "functional" region of WhiB7 proteins (Figure 2) restored antibiotic resistance (Table 1). This indicated that the variable N- and C- termini do not contribute to WhiB7's antibiotic resistance function.

Table 1. Minimum inhibitory concentrations of *M. smegmatis* and *whiB7* KO expressing WhiB7 and WhiB7ΔC19, as well as *M. smegmatis* FB7

	MIC (μg/mL)[a] *M. smegmatis* mc^{2}155							
Strain:	Parental			*whiB7* KO				
Vector:	pMV261	pFB7	pFB7AT	pMV261	pFB7	pFB7AT	pFB7d	pB7fun
spectinomycin	80-40	80	40	5	80	2.5	10	160-80
tetracycline	1	1	0.5	0.13	1	0.063-0.03	0.25-0.13	1
clarithromycin	3	3	1.5	≤0.094	3	≤0.094	0.094	6
roxithromycin	24	24	12	≤0.38	24	≤0.38	≤0.38	24

[a]MIC ranges represent three independent transformants.

In *Mtb*, the SigA R515H mutant is less virulent, mimicking the phenotype of a mutation of the WhiB7 paralog WhiB3 (*71, 93*). Binding of WhiB7 and SigA was similarly prevented by the SigA R515H or WhiB7 E63D mutations (Figure 10), predicting that these mutations might generate a multi-drug sensitivity phenotype found in the *whiB7* KO. I replaced wild type *sigA* with an R515H mutant allele to construct *M. smegmatis* Sig515 (Figure 18a). While levels of resistance to representative antibiotics not in the *whiB7* sensitivity spectrum (including danofloxacin and isoniazid) were not significantly changed (Table 2), the mutant was at least fourfold more sensitive to antibiotics within the *whiB7* sensitivity spectrum (including tetracycline, spectinomycin and clarithromycin) (Table 2). Interestingly, the decrease in sensitivity to spectinomycin was affected less by the SigA R515H mutation than by the *whiB7* deletion. Disk assays were done to further evaluate resistance levels (Figure 18b). The Sig515 mutant was slightly more resistant to clarithromycin and tetracycline than the *whiB7* KO mutant, but was much more resistant to spectinomycin (Table 2). To ensure that *whiB7* was not disrupted in the Sig515 strain, the presence of the gene and its promoter were confirmed by PCR (Figure 18c).

Finally, the ability of WhiB7 E63D (pFB7d) to complement the *whiB7* KO mutation was tested. Similar to the SigA R515H mutation, the pFB7d-complemented strain showed the same multi-drug susceptibility profile as the *whiB7* mutant (Table 1) confirming that WhiB7 E63D did not activate an antibiotic resistance response. Overall, these results show that WhiB7:DNA as well as WhiB7:SigA binding are essential interactions for WhiB7-mediated resistance.

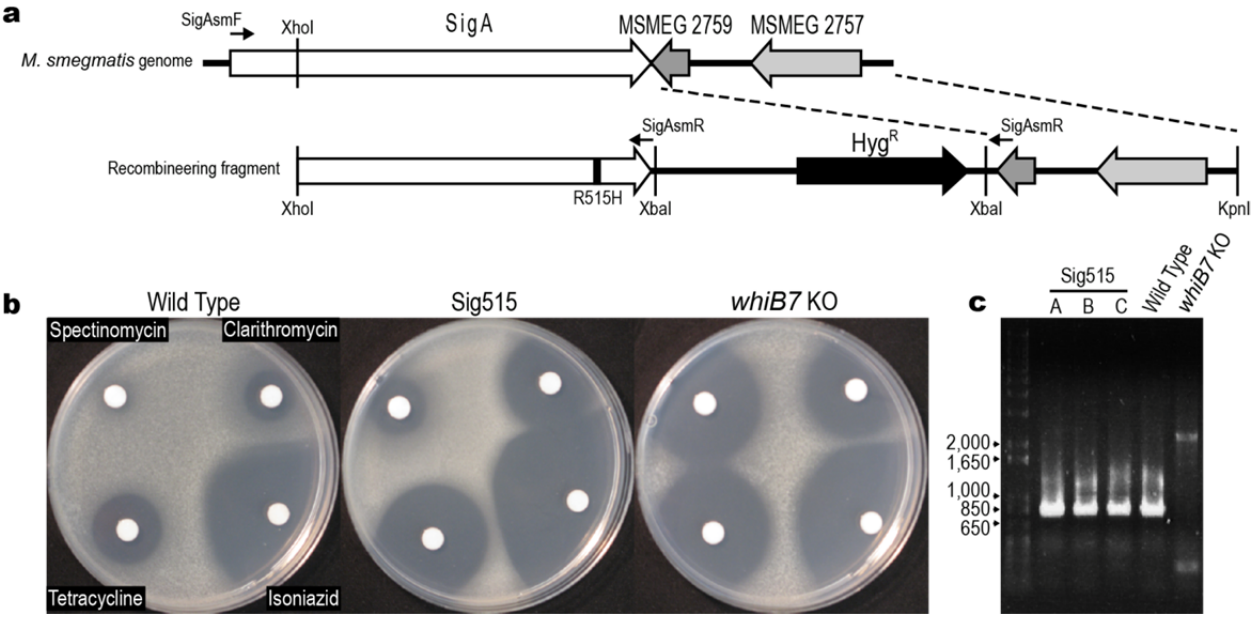

Figure 18. The susceptibility of *M. smegmatis* and its SigA R515H and *whiB7* KO derivatives to several antibiotic. (a) Outline of the recombineering (*140*) strategy used to construct *M. smegmatis* Sig515. A double recombination event replaced a region of the SigA gene (top) with a mutated allele R515H (bottom). The primers used to confirm insertion of the mutation are indicated. **(b)** Disk assay for the resistance of *M. smegmatis* Parental (left), Sig515 (middle), and *whiB7* KO (right). The results are representative of three independent Sig515 recombinants or the other strains performed in triplicate. **(c)** PCR products of the amplification of *whiB7* and its promoter from *M. smegmatis* parental, the three Sig515 recombinants, and *whiB7* KO. A ca. 800 bp product was expected for a native *whiB7* allele. Sizes of the ladder (left) are indicated.

Table 2. Comparison of drug susceptibility of *M. smegmatis* parental, Sig515, and *whiB7* KO in liquid and on solid media

	Mycobacterium smegmatis mc^{2}155					
	Parental	Sig515	*whiB7* KO	Parental	Sig515	*whiB7* KO
Antibiotic	MIC (μg/mL)[a]			Diameter of inhibition zone (mm)[b]		
spectinomycin	80	20	10	0	18.1 ± 2.6	34.3 ± 1.3
clarithromycin	1.5	0.19-0.09	0.094	15.3 ± 0.3	27.5 ± 1.2	30.3 ± 0.6
tetracycline	2	0.5-0.25	0.5	21	31.9 ± 0.9	35.3 ± 0.3
isoniazid	16	8	16	48	49.8 ± 0.4	46.7 ± 1.2
danofloxacin	0.35	0.35	0.35	-	-	-

[a] MICs represent the range of three biologically independent replicates for parental and *whiB7* KO strains. They are the range of three independent Sig515 mutants.

[b] Diameters are the average of triplicate experiments for parental and *whiB7* KO strains. For Sig515 they are the average of three independent recombinants performed in duplicate. If measurements showed variation the standard deviation is indicted as '±'. Total μg spotted: spectinomycin 145, clarithromycin 2.9, tetracycline 0.725, isoniazid 145.

While Wbl proteins have attracted the attention of many laboratories, structural data are not available for any of these proteins. This is generally attributed to structure predictions that their peptide sequences are primarily disordered and the fact that FeS cluster containing regulatory proteins are notoriously unstable (*141*). WhiB7 in *Mtb* is a 92-residue protein (UniProt accession number: Q6MX01) that does not have sufficient amino acid sequence similarity with any protein of known structure for homology modeling or structure-sequence threading. Having established points of interaction between WhiB7, SigA and DNA, these results were able to spatially constrain WhiB7 and its partners. This allowed our collaborators Michael Hsing and Peter Axerio-Cilies, from Dr. Artem Cherkasov's lab, to generate a *de novo* 3D structural model of WhiB7 using the Robetta server (*142*). The top 10 WhiB7 models were examined for positioning of the four cysteine residues to coordinate a [2Fe-2S] cluster, and a C-terminal loop resembling an AT-hook (*143*). My experimental data predicted an interaction between E61 of WhiB7 and R515 of SigA. Using this information, a homology model of SigA region 4 of *Mtb* (UniProt accession number: P0A602) was built using MODELLER (*144*) based

on the *E. coli* SigA structure (PDB: 4IGC_X; (*145*)). Regions 4 of the *E. coli* and *Mtb* vegetative sigma factors share 51% amino acid sequence identity. The potential interacting poses between WhiB7 and SigA were then evaluated by using protein-protein docking predictions from the ClusPro 2.0 server (*146*) and ensuring they contained the E61 – R515 interaction shown experimentally. To further define DNA-binding residues, the most likely protein docking model (best of 12 candidates) was superimposed with the RNA polymerase holoenzyme-DNA complex (PDB: 1L9Z; (*147*)). Using the positions of expected binding sequences for WhiB7 and SigA, the model of the complex was energy minimized in the AMBER99 force field. Figure 19a illustrates the overall structural model of WhiB7, SigA and DNA. The predicted interface between WhiB7 and SigA based on protein-protein docking was further examined for interacting residues. Remarkably, the electrostatic surfaces of WhiB7 (Figure 19b) and SigA (Figure 19c) had complementary charges and shapes. In addition to the E61 and R515 interaction, there were numerous potential close (within 4.5 Å) interactions (Table 3) between WhiB7 and SigA that were identified using the Molecular Operating Environment suite. Interactive residues corresponding to conserved WhiB7 amino acids are diagramed in Figure 19d. Interestingly, a glutamate residue downstream of the tryptophan turn, E69 (E71 in *M. smegmatis*), was identified as a partner for a second potential ionic interaction with SigA. To provide evidence for the validity of the model, E71 in *M. smegmatis* was mutated to an aspartate (pBTW71d) and tested by the two-hybrid assay. Unlike the E63D mutant, the E71D mutant in combination with $SigAC_{170}$ promoted growth under selective conditions, although not as strongly as the wild type or W65Y mutant (Figure 19e). The decreased growth (corresponding to a tenfold dilution) suggested that WhiB7:SigA interaction was indeed weakened by the E71D mutation, but not as

effectively as the E63D mutation. Thus the model correctly identified E71 as a residue contributing to SigA interaction.

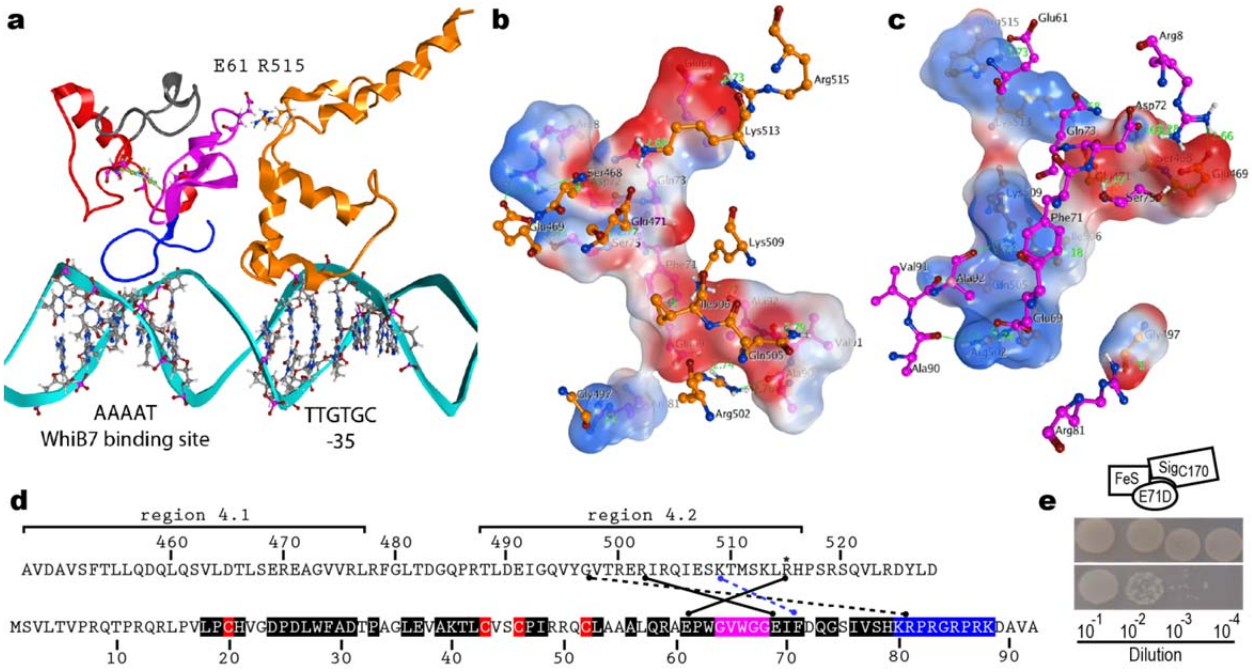

Figure 19. Structural prediction of WhiB7 and its interaction with SigA and DNA. (a A structural model of *Mtb* WhiB7, SigA and DNA. WhiB7 is shown as a ribbon with the three functional regions highlighted; variable N-terminus (grey), FeS cluster binding region (red), middle region (pink), and AT-hook (blue) positioned in the DNA minor groove. The homology model of *Mtb* SigA Region 4 (based on *E. coli* SigA *E. coli* (PDB: 4IGC_X)) is shown as an orange ribbon, interacting with the DNA at the -35 position. Interaction surfaces of **(b)** WhiB7 as viewed by SigA (interactive SigA residues are superimposed) and **(c)** SigA as viewed by WhiB7 (interactive WhiB7 residues are superimposed). The electrostatic surfaces of interacting residues are shown (blue: positively charged, red: negatively charged). Hydrogen and ionic bonds are displayed as green lines with the distance in Ångstroms. For clarity, hydrogen atoms not involved in interactions are hidden. Colors of amino acids modeled correspond to those in (a). **(d)** Potential conserved interactions between WhiB7 (below) and region 4 of SigA (top). The experimentally determined point of interaction (R515) is starred. The *Mtb* WhiB7 maintains the colouring from Figure 2 to highlight conserved residues. Ionic bonds are indicated by solid lines, hydrogen bonds as dashed lines, and hydrophobic interactions as dashed blue lines. **(e)** As in Figure 10, $SigA_{C170}$ was partnered, using the two-hybrid system, with a WhiB7 E71D mutant as bait disrupting the other potential ionic interaction as indicated by '**d**'. A 10 times higher dilution of cells was need for minimal growth relative to Figure 10.

Table 3. Possible interactions between modeled *Mtb* WhiB7 and SigA

Interaction type	WhiB7_MTB residue	SigA_MTB residue
Hydrogen bond	R8.N_{H1}	S468.O_G
Ionic bond	R8.N_{H2}	E469.O_{E2}
Ionic bond	E61.O_{E2}	R515.N_{H2}
Ionic bond	E69.O_{E2}	R502.N_{H2}
Hydrophobic contact	F71.C_{E2}	I506.C_{D1}
Hydrogen bond	D72.O_{D2}	S468.O_G
Hydrogen bond	Q73.O_{E1}	K513.N_Z
Hydrogen bond	S75.O_G	E469.O_{E1}
Hydrogen bond	S75.N	E471.O_{E2}
Hydrogen bond	R81.N_{H1}	G497.O
Hydrogen bond	A90.O	R502.N_{H1}
Hydrogen bond	V91.O	Q505.N_{E2}
Hydrogen bond	A92.O	K509.N_Z

2.6 Discussion

In *Mtb*, seven *whiB* genes are implicated in a variety of fundamental metabolic processes. Whether the corresponding gene products act exclusively as transcriptional regulators and/or have additional functions as thioredoxins or chaperones continues to be debated. To better understand factors that affect WhiB7-mediated intrinsic resistance of mycobacteria, I established a reporter system to monitor *whiB7* transcription and identified the essential components of the *whiB7* promoter. Additionally experiments were performed to generate a model of WhiB7-mediated transcriptional activation. *In vitro* run-off experiments provided the first direct biochemical proof of transcriptional activation by a WhiB protein. WhiB7's predicted functional regions (Figure 2) were shown to contribute to protein stability (FeS cluster binding region), binding of SigA (middle region), and targeting RNA polymerase to a specific subset of vegetative promoters (AT-hook). The experimental data was then combined with bioinformatics approaches to generate a *de novo* 3D structure of the WhiB7:DNA:SigA complex (Figure 19).

My data established that WhiB7 was essential for transcriptional activation of *whiB7* (Figure 6). Importantly, the *Mtb whiB7* promoter (pTB674lux) was activated by erythromycin in *M. smegmatis* (Figure 5) in a similar fashion to pMS689GFP containing the *M. smegmatis whiB7* promoter. This showed that the regulatory elements of *whiB7* transcription are likely conserved across mycobacteria, and perhaps other Actinobacteria, and that the system's effectors, like WhiB7, are also conserved. Surprisingly, unlike eGFP fluorescence (Figure 6), LuxABCDE fluorescence was somehow dependent on WhiB7 (Figure 5). As the bioluminescence reaction is complex requiring RCHO, $FMNH_2$, and O_2, this implies that WhiB7 may have additional biological functions outside of antibiotic resistance that contribute to the Lux system. These may include cell wall biosynthesis, where the RCHO precursor is synthesized, or redox cycling for the reduction of FMN.

The identified nucleotide region required for antibiotic induction of *whiB7* in *M. smegmatis* contained a promoter motif that is conserved in Actinobacteria (Figure 7), providing further evidence that the mode of *whiB7* transcriptional activation is conserved. A comparison of the *whiB7* promoter to consensus sequences for all *Mtb* sigma factors (*148*) showed that its -35 and -10 promoter elements and their spacing was most similar to SigA, the primary vegetative sigma factor. The presence of an AT-rich sequence upstream of the -35 site was important for maximal antibiotic activation of the *whiB7* promoter (Figure 9), suggesting that WhiB7 may act as a bridge to stabilize promoter-RNAP interactions during transcriptional initiation. Since *whiB7* contains an AT-hook (*55*), a motif known to bind the minor groove of AT-rich DNA (*108*), the results imply that the AT-rich sequence serves as the WhiB7 binding site. Similarly to *whiB7,* antibiotic resistance genes proposed to be regulated by WhiB7 also contained an AT-rich sequence 3 bp upstream of their promoters (Figure 9) supporting the hypothesis the mode of

WhiB7 induction has been conserved across the regulon. In addition, although the rate of antibiotic induction of the *whiB7* promoter was strongly decreased in the *whiB7* KO background, a slow but progressive increase in activity was observed (Figure 6). This may reflect the participation of other regulatory elements that either repress under non-inducing conditions or activate upon induction. Together these results show that after antibiotic treatment, WhiB7 may interact with SigA (and/or perhaps other sigma factors), targeting genes within its regulon, thus generating a response tailored to combat the antibiotic-induced stress. The variable -10 and -35 promoter elements may determine the levels of activation for individual promoters controlling transcription of genes in the *whiB7* regulon.

The *M. smegmatis* genome contains 5,954 regions with blocks of at least five adjacent A or T nucleotides (searched with '[AT]{5}' in DNA Pattern Search available at www.geneinfinity.org). The large number of possible WhiB7 binding sites implies additional modes of specificity would be required to target a subset of genes. Since many WhiB proteins do not encode obvious AT-hooks, other regions of the protein may be involved in DNA-binding, or targeting of specific promoters may occur via additional interactions with SigA or other transcription activators. Further experiments showed that WhiB7 was indeed a redox-sensitive transcriptional activator *in vitro*; thereby proving a direct role in transcriptional activation implied by the previous genetic studies and bioinformatics data. The *in vitro* data supports *in vivo* work showing promoter specificity requires an AT-rich sequence upstream of the *whiB7* promoter, and sensitivity of WhiB7 function to redox conditions (Figure 17). How each of WhiB7's three regions (Figure 2) contributed to its function was then investigated.

Isolation and sequencing of Wbl proteins predicted that positively charged amino acids within their C-terminal regions determine DNA-binding specificity (*56*). Mutations in equivalent

residues impair DNA-binding activities of some mycobacterial WhiB proteins as well as their functions *in vivo* (*67, 139*). My studies of WhiB7 showed that removal of its C-terminus, containing an AT-hook motif, prevented activation of *whiB7*-specific antibiotic resistance *in vivo* (Table 1). Evidence for interaction between the AT-hook and the *whiB7* promoter was provided by experiments showing that deletion of a conserved AT-rich sequence immediately upstream of the *whiB7* promoter also prevented WhiB7-mediated transcriptional activation *in vivo* (Figure 9) or *in vitro* (Figure 17). There is little information about AT-hook containing proteins in prokaryotes, but in eukaryotes the motif is found in a variety of DNA-binding regulatory proteins (*149*). The AT-hook binds the minor groove of AT-rich DNA (*108*) rather than specific sequences recognized by many other DNA-binding motifs. It is often found on proteins containing additional DNA-binding modules, suggesting that their AT hooks alter their affinity or specificity (*149*) rather than act as discreet DNA-binding modules. The *whiB7* promoter strongly resembles the consensus sequence of SigA-targeted promoters, and the proximity of the AT-hook binding motif to the -35 promoter element suggested that WhiB7 might act by stabilizing sigma factor–DNA binding (*91, 92, 137*). WhiB7 bound to SigA would add the AT-hook to the repertoire of SigA DNA-binding modules, providing additional specificity for promoters containing upstream AT-rich sequences. In essence, the AT-rich sequence recognized by WhiB7 would act as a discriminator similar to *cis*-acting promoter features that enhance sigma factor selectivity for distinct promoters (*150*).

Complementary data proved that WhiB7 bound to the C-terminus (region 4) of SigA (Figure 10). Steyn and collaborators reported that the SigA R515H mutation prevented interaction between SigA and WhiB3 (*70*) and had a decreased virulence phenotype corresponding to that of a *whiB3* mutant (*71, 93*). My data demonstrated that the SigA R515H

mutation also prevented interaction with WhiB7 and caused WhiB7-specific multi-drug susceptibility *in vivo* (Figure 10; Table 2). The fact that the SigA R515H mutant had a slightly different antibiotic sensitivity profile may indicate that R515 interacts with other proteins (including WhiB3) that have roles in intrinsic resistance. Region 4 of SigA binds a variety of transcriptional activators, generally mediated by interactions between its positively charged residues and negatively charged residues of a regulatory partner protein (*91*). I found that E63 of WhiB7 was an essential residue for WhiB7:SigA binding (Figure 10) and was required for antibiotic resistance *in vivo* (Table 1). Importantly, this glutamate, along with adjacent residues (proline and tryptophan), are conserved across WhiB7 orthologs and similar in WhiB3 (Figure 10). This implies that WhiB7 and WhiB3 bind SigA in a similar manner. While conservation of this tripeptide motif was necessary for SigA binding, the middle region (Figure 2) alone was unable to bind (Figure 10). This suggested additional sequence requirements that must be located upstream since the C-terminal DNA-binding domain was dispensable. I conclude that sequences within the N-terminal domain, encoding FeS cluster binding residues, either interact directly with SigA or are needed for proper folding of regions within the middle region that interact with SigA.

Wbl homologs contain four conserved cysteines at their N-termini that typically co-ordinate an FeS cluster. Alterations of FeS clusters, either conversion from [4Fe-4S] to [2Fe-2S], change of their redox states, or ejection of FeS clusters, are all mechanism of activation for FeS-containing transcriptional regulators (*151*). These events alter tertiary structure to either activate or restrict transcriptional activity of the protein. This versatility allows the evolution of FeS cluster-containing proteins able to respond to redox signals of different strengths. WhiB7:SigA complexes contained a near stoichiometric ratio of [2Fe-2S] clusters (Figure 12) that may

provide essential tertiary stability allowing the middle domain of WhiB7 to interact with SigA, thereby promoting transcription. Importantly, WhiB7 catalyzed run-off transcription was inactivated by oxidation with diamide at concentrations that did not affect transcription of P_{HSP60}, a standard vegetative promoter (Figure 17). Additionally, WhiB7 cysteine mutants could not be stably expressed in *E. coli* (Figure 14). Together these data strongly suggest FeS cluster binding by WhiB7 is essential to establish interaction with SigA.

Underlying their wide variety of functions, each Wbl protein may have unique partnerships with sigma factors, which may be further modulated by multiple redox states. While comparisons of redox-sensitive Wbl proteins using different genetic and biochemical assays is often challenging, conserved themes of their transcriptional regulatory activities have emerged. *Mtb* and *M. smegmatis* SigA R515H mutants are viable, suggesting that essential WhiB proteins (WhiB1 and WhiB2) do not interact with SigA in the same way as WhiB7 and WhiB3, or that they partner with other sigma factors. WhiB5 does not interact with SigA in a two-hybrid assay (*75*). By analogy to the *in vitro* run-off with WhiB7, WhiB3 probably activates promoters directly via similar, redox-sensitive interactions with SigA. However, both holo WhiB3 and the oxidized form of apo WhiB3 bind DNA with different affinities (*71*). It is still unclear in which state WhiB3 might promote transcription. Apo WhiB1 represses transcription *in vitro* and therefore may not depend on interactions with a sigma factor (*62, 139*). Overall, it is clear that SigA binding is not a universal feature of Wbl proteins, and that individual Wbls may have unique redox-sensitive interactions with different sites within SigA or alternative sigma factors. This is supported by the observation that four of the 12 *S. coelicolor wbl* genes are located proximal to genes encoding sigma factors that may serve as their binding partners (*152*); one

plasmid-encoded Wbl protein is translationally fused to a sigma factor (*153*). Many of the questions raised by these data could be clarified by structural analysis.

With my experimentally determined constraints and the crystal structure of the SigA ortholog in *E. coli*, our collaborators were able to generate a model of WhiB7 and its interactions with SigA and DNA (Figure 19). The model of the protein complex predicted that WhiB7 has a distinct negatively charged face that complements remarkably well with the positively charged face of SigA region 4. In further support of the model, a predicted glutamate (E71) - arginine (R502) interaction was confirmed to play a role in WhiB7:SigA binding (Figure 19). Interestingly, the glutamate responsible for this additional ionic interaction is not conserved in WhiB3; evidence that other residues that are not conserved in WhiB7 and WhiB3 may determine unique interactions with SigA. This may lead to various SigA affinities that could impact WhiB7 or WhiB3 biological activity. Overall, the model of WhiB7:SigA interaction predicts that WhiB7's AT-hook is in both the proper orientation and distance for DNA-binding, allowing it to trigger transcriptional activation. Future biochemical and genetic dissection of WhiB7:SigA affinity will provide additional insight into how WhiB7 promotes transcription. Importantly, the 3D model may serve as a platform for the rational design of small molecule inhibitors to inhibit WhiB7-mediated antibiotic resistance.

In summary, this work has defined three distinct WhiB7 domains that function interactively to form a redox-sensitive transcriptional activator of intrinsic antibiotic resistance genes. The FeS cluster binding domain likely stabilizes the tertiary structure of the holo-protein, allowing the middle region to bind SigA. The AT-hook of WhiB7 allows the RNA polymerase complex to target and specifically increase the expression of a family of promoters (the WhiB7 regulon) that contain an AT-rich sequence shortly upstream of their -35 promoter element. By

analogy to genetic studies, chemical inhibition of WhiB7's AT-hook:DNA or WhiB7:SigA interaction would prevent WhiB7 function and lead to multi-drug susceptibility. The fact that WhiB7 and WhiB3 bind to the same region of SigA to target genes in their respective regulons suggests that an inhibitor could prevent binding of both WhiB7 and WhiB3, thereby increasing susceptibility to diverse antibiotics as well as decreasing virulence. The C-terminal 33 amino acids of *Mtb* SigA are highly conserved across Actinobacteria, indicating that the molecular mechanism of WhiB7 and WhiB3 action may also be conserved. Therefore, inhibitors of WhiB7 or WhiB3 interactions with SigA could likely be applied to pathogens in related genera including *Corynebacterium* and *Nocardia*. Future characterization of these important proteins will not only provide strategies to understand intrinsic drug resistance, but also generate important insights into how Actinobacteria integrate their physiology, division, and differentiation programs.

3 Investigating the mechanism of *whiB7* induction

3.1 Information about collaborators

I thank Dr. Gaye Sweet for assembling the Sweet library of antibiotics and Quinn Parker for assembling the CID list of the library for structure clustering. Charles Howes generated Figure 21. I thank Dr. Steven Hallam for the use of the Varioskan and RT-qPCR machine, and Keith Mewis for technical support with the Varioskan. Dr. Santiago Ramón-García in collaboration with Dr. Anaximandro Gómez-Velasco (supervised by Dr. Yossef Av-Gay) designed, performed, analysed and wrote the methods for the mycothiol determination.

3.2 Introduction

Our current understanding of how WhiB7 responds to a diverse repertoire of inducers and then activates transcription of a variety of intrinsic resistance genes has emerged primarily from studies of *whiB7*'s autoregulated promoter. Transcriptional responses to stress are typically mediated by specialized sigma factors that activate general or stress-specific responses in other bacteria. However, the *whiB7* promoter motifs, conserved upstream of all representative homologs, strongly suggest that *whiB7* is transcribed by the primary vegetative bacterial sigma factor (SigA; Section 2.3). WhiB7:SigA interaction would adapt SigA to react to WhiB-specific metabolic stress signals without the participation of specialized sigma factors

Antibiotics exert diverse secondary effects that might provide signals of metabolic distress. These global changes of gene expression can help predict an antibiotic's mode of action (*154*). Conversely, generating a comprehensive list of inducers for discreet antibiotic resistance systems may uncover the signals that lead to their expression. Understanding the activation and

function of the global response to antibiotic exposure may provide new strategies to overcome antibiotic resistance.

Identification of small molecules inducers has been dependent on increased susceptibility in the *whiB7* KO background. Here, I use my eGFP-based *whiB7* reporter (pMS689GFP) to develop a screen for small molecule *whiB7* inducers in an attempt to identify either a common target or structure.

3.3 Comprehensive identification of small molecule *whiB7* transcriptional activators

To investigate *whiB7* transcriptional activation, a custom compound library (Sweet library) was assembled and screened using the pMS689GFP reporter system. The 591-compound library included the majority of commercially available antibiotics targeting synthesis of DNA, RNA, protein, cell envelope, essential metabolites, or other physiologically active compounds. Unlike other chemical libraries that are dissolved exclusively in dimethyl sulfoxide, each compound in the Sweet library was dissolved in an optimal solvent (water, dimethyl sulfoxide, ethanol, methanol, or dimethylformamide) to ensure solubility and maximize hit discovery. A semi-high throughput screen was devised to assay the library for activators of *whiB7* transcription (Figure 20). Each compound was surveyed across a broad (2,500-fold) concentration range (0.02 μM to 50 μM). Hits were identified as compounds that induced a greater than fourfold increase in fluorescence in at least two out of three trials. In total, 86 *whiB7* activators were identified. The reliability of the screen was validated by RT-qPCR analysis of 23 representative hits confirming that all induced *whiB7* transcription, while four non-hits did not.

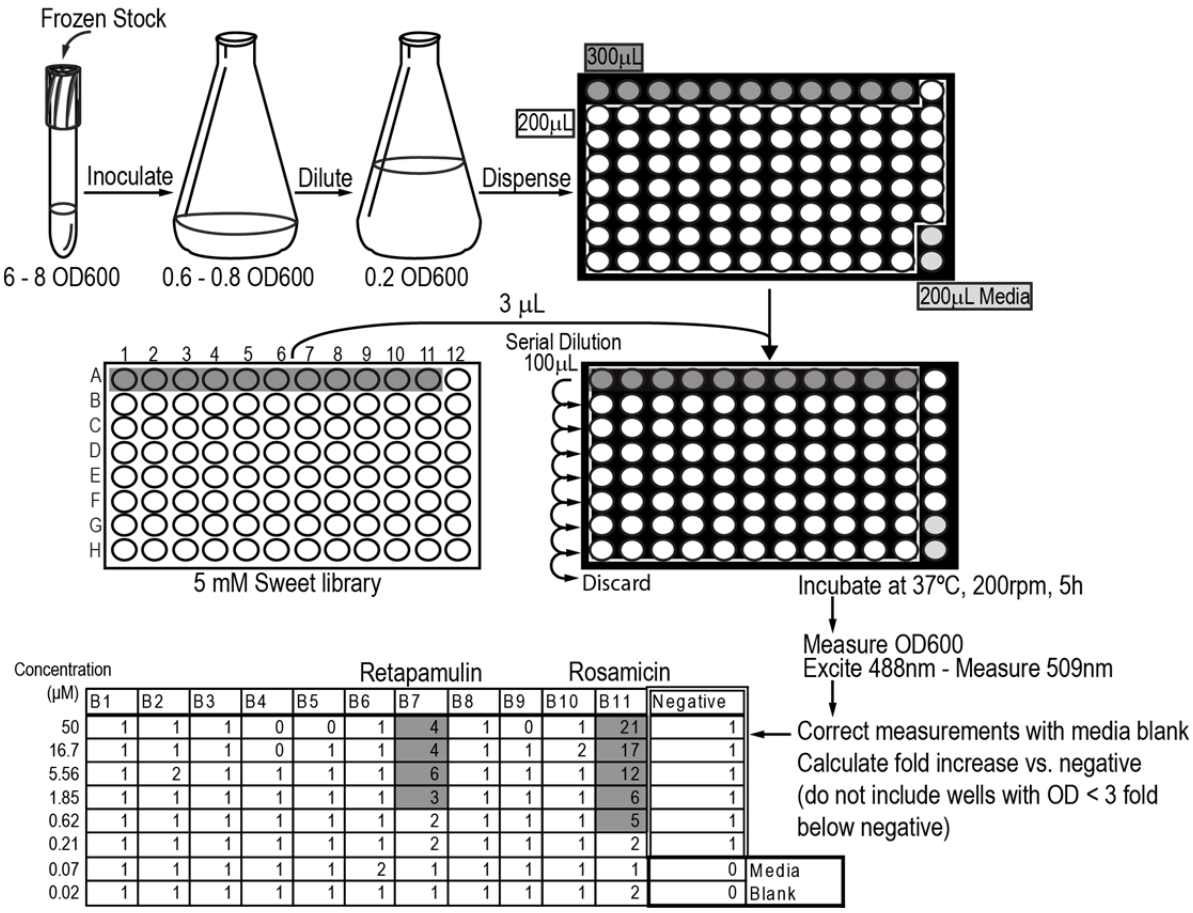

Concentration (µM)	B1	B2	B3	B4	B5	B6	B7	B8	B9	B10	B11	Negative	
							Retapamulin				Rosamicin		
50	1	1	1	0	0	1	4	1	0	1	21	1	
16.7	1	1	1	0	1	1	4	1	1	2	17	1	
5.56	1	2	1	1	1	1	6	1	1	1	12	1	
1.85	1	1	1	1	1	1	3	1	1	1	6	1	
0.62	1	1	1	1	1	1	2	1	1	1	5	1	
0.21	1	1	1	1	1	1	2	1	1	1	2	1	
0.07	1	1	1	1	1	2	1	1	1	1	1	0	Media
0.02	1	1	1	1	1	1	1	1	1	1	2	0	Blank

Figure 20. A flow chart of the eGFP-based *whiB7* promoter activity assay. The pMS689GFP reporter strain was inoculated into 3 mL of kanamycin-containing media and grown to stationary phase. The culture was diluted into fresh antibiotic-free media and grown to early exponential phase. The OD_{600} was standardized to 0.2 and the culture dispensed into a clear bottom, black 96-well plate that prevented light transmission between wells. Compounds (at 5 mM) were transferred from the Sweet library to the black plate and serially diluted. The plate was incubated for 5 hours and fluorescence was then measured. Fold increase in fluorescence was calculated and analyzed for activator compounds. Because eGFP continued to fluoresce in cells lysed by antibiotic treatment, wells with an OD_{600} less than one third of the untreated wells were disregarded (set as '0'). A sample plate is shown with retapamulin and rosamicin identified as activators. Note that the varied solvents used within the antibiotic library (water, dimethyl sulfoxide, ethanol, methanol, or dimethylformamide) did not induce fluorescence.

Structure clustering analyses (http://pubchem.ncbi.nlm.nih.gov/assay/assay.cgi?p=clustering) allowed visualization of potential similarities in the chemical structures of *whiB7* activators (Figure 21). Compounds with statistically similar structure, suggesting similar bioactivities, are

defined by a Tanimoto score greater than 0.7 (*155*). The cluster analysis identified groups of active compounds having similar structures (including macrolides, aminoglycosides, fluoroquinolones and tetracyclines) but showed activators were dispersed throughout the library structures. Analysis of only *whiB7* activators (Figure 22) showed they fall within 24 unique structural clades. Therefore, *whiB7* transcriptional activation is not due to a common structural motif of the compounds.

The structural diversity of the identified activators was also reflected in the diversity of their documented targets. Half of the identified *whiB7* activators including macrolides, tetracyclines, lincosamides, and aminoglycosides inhibited protein synthesis by targeting different sites within the 50S or the 30S subunits of the ribosome (*156*). The second major target was DNA replication which was inhibited by fluoroquinolones (*157*) and DNA intercalators including netropsin (*158*), nogalamycin (*159*), and phleomycin (*160*). Other potent activators (including acivicin, dequalinium, beauvericin, and A23187) are known for their pleiotropic effects on cell metabolism (*161-164*). These data show that induction of *whiB7* transcription does not result from direct inhibition of a single target or function, and implies a common, downstream effect of the activators on metabolism. Curiously, cell wall biosynthesis inhibitors, including the extended family of β-lactams, did not induce transcription.

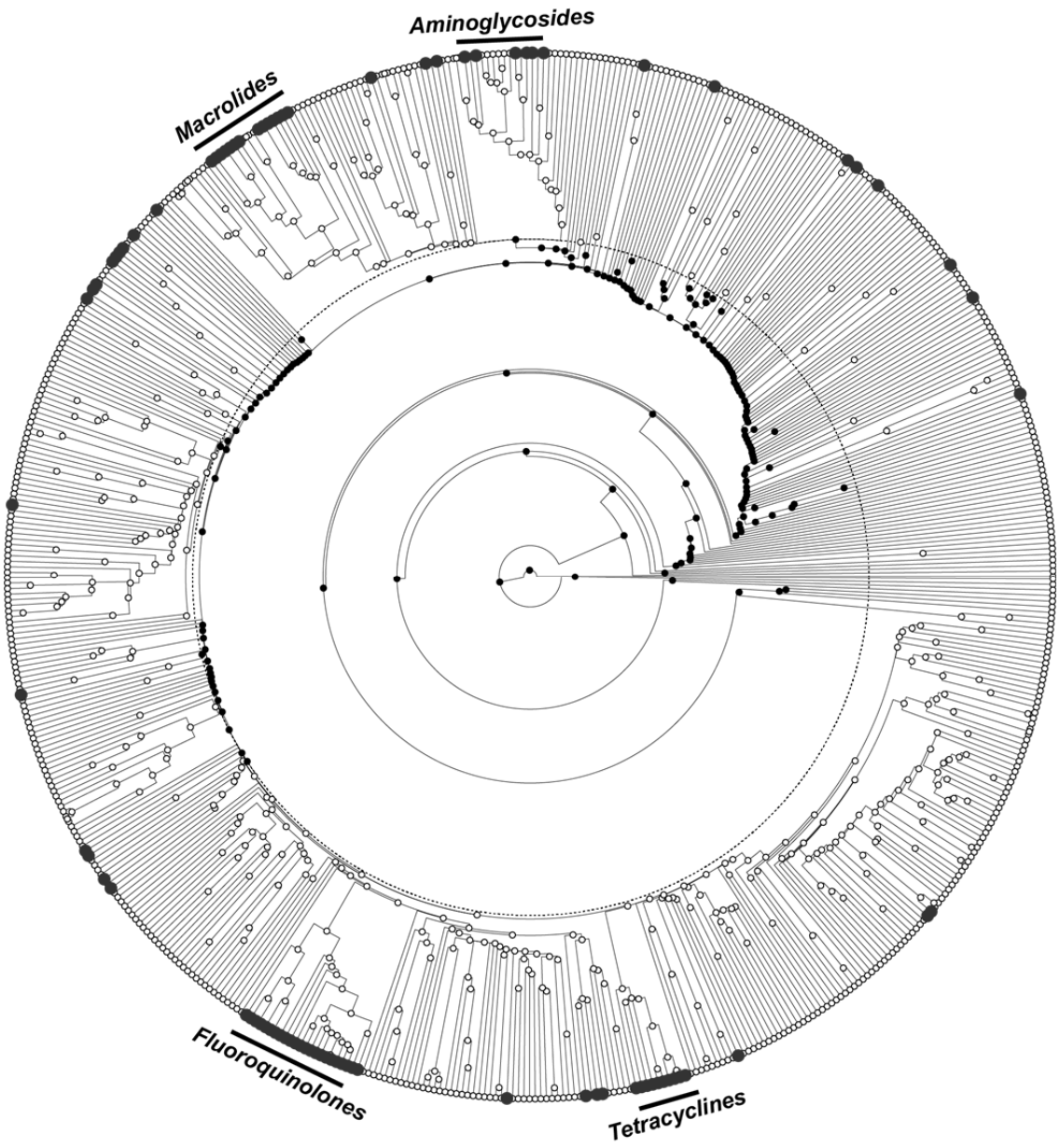

Figure 21. Comparison of structural similarity of compounds within the Sweet Library. The entire Sweet library was grouped using factors that reflect chemical structure by the Tanimoto structural clustering algorithm (compounds that induce *whiB7* expression are shown as large grey dots). The analysis is presented as a tree similar to those used to compare gene or protein homologies. It allows visualization of the structural heterogeneity. Branches that occur within the dashed circle are structurally dissimilar (Tanimoto < 0.7; black nodes) and are likely to have different bioactivities. Several larger groups of compounds that induce *whiB7* expression are indicated.

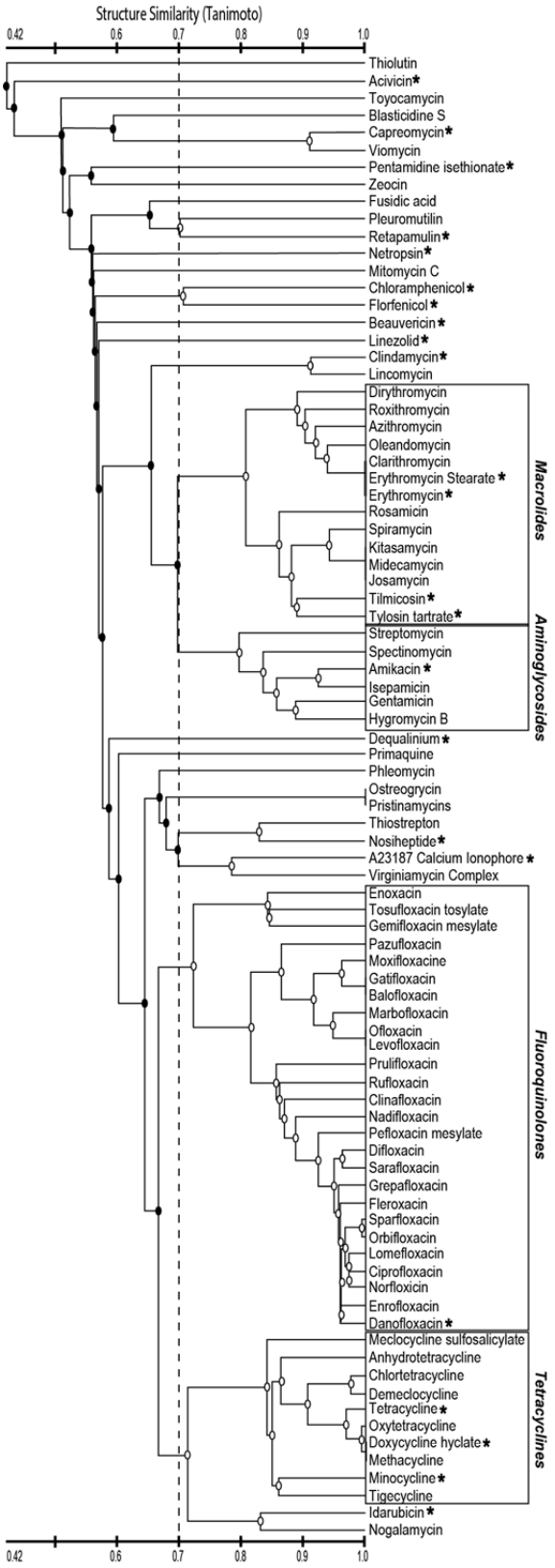

Figure 22. Structural comparison of identified *whiB7* promoter inducers. Identified activators were clustered according to chemical structure similarity. Nodes not considered structurally similar (<0.7 Tanimoto) are solid black. Numerous activators that clustered within distinctive structural classes are highlighted. Activators confirmed by RT-qPCR are indicated by a star (*).

3.4 Investigating unique themes as identified by the inducer screen

3.4.1 The dependence of *whiB7* activation on antibiotic structure

The results from the *whiB7* inducer screen indicate that neither a common antibiotic structure nor a primary target of inhibition predicts *whiB7* transcriptional activation. To provide further evidence that direct recognition of antibiotic structure was not needed for *whiB7* activation, the *Mtb* ribosomal methyltransferase (encoded by *ermMT*), that confers macrolide resistance by preventing interaction between macrolide and its ribosomal target (*121*), was constitutively expressed from the HSP60 promoter in *M. smegmatis* (*ermMT* OE).

If the *whiB7* promoter was induced in response to macrolide structure, independent of translation inhibitory effects, the level of pMS689GFP activation would be the same in wild type and in the *ermMT* OE strain. Alternatively, if *whiB7* transcription responded to the stress generated by toxicity resulting from macrolide-ribosome interactions, macrolides would elicit reduced *whiB7* activation in the resistant strain. When *M. smegmatis ermMT* OE/ pMS689GFP was exposed to various macrolides (erythromycin, dirithromycin, roxithromycin, or azithromycin) at concentrations that activated pMS689GFP in the wild type background, the level of induced fluorescence was ~fivefold lower (Figure 23). The level of activation by doxycycline, an antibiotic whose activity is unaffected by ErmMT, was unchanged. This clearly demonstrates that *whiB7* response is due to toxic macrolide-ribosome interaction and not macrolide structure.

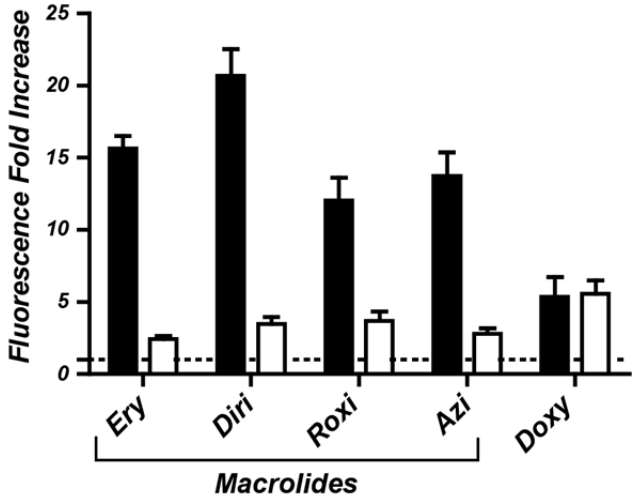

Figure 23. The *whiB7* promoter response to macrolides in wild type and macrolide-resistant *M. smegmatis*. *M. smegmatis* wild type (black) and *ermMT* OE (white; both containing pMS689GFP) were treated with 1.85 μM erythromycin (Ery), 0.62 μM dirithromycin (Diri), 0.62 μM roxithromycin (Roxi), 0.62 μM azithromycin (Azi), and 0.069 μM doxycycline (Doxy) for 5 hours and the fluorescence compared to untreated cultures. All drugs were pretested to define their most effective concentrations for *whiB7* induction in *M. smegmatis* wild type. Values plotted are the mean ± SEM of three biologically independent experiments.

3.4.2 *whiB7* activation generates a non-specific resistance state

The broad range of *whiB7* inducers implies that WhiB7-mediated resistance is not tailored to specific activators, but that WhiB7 generates a 'one-size fits all' global resistance response. Interestingly, several activators were not within the *whiB7* sensitivity spectrum. For example, while dequalinium, linezolid and danofloxacin, all induced *whiB7* expression, the *whiB7* KO mutant was not more sensitive to these compounds (Table 4).

Table 4. Evaluating *whiB7* transcriptional activators for WhiB7-mediated resistance

Compound	MIC (μM)[a]		Fold increase in susceptibility	Fold increase[b] of *whiB7* mRNA (treatment concentration in μM)[c]
	wild type	*whiB7* KO		
erythromycin stearate	32	2	16	320 (1)
retapamulin	100	6.25	16	660 (50)
capreomycin	3	1.5	2	24 (1.9)
tilmicosin	1.5	0.75	2	47 (1.85)
doxycycline hyclate	0.5	0.25	2	1900 (0.21)
amikacin	1	1-0.5	1-2	100 (16.7)
dequalinium	0.78	0.78	1	40 (1.85)
linezolid	0.375	0.375	1	140 (1.9)
danofloxacin	0.75	0.75	1	31 (16.7)
acivicin	>800	>800	-	65 (50)
A23187	>25	>25	-	590 (5.56)
erythromycin	16-32	nd	-	94 (1)
isoniazid	116-232	nd	-	0.3 (50)

[a]MICs were determined in three biologically independent samples.

[b]Fold increase in mRNA (ratio of treated/ untreated) was determined from a sample analyzed in duplicate after 3 hours of induction (concentration shown in brackets).

[c]Concentrations correspond to the highest fold increase of pMS689GFP fluorescence in the chemical screen.

nd = not determined

This further strengthened the argument that WhiB7-mediated resistance is in response to a common, downstream stress generated by the inducers leading to a broad-spectrum resistance response, rather than the more classical one drug/one resistance system type of response. By this logic, any *whiB7* inducer should generate a cross-resistance state.

To investigate this hypothesis I used a hyper-macrolide resistance phenomenon in mycobacteria. A previous study had demonstrated that treatment of *M. smegmatis* with sub-inhibitory concentrations of macrolides greatly increased resistance to these drugs in an *erm(38)* dependent manner (the *M. smegmatis ermMT* ortholog; *MSMEG_1646*) (*122*). As *erm(38)* expression, like *ermMT*, was thought to be controlled by WhiB7, work in our lab confirmed that macrolide pre-treatment increased resistance to macrolides in a *whiB7*-dependent manner (*137*), but not to other non-macrolide WhiB7-specific antibiotics. My hypothesis was that if WhiB7 up-regulates *erm(38)* in response to macrolides, which are *whiB7*-inducers, this would occur with

any *whiB7* inducers. Therefore, a *whiB7* response to any activator compound or metabolic signal should similarly increase macrolide resistance. The data demonstrated that pre-treatment with acivicin, a non-macrolide *whiB7* activator, resulted in increased resistance to macrolides (roxithromycin and clarithromycin; Table 5). This shows that *whiB7* induction activates the entire WhiB7-controlled regulon leading to a cross-resistance state regardless of inducer structure, target, or the ability to generate resistance.

Table 5. Effect of pre-treatment of *M. smegmatis* with sub-inhibitory concentration of acivicin on macrolide resistance

	[a]MIC (μg/mL)		
Antibiotic	Untreated	[b]Pre-treated	[c]Fold
clarithromycin	2	8	4
roxithromycin	8	32	4

[a]MICs were assayed over a range of twofold serially diluted drugs.

[b]Early exponential cells (~0.3 OD_{600}) were incubated in the presence of 100μM acivicin for 6 hours. Cultures were then diluted to 0.005 OD_{600} and MIC determinations carried out against the listed antibiotics.

[c]Fold increase in resistance as compared to the respective MIC of non-treated *M. smegmatis* mc^2155 cells

3.4.3 The dependence of *whiB7* activation on amino acid metabolism and redox balance

The observation that compounds targeting cell wall synthesis do not induce *whiB7* transcription argues against cell wall defects as a trigger of *whiB7* transcription. Although the effects of antibiotics were classically perceived to reflect inhibition of a single target, they are now known to have additional, far reaching consequences on gene expression and cell metabolism. One such example is the *whiB7* inducer acivicin. Acivicin is a gamma-glutamyl transferase inhibitor triggering a stress response described as "metabolic mayhem" in *E. coli* (*163*). This suggests that perturbations in amino acid metabolism may be a root cause of *whiB7* induction. Here, I used

ideas generated by unique *whiB7* inducers to narrow down the contribution of cell physiology to WhiB7-mediated resistance.

To test the dependence of *whiB7* induction on amino acids, glutamate, the only amino acid in standard 7H9 medium, was replaced with glutamine, aspartate, asparagine, arginine, or histidine, and cultures were treated with erythromycin. As summarized in Figure 24, levels of *whiB7* induction were increased in cultures grown in the presence of asparagine and, to a lesser extent, glutamine. This suggests that amino acid metabolism does contribute to the WhiB7 resistance pathway.

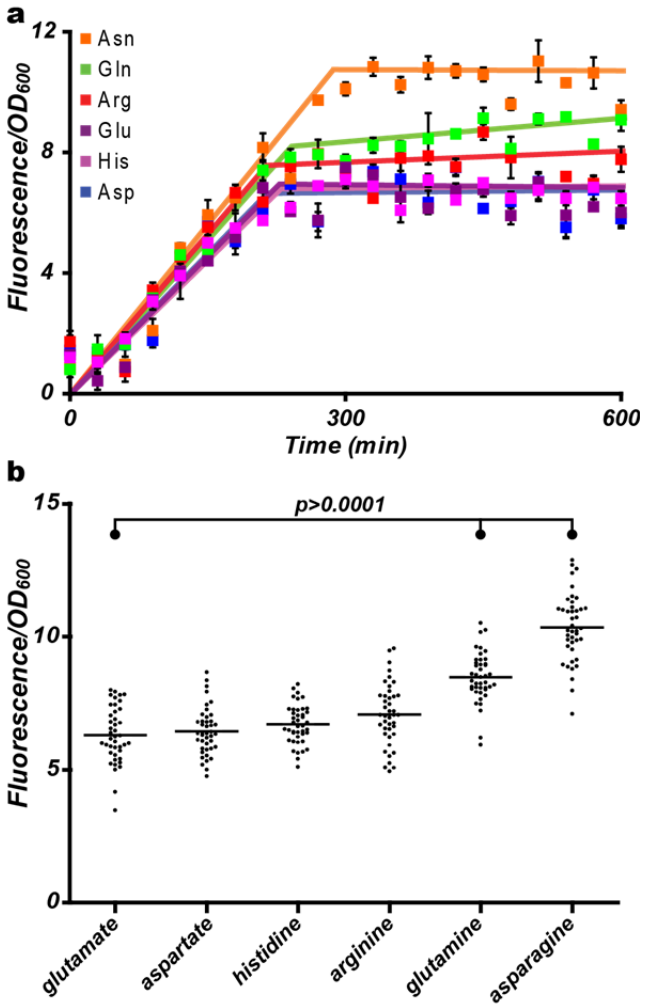

Figure 24. Strength of *whiB7* promoter activation in response to altered amino acid composition in 7H9. (a) *M. smegmatis* pMS689GFP cultured in 7H9 (- glutamate) supplemented with aspartate, asparagine, arginine, glutamine, glutamate or histidine were treated with 1 µM erythromycin. Cultures grew at similar rates in all of these media with no amino acid-dependent effects on fluorescence under non-inducing conditions (data not shown). The fluorescence signal standardized to OD_{600} is plotted as the mean ± SEM with the trend highlighted by coloured lines. **(b)** Values from '**a**' at the peak fluorescence (after 410 min) of the three biological replicates were plotted. The unpaired t-test at a 99 % confidence shows the level of induction in asparagine and glutamine was significantly higher compared to glutamate.

In vitro studies show that WhiB proteins, including WhiB7, have O_2-sensitive FeS clusters *(61, 71)* that may affect their abilities to modulate transcription (*62*). My results indicated that loading of an FeS cluster is essential for WhiB7 function. Both purified WhiB7 and a WhiB7:SigA complex contained FeS clusters and, importantly, WhiB7 which had lost its FeS cluster through oxidation did not promote transcription *in vitro*. As WhiB7 regulates its own promoter (Chapter 2), experiments were carried out to explore the hypothesis that oxidizing or reducing reagents (diamide or DTT) might affect *whiB7* promoter activity *in vivo*.

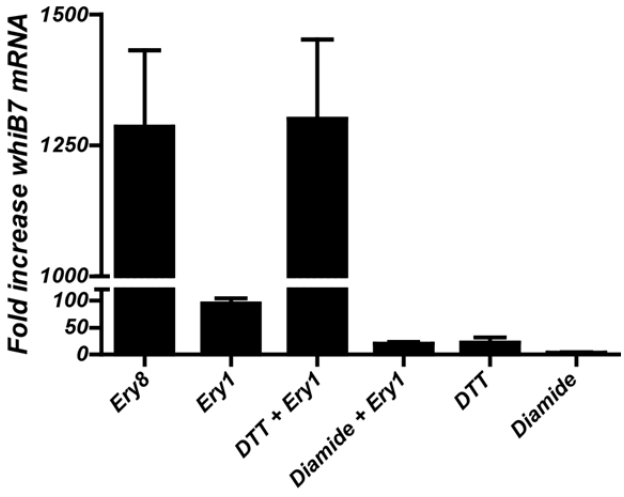

Figure 25. *whiB7* promoter activation under altered intracellular redox conditions. Increase of *whiB7* mRNA in cultures treated with 8 μM erythromycin (Ery8), 1 μM erythromycin (Ery1), 1 μM erythromycin under reducing conditions (10 mM DTT + Ery1), 1 μM erythromycin under oxidizing conditions (Diamide (5 mM) + Ery1), reducing conditions (DTT (10 mM)) and oxidizing conditions (Diamide (5 mM)) relative to a non-treated control. Results plotted are the mean ± SEM of duplicate measurements and representative of three experiments.

In the absence of erythromycin, the thiol reductant DTT moderately induced expression (Figure 25). Treatment with DTT in combination with a low dose of erythromycin generated a strong, synergistic (~1,300-fold) increase in mRNA levels (Figure 25). Conversely, the thiol oxidant diamide generated a negligible increase in *whiB7* mRNA and decreased the level of

induction by erythromycin approximately fivefold (Figure 25). These data indicate that a reducing intracellular state favors *whiB7* transcriptional activation. This provided further evidence that *whiB7* activation is intimately linked with cell metabolism and promoted by a reducing environment.

Table 6. Levels of reduced and oxidized mycothiol in *M. smegmatis* and its *whiB7* KO derivative

		Strain	
Treatment	[A]Mycothiol	wild type	*whiB7* KO
Untreated	MSH	54 ± 4	4.4 ± 2
	MSSM	0.32 ± 0.05	0.15 ± 0.09
	MSH+MSSM	54.3 ± 4.1	4.6 ± 2.1
[B]Erythromycin	MSH	60 ± 10	3.7 ± 2
	MSSM	0.002 ± 0.0003	0.19 ± 0.07
	MSH+MSSM	60 ± 10	3.9 ± 2.1

[A]Values expressed as nmoles/10^9 cells, represent the mean of three independent quantifications ± standard deviation.
[B]Erythromycin treatment was for 1 h at 256 µg/mL

In mycobacteria, the ratio between MSH and MSSM serves as an indicator of intracellular redox potential, with a basal balance of about 200:1 (MSH:MSSM) in *M. smegmatis* (*165*). Because WhiB7 activity responded to redox modulation, our lab in collaboration with Dr. Av-Gay's lab investigated the effect of the *whiB7* mutation as well as antibiotic treatment on mycothiol. After treatment with erythromycin, total mycothiol levels (MSM+MSSM) were relatively unchanged in wild type cells or the *whiB7* KO background (Table 6). Interestingly, without an antibiotic inducer, the *whiB7* KO contained one tenth the amount of MSH and half as much MSSM than the wild type (Table 6), reflecting in a ~fivefold decrease in MSH:MSSM (Figure 26). Importantly, erythromycin treatment virtually eliminated detectable MSSM in wild type cells, but had no effect on levels in the *whiB7* KO (Table 6). Overall, erythromycin treatment resulted in a ~180-fold MSH:MSSM increase in wild type cells indicating a hyper-reduced environment (Figure 26). As WhiB7 activity is increased under reducing conditions

(Figure 25) this implies that a part of WhiB7's role is to generate an environment promoting its own function in the presence of antibiotics.

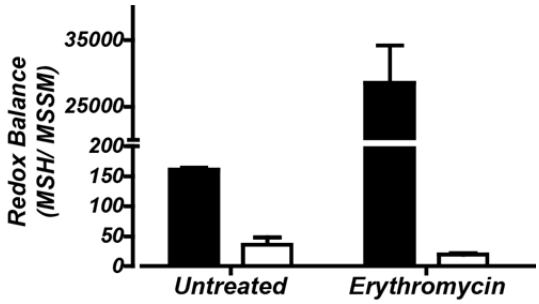

Figure 26. Redox balance changes upon erythromycin treatment in *M. smegmatis* wild type and *whiB7* KO strains. The redox balance (MSH:MSSM) was calculated from mycothiol levels (Table 6) within untreated or 256 μg/mL erythromycin-treated *M. smegmatis* wild type (black) or *whiB7* KO strains (white). Values are the mean ± SEM.

To determine whether the reduced MSH:MSSM ratio in the *whiB7* KO or the increased MSH:MSSM ratio generated by treatment with erythromycin reflected broader effects on redox metabolism, the levels of reduced (NADH) and oxidized (NAD^+) nicotinamide adenine dinucleotide were quantified. During exponential growth the *whiB7* KO strains contained lower levels (40% decreased) of NADH compared to wild type (Figure 27a). Upon erythromycin treatment, the levels of both NADH and NAD^+ increased in both strains. The increase was more pronounced in the *whiB7* KO; after 2 hours of erythromycin treatment NADH levels increased ~threefold and NAD^+ levels ~twofold, while the increases in wild type were ~1.6 and ~1.2-fold, respectively (Figure 27a). The NADH:NAD^+ ratio was ~1.6-fold lower in the *whiB7* KO relative to wild type in exponentially growing cultures, and the ratio in both strains increased after erythromycin treatment (~1.3 and ~1.7-fold after two hours in the wild type and *whiB7* KO; Figure 27b). These differences are not as drastic, suggesting that WhiB7-mediated, antibiotic-

induced changes in redox metabolism are mediated primarily through mycothiol rather than a broader effect on cellular redox balance.

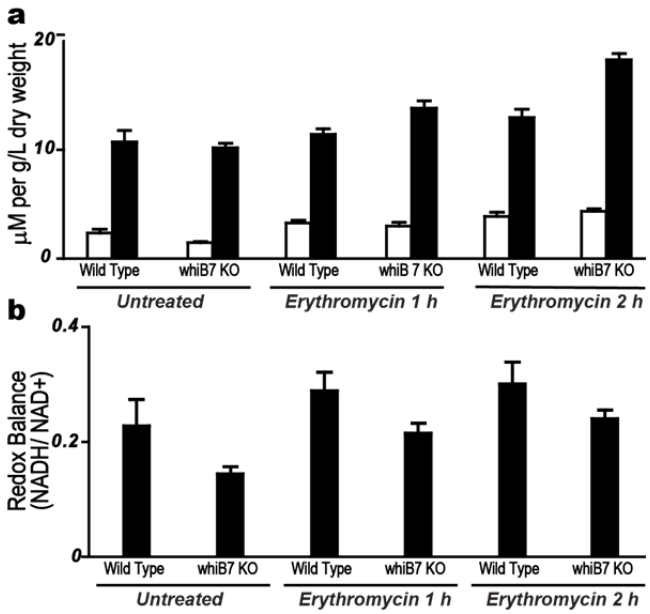

Figure 27. NADH and NAD$^+$ levels upon erythromycin treatment of *M. smegmatis* wild type and *whiB7* KO strains. (a) NADH (white) and NAD$^+$ (black) were quantified in *M. smegmatis* wild type or *whiB7* KO. Cultures were either untreated or treated for 1 or 2 hours with 256 µg/mL erythromycin. Results are plotted as the mean ± SEM of three biologically independent experiments. **(b)** The redox balance (NADH/NAD$^+$) was calculated from levels plotted in 'a'.

3.5 Discussion

To better understand factors that affect the intrinsic resistance of mycobacteria to antibiotics, I identified the spectrum of inducers that activate *whiB7* transcription using an eGFP reporter system. The chemical screens and investigations of redox metabolism provided new insights into the biological activation of *whiB7* expression. Results suggest that inducers that inhibit diverse cellular targets may ultimately shift the intracellular conditions to a more reducing environment,

which in turn leads to an increase in the activity of WhiB7 to activate transcription of its intrinsic antibiotic resistance regulon.

Identification of compounds that activate *whiB7* transcription has been limited by a lack of effective tools to monitor *whiB7* promoter activity. Previously, activators were identified by falling within the sensitivity profile of the *whiB7* KO (*55*), microarray studies (*166*), or by RT-PCR analysis of a limited set of stress conditions (*69*). Here, I established an effective and reliable assay to screen compounds for *whiB7* promoter activation (Figure 20). The screen included a broad concentration range (2,500-fold) for all antibiotics allowing it to identify activation by subinhibitory, inhibitory, and cidal treatments. The screen revealed that the *whiB7* promoter was induced by a wide variety of compounds (Figure 22) at concentrations much lower than their MICs (Table 4). Importantly, the screen was able to show that the ability of WhiB7 to mediate resistance was not required for *whiB7* induction (Table 4). Many *whiB7* transcriptional activators perturb respiration, redox balance, or transmembrane ion flux. One of the most intriguing inducers was the glutamine analog acivicin, an inhibitor of glutamine amidotransferases. In *M. smegmatis* cultures, acivicin did not inhibit growth at the highest concentration tested (800 μM). The fact that it substantially increased *whiB7* transcription even at sixteenfold lower concentrations (50 μM; Table 4) clearly illustrated the concept that activation was due to a drug-induced metabolic signal. In fact, growth of *M. smegmatis* in the presence of various amino acids determined the strength of *whiB7* induction (Figure 24). Exactly how amino acid metabolism contributes to WhiB7-mediate resistance remains unknown, but Morris *et al.* (*55*) identified two putative aspartate aminotransferases as being either up-regulated (*aspC*) or down-regulated (*aspB*) upon antibiotic treatment in a *whiB7*-dependent manner.

Overall, this provides further evidence that amino acid metabolism may play a key role in WhiB7-mediated resistance.

The observation that not all toxic compounds induced *whiB7,* throughout a range of growth inhibitory, non-inhibitory, or toxic concentrations, demonstrated that the signal was not a common feature associated with cell death. Active compounds apparently induce a unique metabolic stress signal that activates *whiB7*. In fact, *whiB7* inducers were enriched for compounds that inhibit protein biosynthesis, demonstrated by a dose-dependent effect on ribosomes by macrolides (Figure 23). Insights into specificity were also provided by the observation that none of the 50+ cell wall targeting compounds in the Sweet library induced *whiB7* expression. Transcriptomic studies have shown that antibiotics with different modes of action, such as inhibitors of cell wall biosynthesis or protein biosynthesis, generate discreet expression patterns associated with regulons responding to distinctive stress signals (*167*). These patterns can be used to predict the mode of action of new antibiotics (*154*). Importantly, a *whiB7* response to any activator results in the activation of the entire WhiB7 resistome leading to cross-resistance (Table 5). The clinical relevance of this induced intrinsic resistance phenomenon has recently been demonstrated in multi-drug resistant strains of *Mtb.* Pre-treatment with rifampicin induced expression of multiple efflux pumps leading to increased resistance to ofloxacin, a quinolone (*120*). Rifampicin pre-treatment of these strains increased expression of *whiB7*, and presumably a multidrug transporter that it activates (*tap*, Rv1258c) contributing to the resistance state (*55, 120*). These observations support a clinically important concept; exposure to *whiB7* inducers activates expression of genes and a metabolic state that provides cross-resistance to diverse drugs.

During investigation into alterations in cell metabolism that may lead to, or modulate, WhiB7-mediated resistance, I discovered that the WhiB7 response was not only altered by amino acid metabolism but also by redox balance (Figure 25). DTT (providing reducing potential) activated a low level of *whiB7* transcription, but combining these reducing conditions with a low concentration of erythromycin synergistically increased *whiB7* transcription, mimicking treatment by a much higher concentration of erythromycin. In contrast, oxidizing conditions (diamide) decreased induction. Importantly, the reducing conditions were mirrored in the mycothiol levels upon erythromycin treatment in a *whiB7* dependent manner (Figure 26). This implied that the *whiB7* response to macrolides (and other drugs) is dependent on a metabolic shift to increases in cytoplasmic reducing potential.

Analyses of MSH, MSSH, and their ratio (MSH:MSSM) revealed differences between wild type and *whiB7* KO strain, both untreated and in response to erythromycin (Table 6). These studies revealed that *whiB7* participates in maintaining a reduced cytoplasmic (MSH:MSSM) environment under normal growth conditions and directly or indirectly controls the concentration of mycothiol. Furthermore, the fact that erythromycin treatment of the wild type strain resulted in a *whiB7*-dependent decrease in the pool of oxidized mycothiol suggested that WhiB7 had an active role in regulating MSSM reduction. By analogy to other WhiB proteins, the activity of WhiB7 as a transcriptional activator may respond to such changes in the redox environment. In support of this model, DTT studies indicated that a highly reduced environment potentiated induction of *whiB7* transcription (Figure 25). In contrast, erythromycin treatment of the *whiB7* KO did not affect levels of oxidized mycothiol or its MSH:MSSM ratio (Figure 26). By comparison, changes in NADH and NAD^+ were relatively small, suggesting that the *whiB7*-dependent mycothiol redox changes were an initial response to erythromycin, reflected by slower

changes in NADH/NAD^+ pools. While increased NADH and NAD^+ pools might be needed to provide longer term responses to erythromycin, they appear to be metabolically isolated from MSH/MSSM pools under the condition of the experiment.

It has been reported that catabolism of host fatty acids by *Mtb* within macrophages results in reductive stress caused by the accumulation of NADH/NADPH (*71, 168*). The stress is dissipated by a WhiB3-dependent shift to the production of virulence lipids (*71*), but the initial reductive burst may explain the activation of *whiB7* in the *Mtb* complex soon after infection of macrophages (*78*). Additionally, macrophages utilize glutathione as the major antioxidant for defence against *Mtb* infection (*169*). Exposure to glutathione may provide additional reductive stress to facilitate activation of *whiB7.* Finally, the observation that the *whiB7* KO strain has a more oxidized cytoplasm and lower levels of NADH rationalizes the reduced output of LuxABCDE bioluminescence (Figure 5b) which requires reducing power to generate reduced riboflavin mononucleotide (Figure 4b), an essential cofactor for the light generating reaction (*126*).

Transcriptional regulators containing redox-sensitive disulfide bridges or iron-sulfur clusters regulate critical redox responsive functions in bacteria (*170*). WhiB1, WhiB2, WhiB3, and WhiBTM4 (a bacteriophage encoded WhiB2-ortholog) proteins also interact with target promoters in a redox-sensitive manner (*62, 68, 71*). WhiB7, like all WhiB family proteins, contains four conserved cysteine residues that are able to bind a redox-sensitive FeS cluster or form disulfide bonds. By analogy to biochemical studies of WhiB1, the FeS cluster-bound WhiB7 may be an inactive form of the protein that does not bind DNA (*62*). However, my studies in Chapter 2 support the conclusion that an FeS cluster-bound WhiB7 is the active form. Removal of FeS clusters by diamide inhibited WhiB7-mediated transcriptional activation, and

WhiB7 cysteine mutants, presumably unable to bind an FeS cluster, could not be stably expressed in *E. coli*.

WhiB7's link to reducing conditions and stable binding of an FeS cluster is important for its antibiotic resistance role, and highlights the emerging theme that antibiotic-induced effects extend far beyond inhibition of single targets and resonate through cell metabolism. In mycobacteria, mycothiol, the major thiol protectant, plays a role in resistance to oxidative stress and some antibiotics (*102*). Therefore, generation of WhiB7-mediated reducing potential may provide resistance to antibiotics by promoting WhiB7 transcriptional activation of discrete resistance genes and/or metabolic systems. Previous microarray data (*55*) did not indicate *whiB7*-dependent transcriptional changes of genes in the mycothiol biosynthesis pathway, suggesting the reductive shift may be due to an another WhiB7 activity, perhaps acting as a thioredoxin or activating other thiol reductant systems (*61*). It is also important to note that over-expression of WhiB7 in *Mtb* activates its regulon in the absence of antibiotics (*55*). This implies that WhiB7 only has to be produced with an FeS cluster to function, which correlates with my *in vitro* run-off data. Once induced, expression of WhiB7 generates a resistance state that is not tailored to the inducing antibiotic. Instead it provides broad spectrum resistance reflecting a generalized metabolic shift. The transcription of different *wbl* genes is induced by a variety of different conditions *in vivo*, presumably corresponding to the different metabolic functions of the Wbl proteins.

Studies of antibiotic resistance in bacterial pathogens have traditionally focussed on genes carried by transmissible elements that provide drug resistance to pathogens. However, there is growing recognition that chromosomal genes having physiological functions can have alternative roles as antibiotic resistance genes. This new concept has important evolutionary

implications, rationalizing the recruitment and evolution of metabolic genes to serve as antibiotic resistance genes or alternatively, to provide physiological functions for genes under selective pressure as resistance genes. My studies revealed that WhiB7 is at a crossroads between physiology and antibiotic resistance with functions linked to the maintenance of balanced reducing potential as well as activation of resistance genes. Activation of *whiB7* creates a non-specific resistance state that provides cross-resistance to diverse drugs. Understanding how WhiB7 senses antibiotic-induced signals to activate intrinsic resistance genes may allow more effective uses of drug combinations (*109*) for treatment of mycobacterial diseases including tuberculosis.

4 Additional genetic elements modulating *whiB7* expression or WhiB7 function

4.1 Information about collaborators

I thank Dr. Corey Nislow, Dr. Sunita Sinha and Jennifer Chiang for helpful discussions on high-throughput sequencing and Nextera tagmentation. Dr. Sinha, supervised by Dr. Nislow, performed the MiSeq sequencing. Dr. Eric Rubin provided ΦMycoMarT7. I also thank Eric Stroczynski for his assistance in preparing several of the knock-out and constitutive expression strains.

4.2 Introduction

WhiB7 plays an essential role in the induction of its own promoter by antibiotics. However, there is also a WhiB7-independent increase in promoter activity (Figure 6b), suggesting another regulatory system. Recent studies indicate that *whiB7* repression may be post-transcriptionally regulated through its large 5'- untranslated region (5'-UTR) (*171, 172*). Analysis of the 5'-UTR of *whiB7* across representative mycobacteria reveals that the only conserved motif is a large palindrome (Figure 7a). A recent study shows that upstream of the palindrome, in the non-conserved region, is an unannotated open reading frame (*uORF)* which is transcribed from the *whiB7* promoter in *M. bovis* and *Mycobacterium marinum* when they are grown in 7H9 (*171*). The full length *whiB7* transcript, however, is not made under these conditions since the large palindrome likely acts as a Rho-independent terminator under non-inducing conditions (*171*). Importantly, single nucleotide insertions or deletions within the *uORF* in *Mtb* lead to constitutive

whiB7 expression implying removal of repression (*172*). Exactly how termination is switched off remains unclear, as discussed below. Furthermore, there are unknown metabolic contributions to WhiB7 function as highlighted by the observation that amino acid and/or redox metabolism modulate WhiB7 activity (Section 3.3.3). Together these data indicate complex regulation of *whiB7* transcription and/or WhiB7 function. Initiation of transcription could be controlled by activators or repressors. Additionally, the ability of the WhiB7 protein to regulate transcription may be controlled by the redox state of the cytoplasm. My goal was to investigate the contribution of the *uORF* to *whiB7* regulation, as well as to identify additional genetic elements contributing to WhiB7-specific antibiotic resistance.

Discoveries in bacterial genetics have largely relied on classical experimental design with selected genes being knocked out or constitutively expressed, and a phenotype observed. These types of studies have assigned the functions of many genes in several model organisms, but the rate of discovery is time-consuming. With the advent of high-throughput sequencing, many bacterial genome sequences have become available, but the function of the majority of genes remains unknown. While functions can often be predicted by sequence similarity, the increasing recognition that homologs can carry out divergent functions makes these identifications unreliable. Tn-seq, which couples next-generation sequencing with high-density transposon mutagenesis, allows for the rapid, high-throughput functional studies of genes (*173, 174*).

Identification of high-density transposon insertions has been applied to diverse bacteria. In *Caulobacter crescentus* a transposon library with insertions on average every 8 bp, allowed for high-resolution mapping of its essential genes (*175*). Such resolution also allowed for the identification of mis-annotated open reading frames, non-essential C-terminal protein segments, as well as small non-coding RNAs. Importantly, these studies can be expanded beyond essential

genes for the identification of genetic elements required for unique, niche-related adaptations that promote growth.

Identification of conditionally essential genes can provide important insights into how bacteria adapt to or respond to a change in environmental conditions. Tn-seq has been applied to numerous such studies. A few examples include identification of genes essential for a variety of functions including *Mtb* growth on cholesterol (*176*), *Haemophilus influenzae* growth in the lung (*177*), *Salmonella enterica* bile tolerance (*178*), Type VI secretion system-dependent effector and immunity proteins in *Vibrio cholerae* (*179*), and *P. aeruginosa* intrinsic aminoglycoside antibiotic resistance genes (*46*).

In this chapter, I investigate the contribution of the *uORF* to *whiB7* repression (using RT-qPCR analysis and a GFP reporter) and screen for additional contributors to the WhiB7-resistance pathway by coupling Tn-seq with antibiotic selection.

4.3 Transposon library selection identifies genetic elements potentially contributing to WhiB7-mediated resistance

4.3.1 The *uORF* region of the *whiB7* transcript is required for repression, but is unlikely to encode a functional protein

To determine whether termination of the *whB7* transcript occurs upstream of its structural gene in *M. smegmatis*, I measured transcription of the *uORF* and *whiB7* by RT-qPCR. Transcription of the *uORF* relative to that of *sigA* (the internal standard for the RT-qPCR) was 1.8 ± 0.5, indicating that transcription occurs from the *whiB7* promoter when *M. smegmatis* is grown in 7H9. The amount of *uORF* relative to *whiB7* under these conditions was 20 ± 6-fold higher,

confirming that the palindrome is an efficient early terminator of the *whiB7* transcript. After roxithromycin treatment, at 25% its MIC, the amount of *uORF* increased 62 ± 13-fold, likely reflecting WhiB7-mediated transcriptional activation. Additionally, the ratio of *uORF:whiB7* under roxithromycin treatment decreased to 2.3 ±0.7, showing that the palindrome mediated termination is significantly relaxed.

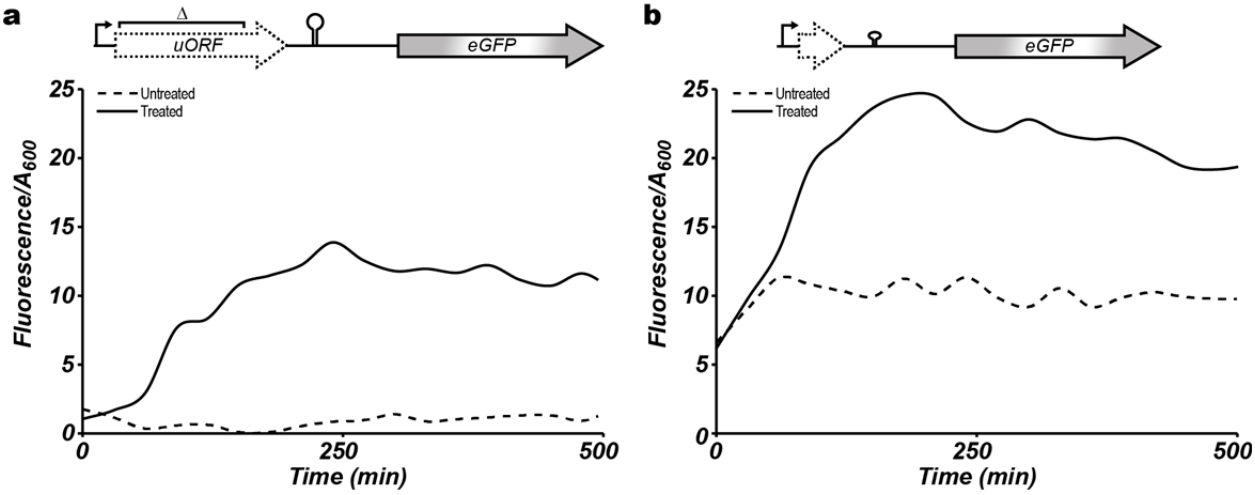

Figure 28. The role of *uORF* in repressing *whiB7*. Exponentially growing *M. smegmatis* containing **(a)** the entire *whiB7* promoter region including the *uORF* fused to *gfp* (pMS689GFP) or **(b)** with the *uORF* deleted (pORFdelGFP) was treated with 1.5 μM linezolid (solid lines) or untreated (dashes line) and fluorescence measured. Data are representative of at least 3 different transformants.

Mutation in the *uORF* led to increased *whiB7* expression in *Mtb* implying the uORF may act as a negative regulator (*172*). To determine whether the *M. smegmatis* uORF contributes to *whiB7* repression, the GFP reporter construct was modified to delete the *uORF*. While pMS689GFP, the full length *whiB7* transcription reporter, showed repression and antibiotic induction in *M. smegmatis* (Figure 28a), deletion of the *uORF* (pORFdelGFP) resulted in loss of repression, but induction was maintained (Figure 28b). Importantly, as the reporter was carried on a plasmid in wild type *M. smegmatis,* an unmodified *uORF* was present *in trans* and could not

complement the truncation. This implies that the uORF is not a functional protein, and that it is the presence of the *uORF* nucleotide sequence that is required for repression of *whiB7*.

Analysis of the 5'-UTR regions across multiple Actinobacteria identified the presence of potential uORFs (Table 7), suggesting they may be a conserved form of *whiB7* regulation. However, nucleotide sequence comparison (Blastn) of the *uORFs* to the *M. smegmatis* sequence showed no significant similarity. Additionally, protein sequence comparison (Blastp) of the uORFs to the *M. smegmatis* sequence showed poor similarity. Only a small region (aa ~60-80) of the *M. smegmatis* uORF showed similarity to *M. marinum* (E-value 0.0006), *Mtb* (E-value 0.07), and *S. coelicolor* (E-value 0.12) uORFs. No similarity was detected with the *R. jostii* RHA1 uORF. The varied lengths and lack of sequence similarity strongly imply that the uORF is not a conserved protein. This makes it unlikely that the uORF encodes a protein that represses *whiB7* transcription.

Table 7. uORF sequences across several genera

Species	uORF sequence	Length (amino acids)	% alanines
M. smegmatis	VSREMISYVNLSEV**A**V**A**GMPGFIPSVVPV**A**VSS**A**PMPHQTPEL **A**H**AA**H**AAA**GWP**AAAA**I**A**PQPKRRRT**AAA**T**A**TS**A**SVDRSPF	83	24.1
Mtb	VIDNN**A**FGVG**AAAA**VPT**A**GTPHSKNRV**AAA**TDESVERGST	40	22.5
M. marinum	MMNMNTFGVGV**AAA**VWYP**AA**RH**AA**RT**A**IP**AAA**GKHRV**AA** **A**TDSSVDRSPT	50	28
S. coelicolor	VLYLHIRGLVRPSPPRRREE**A**SPVISIKSSFIVSST**A**KMTDRS**A**V SLCMLG**A**SHSGTGLSGIR**A**VRP**AAAAAA**P**A**GLPVRERNERPT K**A**LE**AA**V**AA**QA**Q**A**Y**A**FT**A**TG**A**GFRKQTTQHHLMW**A**FRGPE PWSDP**A**	133	18
R. jostii RHA1	VVHIGSRRNGGGSEMTKYQ**A**HET**A**V**AAA**S**A**LFGMN**AA**E**AA** P**A**IVWS**AA**RRRP**AAA**VESVYRSCRGIPR	68	23.5

Note, while the average alanine content in these regions was 23.2 % residues (bold/ underlined), 18 random 133 aa translations of the *M. smegmatis* genome showed, on average, 13.1% alanine.

4.3.2 Library selection to probe genetic elements contributing to WhiB7-specific resistance

M. smegmatis was mutagenized with ΦMycoMarT7 (*180*) to generate a library of transposon mutants (~55,000 inserts as estimated by colony counts). Mutant colonies were harvested from 7H9 plates by scraping and re-suspended in 7H9 with glycerol for storage (OD_{600} of 100). The transposon library was diluted 1/10,000 in 7H9 and incubated for 2 hours before the addition of antibiotics. Cultures were grown until stationary phase and genomic DNA isolated. High throughput sequencing was used to monitor changes in the frequencies of insertion at defined sites (the transposon targets TA sequences) resulting from antibiotic treatment. The protocol is outlined in Figure 29.

Unlike the majority of other protocols that depend on random fragmentation of genomic DNA either by partial restriction digest or mechanical sheering followed by end repair and adaptor ligation, I used Illumina's Nextera tagmentation to do both steps simultaneously. Junctions on both sides of transposon insert sites were then identified by targeted PCR adapted for Illumina MiSeq sequencing. The goal was to identify regions contributing to WhiB7 expression and function; these genes, along with *whiB7*, would be essential for growth in the presence of sub-inhibitory concentrations of antibiotics (Figure 30a). In addition, insertions in downstream resistance genes controlled by WhiB7 would also be selected against, as well as non WhiB7-mediated resistance systems. To attempt to differentiate between the possible resistance systems and focus on the WhiB7 pathway, multiple WhiB7-specific antibiotics were used. The antibiotics roxithromycin, chloramphenicol and tetracycline were used at levels which inhibit the *whiB7* KO cultures (Figure 31) and therefore eliminate transposon insertions which prevented WhiB7-mediated resistance. Alternatively, an antibiotic selection using a macrolide at above-MIC treatment was also used to identify regions contributing to *whiB7* repression (Figure 30b).

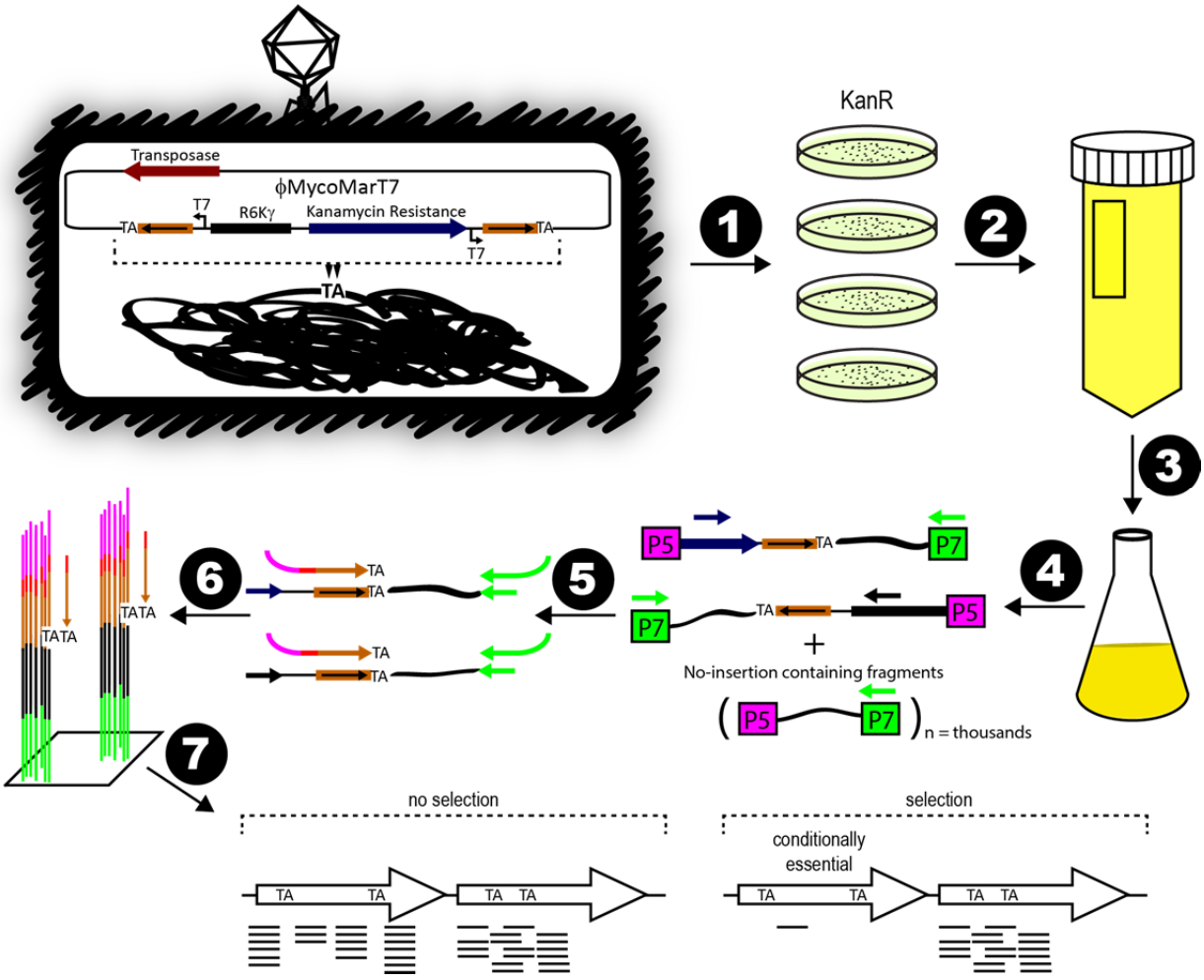

Figure 29. Flow chart of transposon insertion identification protocol. 1) The phage ΦMycoMarT7 carrying a transposase gene (red arrow) and its cognate recognition sequences flanking the transposable region was used to transduce *M. smegmatis*. The transposon contained a R6Kγ origin of replication (black box) and a kanamycin resistance gene (blue arrow) that were flanked by inverse repeats (orange boxed arrow ending in TA) which were targeted by the transposase for insertion into random TA sequences in the *M. smegmatis* genome. *M. smegmatis* which contained this insertion (transposon mutants) were selected on kanamycin-containing growth medium (KanR) under conditions (37 ºC degrees) in which the phage could no longer replicate. **2)** The transposon mutants were scraped from the plates, pooled and **3)** used to inoculate either selective or non-selective media. **4)** After growth under the selective condition (sub or super MIC of an antibiotic), genomic DNA of the culture was fragmented using the Nextera tagmentation procedure. Tagmentation produced random double stranded DNA breaks simultaneous with the insertion of a known sequence (either P5 or P7). These tagged fragments were used as a template for PCR which used a primer targeting the P7 insertion (green arrow) and either a primer targeting the kanamycin resistance gene (blue arrow) or the R6Kγ origin (black arrow). **5)** PCR products were pooled and a second round of PCR was performed using a primer targeting the P7 sequence which contained the additional sequence needed for MiSeq hybridization (hooked green arrow) and a custom primer which contained the inverse sequence (orange boxed arrow

ending in TA) with an added sequence (red line) and the P5 sequence for MiSeq hybridization (pink hook). **6)** The resulting products were sequenced using Illumina's MiSeq. **7)** Sequences corresponded to regions on either side of TA's which contained the transposon insertion. The numbers of reads for individual genes were mapped by the ESSENTIALS software (*181*). This allowed comparisons of read numbers under nonselective and selective (antibiotic presence) conditions. A high frequency of lost reads identified candidate genes which were conditionally essential in the presence of antibiotic.

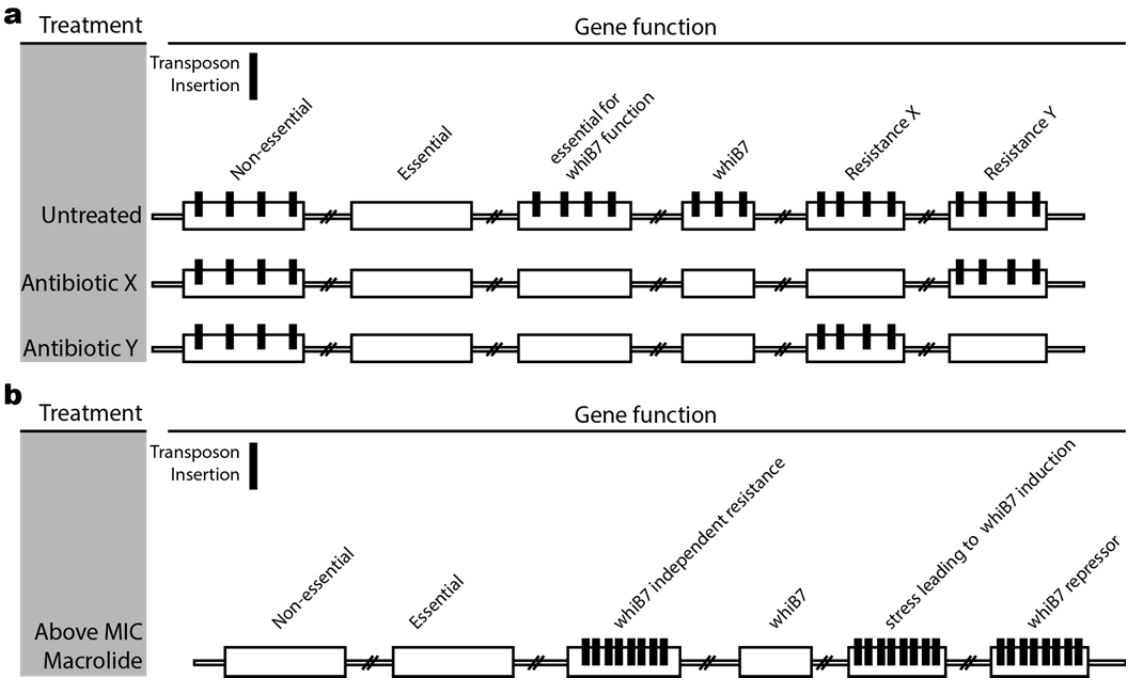

Figure 30. A cartoon representation of the transposon mutagenesis readout designed to identify genes modulating WhiB7 induction or function. (a) By comparing the profiles of sub-MIC treatments with different antibiotics to an untreated control, *whiB7* and genes essential for WhiB7 function can be identified. Downstream resistance genes that are specific for Antibiotic X or Antibiotic Y should not be essential for all conditions. **(b)** Insertions which knock-out *whiB7* repressors (i.e., pre-induce a WhiB7 response), induce a WhiB7 response, or generate alternate macrolide resistance will be selected by an above-MIC treatment with a macrolide.

As noted in Section 3.2.4, pre-induction of *whiB7* with acivicin generated an antibiotic-adapted state with an above-MIC level of resistance to macrolides. Ergo, knock-outs with *whiB7* pre-induction (ex. removal of repression) should also have an above-MIC level of resistance.

Selection was done using roxithromycin at an above-MIC concentration. Genomic DNA was isolated and transposons insertions identified. The untreated condition indicated that the library represented roughly one third coverage of the ~150,000 TA target sequences present in the *M. smegmatis* genome (~57,000 unique TA locations, corresponding to one TA site/50 bp). Of the roughly 7,000 annotated *M. smegmatis* genes, ~1,400 were not identified as disrupted in the transposon library (in the absence of antibiotics). This included ~700 previously described essential genes with an additional ~700 genes that had not been previously identified as essential. The ESSENTIALS software developed by Zomer *et al*. (*181*) was used to map sequencing read frequency to annotated *M. smegmatis* genes. Candidate genes were then analyzed using UGENE (*182*) to determine the number of unique transposon insertions and their associated read counts.

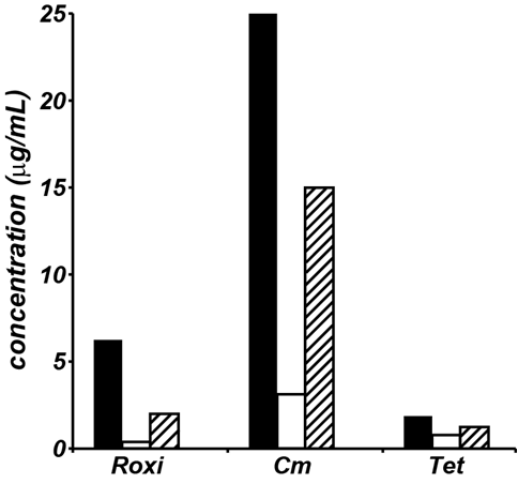

Figure 31. *whiB7* is conditionally essential upon antibiotic selection. The MIC of roxithromycin (Roxi), chloramphenicol (Cm) and tetracycline (Tet) of *M. smegmatis mc²155* (black) and a *whiB7* KO derivative (white) was determined by the resazurin assay. A concentration of each respective antibiotic (stripes) above the MIC of *whiB7* KO, but below the MIC of wild type, was chosen to generate a conditionally essential condition for *whiB7*.

4.3.3 Candidate genes contributing to WhiB7-specific resistance

The ESSENTIALS software identifies conditionally essential genes by comparing the expected number of reads (based on TA per gene, library size, and total reads) to the measured number of reads. Genes are considered essential if this ratio has an adjusted p-value of <0.05. This includes

several steps to minimize false discovery such as gene truncation (disregarding the 3' region that is likely not essential) and normalization of read data. Figure 32 plots the numbers of genes as a function of % read reduction upon antibiotic selection relative to the untreated control. The smooth curve was noticeably distorted at about 20% reads relative to untreated, perhaps reflecting enrichment for strains carrying transposons in genes needed for survival under antibiotic-selective conditions. If so, as many as 140 genes were identified by the ESSENTIALS analysis as potential intrinsic resistance genes. While ESSENTIALs analysis ranked genes based on the frequency of lost reads, it alone was not enough to identify conditionally essential genes.

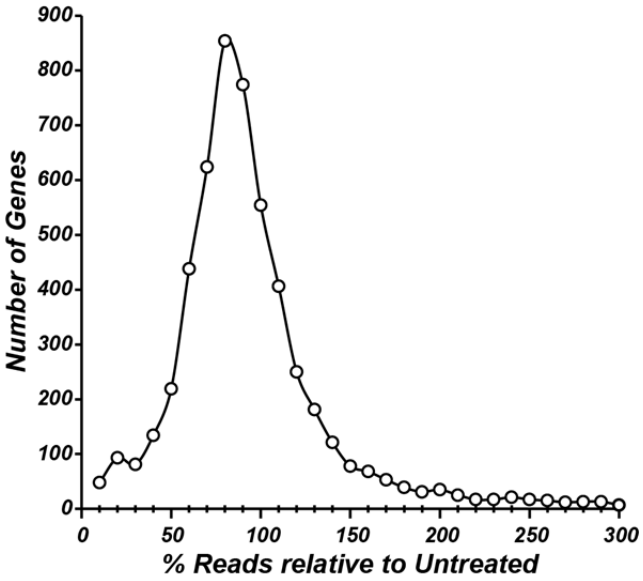

Figure 32. % Read reduction upon antibiotic selection across the *M. smegmatis* genome relative to untreated. The average reads mapped to individual *M. smegmatis* genes, as defined by ESSENTIALS analysis, after roxithromycin, chloramphenicol, or tetracycline treatment were compared to their counterparts in the untreated control. Reductions were then grouped in 10% increments. The total number of genes represents >95% of genes with associated reads.

UGENE allowed for the visualization of aligned reads mapping transposon insertion sites across the *M. smegmatis* genome. UGENE analyses revealed unanticipated ambiguities in the pool of genes identified by ESSENTIALS analyses when comparing read counts in antibiotic treated and untreated cultures. For example, *MSMEG_2370* was one of the best ESSENTIALS hits with a 95.77% reduction in read assignment, resulting in a p-value of 5.69×10^{-9}. UGENE

analysis of *MSMEG_2370* showed that these reads were distributed between the seven different TA locations in the gene. Strikingly, the frequencies of inserts in 6 of the TA insertion sites had reads of about equal value under all conditions, while 1 TA in the untreated condition had a highly disproportional abundance of reads. If that TA insertion was removed, the read content of untreated vs treated conditions was about the same, indicating that *MSMEG_2370* was likely not a conditionally essential gene.

I hypothesized that my protocol to identify TA insertions (Figure 29) may have an unpredictable bias for some insertions. Indeed, library preparation for Illumina sequencing is known to produce sequence bias based on numerous factors such as GC content or something as seemingly trivial as PCR temperature ramp speed (*183*). I reasoned that the use of two separate sets of PCRs to generate sequence-ready products might have introduced an unpredictable bias for random sequences. The initial PCR was a mixture of at least 57,000 discreet junctions with the possibility of each junction fragmented in upwards of 100 varied lengths, and a >1000-fold excess of random genomic DNA fragments. It is reasonable to assume that if an early product was accumulated, it would have a higher probability to be amplified as the cycles continued and therefore build a disproportionate abundance. This would be further amplified by the subsequent PCR reaction required to produce sequence-ready products. As each condition was fragmented separately the initial PCR templates varied. This may have led to a random distribution of abundant products for each condition. Visualizations of read abundance on a global scale using UGENE showed a random distribution of abnormally high read counts that differed between each selection condition. As a result, UGENE analysis of all potential ESSENTIALS hits was performed with the criterion that multiple insertions in the same gene must show the same trend.

It was expected that read abundance of genes conditionally essential under antibiotic treatment would be minimal. This was confirmed by analysis of known antibiotic resistance genes. For example, Erm (MSMEG_1646) is a macrolide resistance gene under WhiB7 control. Without antibiotic treatment, ESSENTIALS analysis showed *erm* contained 128 assigned reads which decreased to 1 under roxithromycin (a macrolide) treatment. UGENE analysis indicated that *erm* contained two unique insertion sites, both of which were lost under roxithromycin treatment. To ensure that the sub-MIC selection converged on WhiB7-mediated resistance, *whiB7* and its surround regions was analyzed.

Analysis of the transposon insertion profile surrounding *whiB7* served as a positive control for the sub-MIC treatments (Figure 33; nb, the *whiB7* structural gene could not be analyzed because it has only one non-essential TA at its C-terminus). Multiple insertions within the *whiB7* promoter and 5'-UTR region were present when no antibiotic selection was applied, but either disappeared or showed very limited read counts when the cultures were treated with sub-MIC antibiotics (Table 8). This was expected since this region was required for *whiB7* expression. Read counts outside of *whiB7* and its 5'-UTR remained relatively unchanged. Surprisingly, insertions at a single TA site (#4; Figure 33) within the *uORF* may be beneficial for growth in the presence of chloramphenicol or tetracycline, as indicated by read count enrichment (Table 8). As previously mentioned, the *uORF* region was required for repression of *whiB7* transcription (*171, 172*). Therefore, the insertion may be alleviating repression leading to a WhiB7-mediated antibiotic resistance state, causing an increase in relative growth rate and population enrichment.

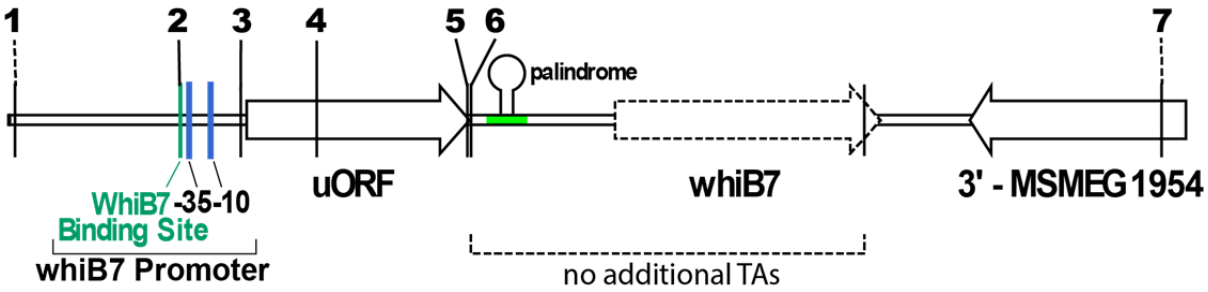

Figure 33. Transposon insertion profile of the *whiB7* genomic region. Transposon insertions with mapped reads are indicated (numbered lines). The *whiB7* promoter, as well as conserved regions across mycobacteria (conserved/ palindrome) are shown. Reads associated with insertions are given in Table 7.

Table 8. Read numbers associated to transposon insertion sites indicated in Figure 33

		[B]Sub-MIC		
[A]T#	Untreated	Roxi	Cm	Tet
1	41	50	32	54
2	12	1	0	0
3	14	0	0	0
4	40	13	385	727
5	55	0	9	6
6	29	1	8	6
7	71	38	22	22

[A]T# indicates the transposon insertion site numbered in Figure 33

[B]Sub-MIC treatments include 2 µg/mL roxithromycin (Roxi), 15 µg/mL chloramphenicol (Cm), 1.25 µg/mL tetracycline (Tet).

Genome-wide screening for loci with decreased transposon insertion frequencies after sub-MIC antibiotic selection identified genes that may contribute to WhiB7 expression or function (Table 9). These were manually screened to ensure the lower read counts represented multiple insertion locations within a gene that were uniformly reduced or disappeared upon selection. They included several known antibiotic resistance determinants some of which are likely to be WhiB7-independent. For example, an antigen 85 (MSMEG_6398) knock-out shows significant cell envelope perturbations which increase the rate of antibiotic penetration (*48*). Similarly, the *ftsX* deletion may also lead to cell wall perturbations (*184*). MSMEG_3069 is annotated as an aminoglycoside/tetracycline-transport integral membrane protein. Additional

genes that were identified included *MSMEG_4269* (*asnB*), a known multi-antibiotic resistance determinant with an unknown mode of action (*41*), as well as several hypothetical genes. Whether the hypothetical genes or *asnB* promote resistance through WhiB7 rather than independent mechanisms was investigated further in Section 4.1.6.

Table 9. Gene candidates that may promote *whiB7* expression or WhiB7 function in the presence of antibiotics (sub-MIC).

		Sub-MIC			
	Untreated	2 μg/mL roxithromycin	15 μg/mL chloramphenicol	1.25 μg/mL tetracycline	Product
MSMEG_3027 (Rv2553c)	291	1	10	1	
	126 (6)	0	3 (2)	0	hypothetical protein
MSMEG_3493 (Rv0559c)	491	60	99	7	
	249 (5)	34 (2)	38 (4)	2 (2)	hypothetical protein
MSMEG_3494 (Rv0455c)	254	7	44	3	
	158 (6)	2 (1)	16 (3)	5 (2)	hypothetical protein
MSMEG_3637 (Rv1842c)	175	3	1	1	
	71 (2)	1 (1)	0	0	hypothetical protein
MSMEG_3638 (Rv1841c)	276	9	3	1	
	160 (4)	3 (2)	4 (2)	0	hypothetical protein
MSMEG_4269 (Rv2201)	71	5	1	1	asparagine synthase (*asnB*)
	35 (6)	2 (1)	0	0	
MSMEG_6099	101	9	20	9	
	96 (6)	5 (2)	11 (4)	6 (4)	hypothetical protein

ESSENTIALS software analysis is shown in white rows. Figures indicate the total number of reads from insertions at target sites within the entire gene.

UGENE analysis is shown in grey rows. The total read counts per gene are indicated with the number of unique transposon insertions associated with the reads shown in parentheses.

Note, ESSENTIALS used PASS alignment (*185*) while UGENE used Bowtie alignment (*186*). Alignment settings for Bowtie were more stringent and therefore lower lead alignments were observed.

If present, orthologs in *Mtb* are given in parentheses. Note that the MSMEG_3493/4 orthologs do not maintain synteny.

In addition to the above experiments using sub-MIC treatments, roxithromycin was also used at an above-MIC concentration. The fact that that pre-induction of *whiB7* with antibiotics increases resistance to macrolides, along with evidence of a system that represses *whiB7*

expression (Figure 28), suggested above-MIC treatment might select for insertions that relieve *whiB7* repression (Figure 30b).

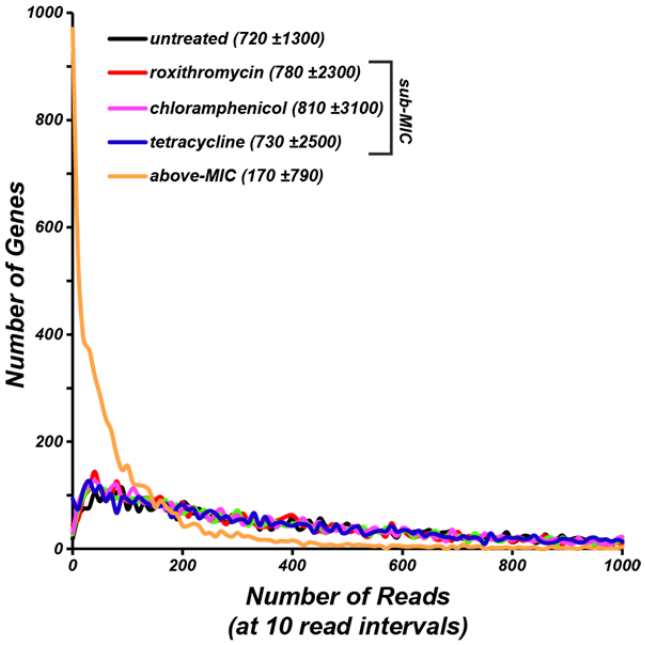

Figure 34. Number of genes corresponding to read counts. Genes were grouped based on the associated read counts as denoted by ESSENTIALS output. The number of genes per 10 read interval were then plotted against the lowest interval value (i.e., value plotted at 0 corresponds to genes with read counts between 0 - 10). The average number of reads per gene ± standard deviation is indicated in parentheses.

The above-MIC selective conditions were expected to inhibit the growth of the majority of the library. This was reflected by a drastically altered read profile where the vast majority of mutants had very low read counts reflecting growth inhibition (Figure 34). As a result, the read counts from above-MIC and sub-MIC (including untreated) conditions could not be directly compared and selection of candidates was based on ranking the observed read counts per gene. Roughly 55,000 inserts could be identified by read alignment, with an average of 174 reads (± 790) per gene. In total, >70 genes were at least one standard deviation above the average read count. However, the probability that these candidates reliably represented resistance to roxithromycin was questionable since they could not be compared to the untreated control. Similarly to the sub-MIC selection process, UGENE analysis was used to confirm that the reads from candidate genes mapped to multiple TA insertion sites.

Table 10. Candidate genes that may repress *whiB7* expression or WhiB7 function in the presence of antibiotics (above-MIC)

		[a]Sub-MIC		
Read count	Above-MIC	untreated	roxithromycin	Product
MSMEG_0965	31212	1300	6918	porin
MSMEG_0385 (Rv1524)	3145	2836	2441	glycosyl transferase family protein
MSMEG_0688 (Rv0337c)	815	0	0	aminotransferase
MSMEG_2691 (Rv2747)	1623	1278	1563	*N*-acetylglutamate synthase
MSMEG_2779 (Rv2680)	2139	622	1375	hypothetical protein
MSMEG_3374	464	2328	60636	hypothetical protein
MSMEG_4060	1681	1716	1367	pseudogene; aspartate aminotransferase
MSMEG_5121 (Rv1178)	3630	169	1884	*N*-succinyldiaminopimelate aminotransferase
MSMEG_5270 (Rv1077)	17282	3590	7708	cystathionine beta-synthase

[a]Sub-MIC experiment was independent of the above-MIC experiment and therefore the absolute read count values are not directly comparable. With the untreated as a negative control, read count enrichment under sub-MIC roxithromycin provides a line of evidence independent of high above-MIC read counts that a disruption of the candidate may promote macrolide resistance. These instances are highlighted grey.

If present, orthologs in *Mtb* are given in parentheses.

In addition to UGENE analysis, additional criteria were used to select genes for further study. To select genes that were more likely to be involved with *whiB7*, special attention was given to those linked to amino acid metabolism (Table 10). This was based on results suggesting that amino acid metabolism played a role in controlling *whiB7* expression. Results obtained by a fellow graduate student, Carol Ng, revealed that an alanine aminotransferase (annotated aspartate aminotransferase) promotes WhiB7 function; my work also implicated amino acid metabolism in modulating *whiB7* expression levels (Figure 24). Additionally, genes with no assigned function were selected to link novel genes to antibiotic resistance and *whiB7*.

The final criterion used to select candidates most likely to represent antibiotic resistant hits was provided by the more reliable sub-MIC roxithromycin dataset. While the sub-MIC experiment focussed largely on mutants that were more antibiotic sensitive, analysis of the data also revealed some mutants with an increased relative read abundance suggesting higher relative growth rate. The fact that some mutants grew faster than the overall population in the presence of low concentrations of antibiotic revealed that the sub-MIC roxithromycin treatment decreased growth of the majority of the library. This pool of genes overlapped in part with super-MIC candidate genes (Table 10), thereby providing further support that these genes played roles in roxithromycin resistance. Importantly, these included *MSMEG_0965*, the major surface porin protein MspA. *mspA* deletions have broad spectrum antibiotic resistance, resulting from the decreased rate of antibiotic entry into the cell (*187*), providing verification of the selection process.

4.3.4 Antibiotic susceptibility of candidate gene deletion or constitutive expression strains

Inactivation of potential *whiB7* regulatory genes identified through selection with sub-MIC antibiotic treatments were expected to show a WhiB7-specific susceptibility profile, reflected by sensitivity to all antibiotic used for Tn-seq selection (roxithromycin, chloramphenicol, and tetracycline). To investigate this hypothesis gene deletion mutant were constructed; *MSMEG_3027* (3027KO), *MSMEG_3493* (3493KO), *MSMEG_3494* (3494KO), *MSMEG_3493/MSMEG_3494* double mutant (3493/4KO), *MSMEG_3637/MSMEG_3638* double mutant (3637/8KO), *asnB* (4269KO), *MSMEG_6099* (6099KO). Surprisingly, several constructs did not have the predicted antibiotic sensitivity profile. The 3027KO and 6099KO strains did not show a difference in susceptibility to WhiB7-specific antibiotics roxithromycin,

spectinomycin, and tetracycline relative to the parent *M. smegmatis* (Table 11). Similarly, the 3493KO, 3494KO, and 3493/4KO strains did not show an increase in susceptibility to roxithromycin or tetracycline, but had a substantial increase in spectinomycin susceptibility. For all the cases, susceptibility to the WhiB7-independent antibiotic biapenem was unaffected. The 4269KO showed an increase in susceptibility to spectinomycin and biapenem, with a possible slight increase in susceptibility to tetracycline, but no change in resistance to roxithromycin (Table 11). Lastly, the 3637/8KO was the only candidate that resulted in a WhiB7-specific susceptibility profile (Table 11). The susceptibility to the WhiB7-independent antibiotic (biapenem) was unchanged, strongly suggesting that MSMEG_3637 and MSMEG_3638 may contribute to WhiB7-mediated antibiotic resistance. In further support, the constitutive expression of MSMEG_3637 (p3637OV) showed a 2-4 increase in roxithromycin resistance suggesting pre-induction of *whiB7* (Table 11).

Candidate genes identified through selection with above-MIC roxithromycin treatment had the potential of repressing *whiB7*. Therefore, constitutive expression of the corresponding genes was expected to generate increased susceptibility to the *whiB7*-specific antibiotics roxithromycin, spectinomycin and chloramphenicol. From the candidates, constitutive expression of *MSMEG_0385* (p0385OV), *MSMEG_0688* (p0688OV), and *MSMEG_5270* (p5270OV) showed no difference in susceptibility to either WhiB7-specific or non-specific antibiotics (Table 11). Additionally, *MSMEG_2691* (p2691OV), *MSMEG_2779* (p2779OV), *MSMEG_3374* (p3374OV), and *MSMEG_5121* (p5121OV) did not show a *whiB7*-specific susceptibility profile, but rather a 2-4 fold increase in macrolide resistance (Table 11). This suggested that these genes do not repress *whiB7* as predicted by Tn-seq analyses. On the contrary, this data suggested that they activate (pre-induce) *whiB7* expression similarly to

constitutive expression of *MSMEG_3637*. To determine whether in the increase in roxithromycin resistance was linked to *whiB7*, p2691OV and p5121OV were transformed into the *whiB7* KO strain where, as expected, they could no longer promote resistance (Table 11). This suggests that both knock-out or constitutive expression of *MSMEG_2691, MSMEG_2779, MSMEG_3374*, and *MSMEG_5121* lead to pre-induction of *whiB7*.

Table 11. Minimum inhibitory concentrations of *M. smegmatis*, its *whiB7* KO derivate, and candidate gene knock-outs or constitutive expression strains to various antibiotics

Treatment	roxithromycin	spectinomycin	tetracycline	chloramphenicol	biapenem
M. smegmatis	2-4	18.75-37.5	0.5-1	25	3-6
3027KO	4-8	18.75-37.5	0.5-1	-	6-12
3493KO	4	<2.3	0.5	-	6-12
3494KO	4-8	<2.3	0.5	-	6-12
3493/4KO	2-4	<2.3	0.5	-	6
3637/8KO	0.125-0.5	4.7-9.4	0.25-0.5	-	6-12
4269KO	4	2.3	0.25	-	0.05
6099KO	2-4	37.5	0.5	-	6
p0385OV	4	37.5	-	25	6
p0688OV	2-4	18.8-37.5	-	25	3-6
p2691OV	8	37.5	-	12.5-25	6
p2779OV	4-8	37.5	1	-	6
p3374OV	4-8	37.5	1-2	25-50	3-6
p3637OV	4-8	37.5	0.25	-	6
p5121OV	4-8	37.5	-	25-50	6
p5270OV	2-4	37.5-75	1-2	25	6
whiB7 KO	0.031-0.063	2.3-4.7	0.125	6.25-12.5	3-6
whiB7 KO/ p2691OV	0.031-0.063	-	-	-	-
whiB7 KO/ p5121OV	0.063	-	-	-	-

Values represent the MIC (μg/mL) as measured from at least three independent recombineered colonies (*140*) or transformants. '-' indicates not-performed. Candidates with WhiB7 specific susceptibility are highlighted grey.

4.3.5 *MSMEG_4060* was a unique candidate with a point mutation

MSMEG_4060 was identified as a candidate for inhibiting WhiB7 activity in the course of verifying the transposon library construction, treatment conditions, and screening technology used to identify other genes listed in Table 10. Selection of mutants for resistance to roxithromycin at above-MIC identified two insertions that were mapped to a TATA sequence 66 bp downstream of *MSMEG_4060* and 228 bp upstream of *MSMEG_4061* (Figure 35; hyper insertion region). My initial hypothesis was that insertions in the region annotated as intergenic, might be promoting WhiB7 activity.

As the insertions were not mapped to a gene, and seemingly too far upstream to affect *MSMEG_4061*, an effect on WhiB7 was puzzling. Therefore, an insertion was engineered into the TATA sequence to directly test an effect on WhiB7-specific antibiotic sensitivity. During construction of the insertion vector, a single base pair deletion (Figure 35; ΔG) was detected with three independent PCR reactions and the subsequent sequencing of the products. Interestingly, the ΔG mutation was not present in the *M. smegmatis* mc^2155 genomic sequences from Oct. 2006 (Accession CP000480) or from Jun. 2009 (Accession CP001663), but was found in the newest sequence Sept. 2014 (Accession CP009494) and the sequences of its two isoniazid resistant mutant strains (INR1/R2). The ΔG mutation shifts the frame within *MSMEG_4060** (the * designating the original short product) resulting in a longer *MSMEG_4060* product (Figure 35). This placed the hyper insertion region within *MSMEG_4060* making it a candidate for the repression of WhiB7 mediated antibiotic resistance. This was further strengthened upon the sequencing of the above-MIC Tn-Seq condition (Table 10). Blastp results of both the short and long translation products showed similarity to an aspartate aminotransferase, but MSMEG_4060 showed a higher level of similarity including the region downstream of the ΔG mutation (Figure

35; grey area). These data indicate that my strain of *M. smegmatis* contains the longer MSMEG_4060 which may be an aspartate aminotransferase repressing WhiB7-mediated resistance.

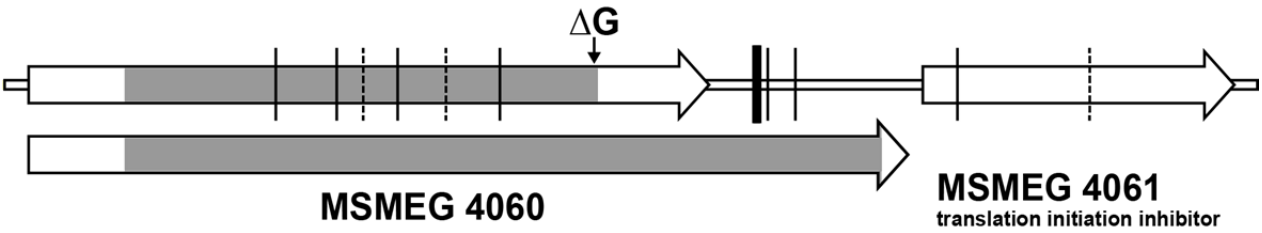

Figure 35. *MSMEG_4060* contained a single nucleotide deletion which shifted the frame of translation to encode a larger aspartate aminotransferase homolog. The original *MSMEG_4060* and the downstream gene *MSMEG_4061* are shown. The G deletion (ΔG) is indicated and transposon insertions into TA nucleotides are indicated by lines. Dashed lines represent insertion found only in the untreated library and not the above-MIC treated sample. The hyper insertion region of two adjacent TA sites is represented by the thicker line. The predicted product of *MSMEG_4060* resulting from the G deletion is also shown (bottom). Areas highlighted grey indicate similarity to an aspartate aminotransferase based on Blastp analysis.

To test the effect of a *MSMEG_4060* knock-out on WhiB7-mediated resistance, an insertion was engineered into the TATA sequence (4060KO) and a constitutive expression plasmid was constructed (p4060OV). As expected, the 4060KO showed a fourfold increase in resistance to macrolides including roxithromycin and clarithromycin (Table 12) indicating *whiB7* pre-induction, but was unchanged in its resistance to other WhiB7-specific antibiotics. Constitutive expression of *MSMEG_4060* decreased resistance not only to macrolides, but also other antibiotics within the *whiB7* sensitivity spectrum including spectinomycin and chloramphenicol (Table 12). Constitutive expression or knock-out of *MSMEG_4060* did not affect resistance of a *whiB7* independent antibiotic, biapenem. Together these results indicate that MSMEG_4060 may be a repressor of *whiB7*.

Table 12. Minimum inhibitory concentrations of *M. smegmatis*, its *whiB7* KO and 4060KO derivatives, and the *MSMEG_4060* constitutive expression strain to various antibiotics

Treatment	roxithromycin	clarithromycin	spectinomycin	chloramphenicol	biapenem
M. smegmatis	2	0.5	25-50	25	6.25
whiB7 KO	0.5	0.0625	6.25	6.25-12.5	6.25
4060KO	8	2	25-50	25	6.25
p4060OV	0.5	0.0625	12.5	6.25	6.25

Values represent the MIC (μg/mL) as measured from at least three independent recombineered (*140*) colonies or transformants.

Note, these experiments were carried out independent of the Table 11 values with different concentration of diluted antibiotic and different antibiotic stocks.

4.3.6 *whiB7* transcription was altered in p4060OV and 3637/8KO

Both the p4060OV and 3637/8KO strains had a WhiB7-specific sensitivity phenotype while their counterparts (4060KO and p3637OV) had an increase in macrolide resistance (Table 11 and 12). This suggested that their respective activities may hinder or amplify the WhiB7 pathway. To determine if this effect was at a transcriptional level, induction of *whiB7* was monitored using quantitative PCR. As indicated by Figure 23, *whiB7* induction was a function of stress rather than absolute antibiotic concentration. Therefore, the macrolide roxithromycin was used at a standard concentration of 25% the MIC of the respective strains, to generate a comparable stress response. The data showed that *whiB7* induction was considerably impaired with a ca. 550-fold and a ca. 100-fold reduced induction in the p4060OV and 3637/8KO, respectively (Figure 36). The lack of induction was not a concentration dependent effect in the case of p4060OV; treatment with roxithromycin at four times the dose (i.e. corresponding to the dose used to treat *M. smegmatis*), did not induce transcription (data not shown). Together the data clearly demonstrate that MSMEG_4060 inhibits *whiB7* transcription, while MSMEG_3637 and/or MSMEG_3638 are required to amplify *whiB7* transcription.

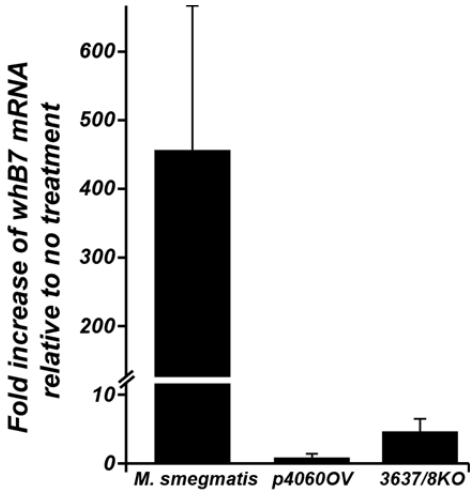

Figure 36. Effect of 3637/8KO and p4060OV on *whiB7* induction. Fold increase of *whiB7* mRNA relative to an *M. smegmatis* untreated control and its derivatives: *MSMEG_4060* constitutive expression (p4060OV) and the *MSMEG_3637/3638* double mutant (3637/8KO). Antibiotic induction was performed with roxithromycin at a 25% MIC for each strain as defined in Table 4. Values represent the average of five, three and four biologically independent results for *M. smegmatis*, p4060OV and 3637/8KO, respectively. Error bars represent standard deviation.

4.4 Discussion

Regulation of *whiB7* is a complex and novel phenomenon that determines resistance to diverse antibiotics in Actinobacteria. I have shown that WhiB7 directly promotes transcription of its own promoter and found evidence for a WhiB7-independent partner(s) that also regulates expression. I carried out three parallel experiments each using one *whiB7*-specific antibiotic for selection of mutants in a high-density transposon library coupled with high-throughput sequencing to identify genetic loci that contribute to WhiB7-mediated resistance. While several candidates were identified, only the hypothetical gene pair *MSMEG_3637/3638* was shown to contribute to *whiB7* activation. *MSMEG_4060*, a putative aspartate aminotransferase, was shown to contribute to *whiB7* repression; repression was also attributed to early termination of the *whiB7* transcript.

The *whiB7* transcript is terminated upstream of the *whiB7* structural gene due to a large conserved palindrome. Upstream of the palindrome was a non-conserved *uORF* which was required for the termination to occur (Figure 28). How the *uORF* contributes to *whiB7* regulation remains unknown, although the uORF is unlikely to be a functional protein as its sequence is highly divergent not only across mycobacteria but other Actinobacteria. Importantly, the *uORF*

is cis acting; deletion of the *uORF* region alleviated repression of the reporter system in *M. smegmatis,* which contained a functional *uORF* in its genome (Figure 28). This provided further proof that the uORF was not a functional protein that directly repressed *whiB7* transcription. A coupled transcription-translation type of regulation, requiring a sequence to be targeted by ribosomes, regardless whether the peptide is functional or not, is the most likely hypothesis.

Post-transcriptional regulation of antibiotic resistance genes to ribosome targeting antibiotics, such as macrolides, is common in bacteria (*188*). Generally, this involves a transcript containing the resistance gene downstream of an actively translated regulatory ORF. The ribosome binding site of the resistance gene is sequestered by RNA secondary structure under normal growth conditions. The addition of a macrolide stalls translation of the ORF leading to a change in RNA secondary structure freeing the downstream ribosome binding site and allowing translation of the resistance gene. Interestingly, a second mode of activation, caused by a ribosome frame shift in response to drug treatment can also act as an activating signal (*189*). In this case, rather than differential RNA structures, the frame shift causes the ribosome to read past the ORF stop codon, thereby supressing the formation of the sequestering structure. Importantly, aminoglycosides, which were potent inducers of *whiB7,* are known to promote mistranslation. While interesting ideas, these types of systems are unlikely to be the cause of *whiB7* repression as it was the level of full length *whiB7* transcript that was altered (Figure 28) rather than sequestering a ribosome binding site in a full length transcript. However, the frame shift read-through may contribute to regulation as point mutations within *whiB7's uORF* relaxed early termination (*172*). Transcriptional attenuation can occur though many mechanisms (*190*).

For example, regulation of the tryptophan biosynthetic regulon in *E. coli* is, in part, regulated by translation-coupled transcriptional attenuation. In this system, transcription pauses

within an upstream ORF that contains a critical tryptophan codon, allowing for ribosome loading. The subsequent translation of the ORF allows transcription to continue. If there are sufficient levels of tryptophan, translation functions at a normal rate and stops at the designated stop codon in the *ORF*. This coupled transcription-translation causes the formation of an early terminator thereby releasing RNAP and generating a truncated transcript. However, if tryptophan levels are low, translation pauses at the tryptophan codon, uncoupling translation from transcription and causing the formation of an anti-terminator structure leading to a full length transcript. As a RNAP pause site was present in the *whiB7* 5'-UTR (*171*), the *whiB7 uORF* may serve a similar function in mediating early termination. However, with tryptophan biosynthesis, several loop structures are required to transition between regulatory states. In the case of *whiB7*, only one large palindrome was conserved implying it was the single element that mediated early termination without the formation of other secondary structures.

A recent study by Zukher *et al.* (*191*) investigated the posttranscriptional regulation of the microcin C biosynthetic operon (*mccABCDE*). Similarly to *whiB7*, an early termination event mediated by a palindrome in the intergenic region between *mccA* and *mccB* resulted in an accumulation of a short *mccA* transcript. While the *mccA* product was the precursor peptide for microcin C, its translation was not required for the termination event. The group showed that for the early termination to occur, the only factor required was for a ribosome to be bound upstream of the palindrome. While a detailed mechanism is unavailable, the group postulates that secondary or tertiary interactions by the ribosome with *mccA* RNA are required for the formation of the terminator. Overall, this mechanism does not fit the observed effects of the uORF as its translation is likely required for termination, but the study raises the idea that a ribosome must be loaded at a specific location in the *whiB7* transcript for termination to occur, for example at the

C-terminal sequence of the *uORF*. If the ribosome stalls the terminator is not formed, or if there is a frame shift read-through of its stop codon, it will also repress terminator formation. This model may very well explain how macrolides or aminoglycosides activate *whiB7* transcription, but it fails to conceptualize why other activators identified, many of which do not target the ribosome, also activate *whiB7* transcription. The most unique of which was the glutamine analog acivicin.

One of the most unique aspects of *whiB7* regulation was its induction by a large number of structurally and functionally independent activators (Figure 22). While all of the compounds converge to induce *whiB7* transcription, their finite levels of activation (as measured by RT-qPCR) are not identical. This implies that circumvention of early termination is not binary (on/off) and suggests a gradient of possible responses. This can be seen directly as when lower concentrations of antibiotic was used for induction, a smaller increase in *whiB7* transcriptional induction was observed. As mentioned, the anti-termination event may be mediated by ribosome stalling within the *uORF*, and therefore the rate of stalling may not be the same for all the activators. For example, macrolides are very effective at ribosome stalling and are strong *whiB7* inducers, but other compounds may generate only moderate stalling leading to lower levels of response. Interestingly, while the *uORF* sequence was highly divergent, and the peptide sequence therefore variable, a common pattern across several Actinobacteria was a noticeable abundance of alanines (Table 7). It is important to note that as Actinobacteria have high GC genomes, random translations of their DNA will include a higher abundance of amino acids encoded by high GC codons including alanine, proline, arginine or glycine. However, only alanines are abundant across five representative sequences, suggesting alanine as a potential regulatory metabolite. As mentioned, amino acid metabolism modulated the level of *whiB7*

activation. Importantly, as Carol Ng in our lab found that, AspC, an alanine aminotransferase, was required for proper levels of *whiB7* activation. Together, these data imply that amino acid pools (specifically alanine) and corresponding charged tRNA pools, may be altered by some *whiB7* inducers, leading to a ribosome stall event in *uORF* translation and thereby alleviating early termination. This may be an alternate route for *whiB7* activation if the compound itself does not directly stall the ribosome or results in frame-shifts. As a result, cell metabolism may perhaps be shifted towards *whiB7* induction by forcing amino acid metabolism away from alanine production. This hypothesis does not rule out additional protein regulators as they may target the conserved palindrome or perhaps modulate RNAP or ribosome activity.

To investigate other genetic loci that could contribute to WhiB7-mediated resistance, high-density transposon mutagenesis coupled with high-throughput sequencing was used in combination with WhiB7-specific antibiotic selection. Several conditions were considered in the experimental design. These were mainly the density of the library and the available sequencing depth. The library constructed included ~57,000 mutants and the MiSeq chemistry chosen was version 2 with 50 cycles (i.e. 50 bp reads) and 15 million reads. To ensure identification of all insertions, a maximum of 5 conditions could be used. This allowed for 50X coverage of the insert library under each condition at the maximal read depth. To maximize the likelihood of discovering WhiB7-specific systems, the sub-MIC treatment conditions chosen contained as many different classes of WhiB7-specific antibiotics as possible (Figure 30a). These included roxithromycin (macrolide), chloramphenicol (phenicol), and tetracycline (tetracycline), as well as spectinomycin (aminoglycoside; spectinomycin was later disregarded from formal analysis). Additionally, the above-MIC condition (Figure 30b) was added as it monitored increased numbers of insertions and therefore required less sequencing coverage, compared to analyses for

loss of insertions which required complete library sequencing. Overall, this protocol was designed to establish methodology and assess the potential of the data. I believe it has done so, and importantly provided numerous insights into how it can be improved, which will be discussed in the concluding remarks.

The sub-MIC treatment condition was designed to identify loci that contributed to WhiB7-mediated resistance. As such, transposon insertions would be selected using concentrations that inhibited the growth of the *whiB7* mutant (Figure 31). In total 7 potential targets were identified (Table 9). These included the hypothetical proteins MSMEG_3027, MSMEG_6099, the pairs MSMEG_3493/ 3494 and MSMEG_3637/ 3638, and MSMEG_4269 (AsnB). To determine predicted effects on WhiB7-mediated resistance, the corresponding genes were disrupted by targeted recombination.

It is important to note, that my investigations with these strains are ongoing and the presented data do not yet provide a complete picture. For example, site directed mutants in *MSMEG_6099,* generated with two independent rounds of recombineering, did not show the drug sensitivity profile that was predicted. However, these mutants could not be confirmed by PCR. Therefore, while 6099KO did not exhibit a WhiB7-like susceptibility profile (Table 11), this may be due to faulty mutant construction. However, the 3027KO mutant was also constructed twice with confirmation of the insertion, and did not show the expected susceptibility profile (Table 11). A similar result was noticed with the *MSMEG_3493/ 3494* gene pair, which only showed increased susceptibility to spectinomycin (Table 11). These false positives may reflect limitations of the MIC assay in resolving different levels of susceptibility.

To illustrate the concept, suppose that *M. smegmatis* has a level of resistance of 100 to an antibiotic and the *whiB7* KO has a resistance of 25. A concentration of 80 is used as selection.

Any genes identified with a resistance defect may not correspond to one at the same level of the *whiB7* KO. If an identified gene has a level of resistance of 60, once its knock-out is generated a defect may not be observed based on the standard MIC assay, as it uses twofold serial dilutions. Testing concentrations of 200, 100, 50, 25, and 12.5 would show the knock-out is inhibited by 100 and not 50, and therefore appear as having resistance comparable to unmodified *M. smegmatis.* Therefore, 3027KO and 3493/4KO may have different levels of susceptibility that are not dependent on *whiB7* at levels undetected by the standard MIC assay. Alternatively the explanation may be as simple as lack of replicates for the transposon insertion assays, a differential phenotype based on the transposon insertion versus the site directed recombineered insertion, or something as exciting as the possibility of a complex diffusible signal generating a community response to the antibiotic that actively selects against the mutants.

Drug sensitivity of the MSMEG_4269 (AsnB) knock-out suggested that it was more susceptible to some *whiB7*-specific antibiotics, but also more sensitive to antibiotics that were not affected in the *whiB7* mutant. AsnB was previously reported as an antibiotic resistance determinant in *M. smegmatis* mediating resistance to erythromycin, rifampicin, novobiocin and fusidic acid; it did not mediate resistance to streptomycin, chloramphenicol, norfloxacin, tetracycline, isoniazid, ethambutol, and beta-lactams (*41*). Intriguingly, while resistance to erythromycin was decreased, resistance to roxithromycin, a semi-synthetic derivate of erythromycin, was not affected (Table 11). Surprisingly, while no tetracycline or chloramphenicol susceptibility was previously reported (*41*), these antibiotics actively selected against insertions in *asnB* indicating susceptibility (Table 9). This may once again be linked to the selection concentration rather than a large increase in susceptibility, although a 2-4 fold drop in tetracycline resistance was observed (Table 11). While there is still no explanation of how

AsnB mediates resistance, due to the lack of convergence of susceptibility to several WhiB7-specific antibiotics (roxithromycin, streptomycin, chloramphenicol), and the increase in susceptibility to non-WhiB7 specific antibiotics (biapenem, rifampicin, novobiocin), it is unlikely that it is linked to WhiB7. However, it is still too early to discount AsnB as several experiments are in progress. Unfortunately, the *asnB* mutant, 4269KO has a severe growth deficiency phenotype and aggregates even in the presence of detergents. This has hampered efforts to gain solid insights into the 4269KO susceptibility profile, as well as to generate RT-qPCR data. These efforts are ongoing.

Assay of knockouts or strains overexpressing *whiB7* by PCR is also being used as an independent criterion for evaluating the significance of genes identified in sub or super MIC experiments. These assays are ongoing, however they have shown that 3493/4KO, has no defect in *whiB7* induction (data not shown) implying its susceptibility to spectinomycin was independent of the *whiB7* induction pathway.

Finally, the gene pair *MSMEG_3637/ 3638* was the only candidate to show a WhiB7-like susceptibility profile (Table 11) that was then linked to a lack of *whiB7* induction (Figure 36). This demonstrated that the transposon assay could indeed identify determinants that contribute to WhiB7-mediated resistance. However, the mechanism of MSMEG_3637 and MSMEG_3638 contribution to WhiB7-mediated resistance remains uncharacterized. Thorough bioinformatic analysis showed that the genes are conserved across mycobacteria and are likely membrane associated, they cannot be linked to a proposed function. Continued investigation will likely provide exciting results in the regulation of the *whiB7* pathway and perhaps contribute our overall understating of Wbl regulation.

In addition to the sub-MIC treatments to identify genes contributing to WhiB7-mediated resistance, an alternate above-MIC treatment was used to identify possible repressors. This treatment relied on the fact that resistance to macrolides was increased by *whiB7* pre-induction, but the selection condition was expected to produce numerous types of hits (Figure 30b). WhiB7-independent resistance was highlighted by inserts in MSMEG_0965, the major surface porin MspA; consistent with a previous report, the corresponding knocked-out generated multi-drug resistance (*187*). Constitutive expression of other candidates did not confirm their predicted functions in drug susceptibility. This included MSMEG_0385, a glycosyl transferase family protein that catalyzes glycosidic linkages to join saccharide moieties, MSMEG_0688 an aminotransferase, and MSMEG_5270 a cystathionine beta-synthase which functions in the transulfuration pathway whose products include cysteine and alpha-ketoglutarate. Surprisingly, constitutive expression of other candidates (MSMEG_2691 a N-acetylglutamate synthase which makes N-acetylglutamate from glutamate and acetyl-CoA, MSMEG_2779 a hypothetical protein, MSMEG_3374 a hypothetical protein, and MSMEG_5121 a N-succinyldiaminopimelate aminotransferase that catalyzes the interconversion between N-succinyl-L-2,6-diaminoheptanedioate and 2-oxoglutarate to N-succinyl-L-2-amino-6-oxoheptanedioate and glutamate (which is an important step in lysine and arginine biosynthesis)) all increased resistance to the macrolide roxithromycin 2-4 fold, but had no other susceptibility changes (Table 11). The increase in roxithromycin resistance mediated by MSMEG_2691 or MSMEG-_5121 overexpression was *whiB7* dependent; the phenotype was not observed when these genes were overexpressed in the *whiB7* KO strain (Table 11). This, together with studies of uORF implies a second regulatory system, an idea that is being explored. Together, this highlights the complicated nature of metabolic factors that regulate WhiB7 and genes in its regulatory cascade.

The stringent response, mediated by an accumulation of ppGpp, shifts cell metabolism towards amino acid synthesis and slows down transcription, translation, and DNA replication in response to nutrient starvation (*192*). The response can directly promote antibiotic resistance. For example, in *P. aeruginosa* mutants that cannot make ppGpp (due to inactivation of both ppGpp synthetic genes *relA* and *spoT* (which also serves to degrade ppGpp)) become sensitive to ofloxacin (a gyrase inhibitor) (*193*), an effect reflecting its inability to activate an intrinsic resistance system.

In mycobacteria, like other gram-positive organisms, ppGpp is synthesized and degraded by the bifunctional Rel protein (corresponding to RelA (MSMEG_2965) in *M. smegmatis*). Analysis of the transposon library showed that inserts in RelA had a roughly 10X increase in read count abundance under sub-MIC chloramphenicol and tetracycline treatments relative to the untreated culture, and increased numbers of reads (1000 compared to average read count of 170) after above-MIC roxithromycin treatment. This implies that the *relA* mutant, lacking ppGpp's global effects on metabolism, increases antibiotic resistance, in contrast to the previous description of ofloxacin sensitivity in the *relA/spoT* mutant in *P. aeruginosa* (*193*). As noted above, amino acid pools, including levels of alanine that allow optimal translation rates provided by a dense assembly of ribosomes on the *whiB7* transcript, could mediate early termination at the palindromic sequence (Figures 7 and 28). Therefore, the stringent response may increase cytoplasmic amino acid (especially alanine) concentrations and promote early termination. This might not occur in a *relA* mutant, leading to an increase of WhiB7-mediated resistance. In support of this concept, microarray analysis of *Mtb* lacking the Rel protein accumulates the *whiB7* transcript under both regular growth (in 7H9) and nutrient starvation (*194*). Overall, these concepts contribute to the hypothesis that intracellular amino acid concentrations may contribute

to transcriptional regulation of *whiB7*. Interestingly, MSMEG_4060 was the only candidate linked to amino acid metabolism that showed repression of WhiB7-mediated antibiotic resistance.

MSMEG_4060 is a putative aspartate aminotransferase that caused a WhiB7-specific antibiotic susceptibility profile when overexpressed (Table 11). Importantly, constitutive expression of MSMEG_4060 led to a lack of *whiB7* induction in response to antibiotic treatment (Figure 36). Aspartate aminotransferases catalyze the interconversion of aspartate and alpha-ketoglutarate to oxaloacetate and glutamate. The direction of this reaction in MSMEG_4060 remains to be investigated, assuming it is an aspartate aminotransferase. If so, *whiB7* may be regulated by glutamate flux, which plays a central role in nitrogen metabolism and amino acid synthesis. Supporting this concept is the observation that MSMEG_2691 and MSMSEG_5121 may also be involved in amino acid metabolism with a common link to glutamate.

Importantly, unlike MSMEG_2691 and MSMEG_5121, blastp analysis indicated that MSMEG_4060 was not conserved across mycobacteria, implying that its regulatory influence on WhiB7 was not a universal feature. Mycobacteria and other Actinobacteria generally have many aminotransferases which may be adapted to MSMEG_4060-like roles, or perhaps serve as unique modulators of the WhiB7 pathway.

As previously mentioned, Morris *et al.* (*55*) identified two putative aspartate aminotransferases as being either up-regulated (*aspC*) or down-regulated (*aspB*) upon antibiotic treatment in a *whiB7*-dependent manner implying their reverse contributions to intrinsic resistance. In our lab, Carol Ng's investigation of AspC characterized it as an alanine aminotransferase that contributed to WhiB7-mediated resistance. Together, along with my work, these data continue to point to physiological variations as major contributors to *whiB7*

inductions. Along with other modes of induction such as ribosome stalling or ribosome frame-shift, amino acid or nitrogen imbalances may result from WhiB7-specific antibiotic treatment and all converge to relieve the palindrome-mediated transcriptional termination leading to a WhiB7 response. This area of exploration will undoubtedly be a key contributor to our understanding of WhiB7 activation and action, and perhaps provide additional paradigms for the Wbl family.

5 Concluding remarks

5.1 Overall significance

The proposed functions of Wbls include transcriptional regulation, thioredoxin activity and chaperone activity. While individual Wbl attributes, like DNA-binding or insulin reduction, have been well documented, a consensus on a Wbl function has not been reached. For example, WhiB1 was shown to repress transcription of the *groEL2* promoter *in vitro* (*88*), but also shown to specifically reduce GlgB (*94*). Many studies utilizing mutated alleles point to dysregulation of various genetic products, but a direct transcriptional role can be countered by examples of thioredoxin modulation of transcriptional regulators such as the eukaryotic NF-kappa B (*195*). While Wbl mediated transcriptional activation has been theorized for more than two decades (*59*), my WhiB7 studies were the first to provide direct biochemical proof of Wbl-mediated transcriptional activation. My characterization of WhiB7 and its mode of action provided concrete evidence that it functions as a transcriptional activator affirming previous hypotheses resulting from microarray studies (*55*). I have shown direct transcription activation *in vitro* and provided more detailed insights into how WhiB7 interacts with the primary sigma factor SigA and targets a specific DNA sequence. In addition, I have provided a thorough investigation of these activities by characterizing the residues required and, most importantly, shown their significance *in vivo*. In my opinion, my work has provided the most complete characterization of any Wbl protein to date and provides a paradigm for Wbl activities that should facilitate many exciting discoveries.

5.2 Limitations of research

The main unachieved goals of my research are the identification of a common activation signal for WhiB7 in Chapter 3 and full exploitation of the new Tn-seq technology in Chapter 4.

While Chapter 3 revealed the broad range of small molecules that induce *whiB7*, as well as several physiological conditions that modulate *whiB7* induction, a unique inducing metabolic signal could not be identified. Both amino acid and redox metabolism were implicated as contributors in the pathways for *whiB7* activation, but their exact contributions have yet to be determined. In combination with the studies in Chapter 4, numerous modes of induction can be proposed. Whether any are valid remains to be established. Nevertheless, my research provides numerous insights for future work.

Chapter 4 documents the application of Tn-seq to identify regulators contributing to WhiB7-mediated antibiotic resistance. The research has identified potential repressors and activators, but it is in its infancy in both method and results. It has generated exciting results and provided important insights into how the methodology could be improved. For example, I chose only WhiB7-specific antibiotics for treatment due to initial limitations. However, the results can be greatly improved by using WhiB7-independent antibiotics. Additionally, multiple selection concentrations of individual antibiotics, including going below the MIC of the *whiB7* KO, would allow for greater differentiation of WhiB7-contributing genetic loci rather than modest contributors to overall resistance. Expansion of the transposon library size is also a consideration, but must be balanced against available sequencing depth.

Overall, the perceived limitations are exciting areas of future research. The fact that elucidation of the basic qualities of WhiB7-mediated antibiotic resistance has raised far more intriguing questions that have been answered underlies the exciting possibilities for future

discovery. This reflects the centrally important regulatory features of Wbl proteins and the challenges of understanding how they interact not only with other proteins but also with their metabolic partners.

5.3 Potential applications

The most exciting applications of my research involve the WhiB7:SigA:DNA complex and the high potential of data mining from my transposon studies. The structural model may serve as a platform for the design of small molecule inhibitors, which can be tested directly with our *in vitro* run off studies. Importantly, my data shows that WhiB3 may bind SigA in a similar manner, suggesting that any inhibitor disrupting WhiB7:SigA interaction would have the same effect on WhiB3:SigA. This would have immense implication for TB treatment since WhiB3 is an important virulence factor. Thus, both intrinsic antibiotic resistance and virulence might be simultaneously targeted. Importantly, my transposon studies may provide numerous other antibiotic resistance targets that are dependent and independent of WhiB7.

The transposon experiment was designed to identify WhiB7 partners that contribute to its function and/or additional transcriptional regulators of *whiB7*. While results were obtained, the wealth of information in the database has yet to be fully exploited. Importantly, analyses of individual treatments can identify direct effectors of resistance for individual antibiotics. For example, the WhiB7-controlled, macrolide resistance determinant, ribosomal methyltransferase *erm* was an obvious essential gene under roxithromycin treatment but was not essential for regular growth or treatment with the other antibiotics. Additionally pairwise analysis can find linked resistance contributors across two or more of the tested antibiotic selections elucidating multi-drug resistance determinants. Analysis can extend beyond conditionally essential genes, by

monitoring frequency of insertions to find genes that make minor contributions to fitness. These types of studies can generate an unprecedented view of antibiotic resistance in mycobacteria, further expanding our appreciation for the contribution of previously unconsidered genes as resistance determinants. Most importantly, the methods I have established can be expanded outside the scope of WhiB7. Identification of intrinsic resistance genes for the current TB therapy of rifampicin, isoniazid, ethambutol and pyrazinamide can provide numerous targets to improve the standard of globally applied treatment regimens.

5.4 Future research

Future studies of the WhiB family of proteins in *Mtb* will not only increase our understanding of the fundamental physiological processes underlying intrinsic antibiotic resistance, redox balance, virulence, and cell division, but may also provide new TB treatment strategies. Many intriguing questions remain to be addressed.

How does metabolism affect intrinsic resistance and what is the role of the WhiB7 protein in regulating metabolism? WhiB7 not only activates antibiotic resistance systems, but also influences redox metabolism under both normal growth conditions and stress. How are these two functions related?

What are the common metabolic or redox signals generated by the diverse array of compounds that activate *whiB7* transcription? While its promoter reacts to thiol redox balance, this is not sufficient for full induction. What are the other metabolites that serve as essential partners in the general response? The introduction of metabolomic approaches should provide important insights into the role of WhiB7 in physiology, complementing expression microarrays that have provided insights into its regulon.

Are the thioreductase activities of WhiB proteins relevant to their functions *in vivo*? Even though evidence continues to build that WhiB proteins indeed function as essential transcriptional regulators of specific promoters, they may have additional functions with their possible roles as thioreductases requiring further clarification.

The fact that core amino acid motifs are conserved in all WhiB proteins and apparently required for their activity, evokes the question of how individual WhiBs react specifically to different stresses and activate specific promoters? WhiB proteins vary primarily in their C-termini, the likely determinants of their DNA-binding specificities. A simplistic model based on their sequence homology, suggests that all should be activated by the same stress signal, and then each activates transcription of its respective regulon. However, studies in liquid cultures show that each *whiB* gene is regulated by a unique repertoire of inducers and stress conditions (*69*). Is their specificity derived from variation at the N-terminus or perhaps subtle changes around the core motifs? *whiB7* transcriptional induction seems partially controlled by another antibiotic-responsive metabolic signal. Likewise, in the case of other *whiB* genes, is the specificity of induction dependent on additional regulators and the root of the differential responses?

Can compounds be developed to inactivate WhiB7 directly or block metabolic activating signals? Inhibiting specific antibiotic resistance determinants is a proven means of increasing antibiotic efficacy (ex. combination therapy with beta-lactams and beta-lactamase inhibitors (*196*)). Understanding the downstream effectors of WhiB7, as well as other WhiB proteins, may lead to the identification of novel targets to treat TB or increase the efficacy of currently available antibiotics. Compounds that inhibit several WhiB target proteins would inactivate multiple systems essential for growth, virulence, and intrinsic antibiotic resistance in *Mtb.* However, the focus of *Mtb* research must expand beyond screens for antimycobacterial

compounds. While identifying novel inhibitors is an essential task, it should be a part of a diversified research program. Understanding the fundamental ways *Mtb* controls essential aspects of its metabolism and intrinsic resistance may lead to novel approaches for TB therapy.

6 Methods

6.1 General methods

6.1.1 Bacterial strains and growth conditions

Unless otherwise specified *Escherichia coli* strains were grown in LB (Sigma) at 37 ºC, shaking at 200 rpm. *Mycobacterium smegmatis* mc^2155 and its derivatives were grown in Middlebrook 7H9 (BD) supplemented with 10 % (v/v) ADC (BD), 0.2 % (v/v) glycerol and 0.05 % (v/v) tyloxapol (Sigma) (henceforth referred to as 7H9) or with ADC replaced with 0.2 % (w/v) glucose (henceforth referred to as 7H9g) at 37 ºC either shaking in flasks at 200 rpm or rolling in test tubes. If needed, appropriate antibiotics were supplemented into the media; hygromycin 50 μg/mL, kanamycin 30 μg/mL, chloramphenicol 34 μg/mL, tetracycline 12.5 μg/mL, apramycin 50 μg/mL and ampicillin 200 μg/mL. *E. coli* TOP10 was used for the majority of cloning. Specialty strains were used as required; *E. coli* MRF' Kan was grown at 30 ºC as specified by Stratagene for the two-hybrid vector cloning, *E. coli* XL10 gold was used for mutagenesis as specified by the QuickChange II kit (Agilent technologies), ΦMycoMarT7 DNA was propagated in *E. coli* DH5αλpir, *E. coli* Rosetta2 (DE3) was used for protein expression.

6.1.2 Cloning

Unless otherwise specified, PCR was performed using Easy-A Hi-Fi polymerase (Agilent) according to manufacturer instructions. Reactions included 3 % (v/v) dimethyl sulfoxide. Restriction enzymes were from New England Biolabs; digests were preformed according to manufacturer instructions. Ligations were performed using T4 DNA ligase (Invitrogen) at room

temperature for 30 minutes and transformed by heat shock. Sequencing of vector constructs was performed at the UBC Vancouver campus NAPS unit (http://naps.msl.ubc.ca/). When necessary custom primers were used to sequence; they are indicated by a 'seq' tag in the primer list. All constructed strains and plasmids are listed in Table 13 with the oligonucleotides used listed in Table 14.

Table 13. Strains and plasmids used in the study

Strains	Description	Reference
Escherichia coli		
TOP10	Cloning and plasmid maintenance	Invitrogen
MRF' Kan	Cloning and plasmid maintenance for pBT, pTRG, and their derivatives; KanR	Stratagene
Rosetta2(DE3)	Protein expression strain containing rare tRNAs; CmR	Novagen
BacterioMatch II reporter	Reporter strain for the BacterioMatch II two-hybrid system; KanR	Stratagene
DH5αλpir	Maintenance strain for ΦMycoMarT7 DNA	Biomedal
Mycobacterium smegmatis mc2155		
wild type	Unmodified lab strain	(*197*)
whiB7 KO	Genomic region 2031710 to 2032094 containing *MSMEG_1953* (*whiB7*) replaced by Hygromycin resistance; HygR	(*107*)
whiB7 KOC	p361comp.apra integrated into the *whiB7* KO strain providing *whiB7* expressed under its own promoter *in trans*; HygR ApraR	This Study
ermMT OE	pERM.hyg integrated into genome constitutively expressing *ermMT* to provide macrolide resistance; HygR	This Study
FB7	N-terminal 3xFLAG tag and *whiB7* fusion	This Study
Sig515	*sigA* mutant expressing SigA R515H; HygR	This Study
3637/8KO	*MSMEG_3637* and *MSMEG_3638* double knock-out mutant; HygR	This Study
3027KO	*MSMEG_3027* knock-out mutant; HygR	This Study
4269KO	*MSMEG_4269* knock-out mutant; HygR	This Study
6099KO	*MSMEG_6099* knock-out mutant; HygR	This Study
3493KO	*MSMEG_3493* knock-out mutant; HygR	This Study
3494KO	*MSMEG_3494* knock-out mutant; HygR	This Study
3493/4KO	*MSMEG_3493* and MSMEG_3494 double knock-out mutant; HygR	This Study
4060KO	*MSMEG_4060* knock-out mutant; HygR	This Study
Plamids	**Description**	**Reference**
pAmilux	source of *luxABCDE* reporter; AmpR	(*124*)
pMV361	Integrative vector containing kanamycin resistance, integrase gene and the HSP60 promoter upstream of a multiple cloning site; KanR	(*198*)
pMV261	Multicopy vector containing kanamycin resistance and the HSP60 promoter upstream of a multiple cloning site; KanR	(*198*)
pMV361.hyg	Modified pMV361 with kanamycin resistance replacing hygromycin resistance; HygR	(*198*)
pMycVec1	Multicopy vector containing kanamycin resistance and promoterless multiple cloning site; KanR	(*199*)
pYUB854	Mycobacterium recombineering vector; HygR	(*140*)
pAB707	Source of the apramycin resistance gene *aac(3)IV*; AmpR	(*9*)
pET19b	T7 RNA polymerase promoter driven protein expression vector; AmpR	Novagen

Plamids	Description	Reference
pColaDuet-1	T7 RNA polymerase promoter driven protein co-expression vector; KanR	Novagen
pBT	Empty bait vector expressing λcI; CmR	Stratagene
pTRG	Target vector expressing the α-subunit of RNA polymerase; TetR	Stratagene
pLGF2	Positive control bait vector with LGF2 fused to the C-terminus of □cI; CmR	Stratagene
pGAL11	Positive control target vector expressing Gal11 fused to the C-terminus of the α -subunit of RNA polymerase; TetR	Stratagene
pUC19	Blue/white selection cloning vector; AmpR	NEB
pGEM-T easy	Blue/white selection cloning vector with A overhangs ; AmpR	Promega
pTB674lux	*luxABCDE* controlled by the *Mtb whiB7* promoter region (up to 674 nucleotides upstream of *Rv3197a*) replacing the HSP60 promoter in the integrative vector pMV361; KanR	This Study
pLUXon	Constitutively expressed *luxABCDE* using HSP60 promoter in the integrative vector pMV361; KanR	This Study
pMS689GFP	*egfp* controlled by the *M. smegmatis whiB7* promoter (up to 689 nucleotides upstream) in the promoterless, multi-copy pMycVec1; KanR	This Study
pGFPon	Constitutively expressed *egfp* using HSP60 promoter on the multi-copy vector pMV261; KanR	This Study
p361comp.apra	Modified pMV361 vector with the HSP60 promoter replaced by *whiB7* under its own promoter and kanamycin resistance replaced by apramycin resistance; ApraR	This Study
pMS497GFP	*egfp* controlled by the *M. smegmatis whiB7* promoter (up to 497 nucleotides upstream) in the promoterless, multi-copy pMycVec1; KanR	This Study
pMS483GFP	*egfp* controlled by the *M. smegmatis whiB7* promoter (up to 483 nucleotides upstream) in the promoterless, multi-copy pMycVec1; KanR	This Study
pMS438GFP	*egfp* controlled by the *M. smegmatis whiB7* promoter (up to 438 nucleotides upstream) in the promoterless, multi-copy pMycVec1; KanR	This Study
pBTW7	Bait WhiB7 fused to the C-terminus of λcI; CmR	This Study
pBTW7ΔC19	Bait WhiB7 lacking the AT-hook fused to the C-terminus of λcI; CmR	This Study
pBTW7mid	Bait WhiB7 fragment, amino acids 50-80, fused to the C-terminus of λcI; CmR	This Study
pBTW7epy	Mutant of pBTW7ΔC19 expressing an AT-hookless WhiB7 W65Y fused to the C-terminus of λcI; CmR	This Study
pBTW7vey	Mutant of pBTW7ΔC19 expressing AT-hookless WhiB7 E63V P64E W65Y fused to the C-terminus of λcI; CmR	This Study
pBTW7d	Mutant of pBTW7ΔC19 expressing AT-hookless WhiB7 E63D fused to the C-terminus of λcI; CmR	This Study
pBTW71d	Mutant of pBTW7ΔC19 expressing AT-hookless WhiB7 E71D fused to the C-terminus of λcI; CmR	This Study
pBTW748	Mutant of pBTW7ΔC19 expressing AT-hookless WhiB7 C48A fused to the C-terminus of λcI; CmR	This Study
pBTW74548	Mutant of pBTW7ΔC19 expressing AT-hookless WhiB7 C45A C48A fused to the C-terminus of λcI; CmR	This Study
pSigASM	Target SigA fused to the C-terminus of the α-subunit of RNA polymerase; TetR	This Study
pTRG170	Target Region 4 of SigA fused to the C-terminus of the α -subunit of RNA polymerase; TetR	This Study
pTRG170.515	Target Region 4 of SigA with the R515H mutation fused to the C-terminus of the α -subunit of RNA polymerase; TetR	This Study
pETB7sm	pET19b derivative for the expression of 10xHis-WhiB7; AmpR	This Study
pETB7epy	Mutant of pETB7sm expressing 10xHis-WhiB7 W65Y; AmpR	This Study

Plamids	Description	Reference
pETB7vey	Mutant of pETB7sm expressing 10xHis-WhiB7 E63V P64E W65Y; Amp^R	This Study
pETB7d	Mutant of pETB7sm expressing 10xHis-WhiB7 E63D; AmpR	This Study
pETB748	Mutant of pETB7sm expressing 10xHis-WhiB7 C48A; AmpR	This Study
pETB74548	Mutant of pETB7sm expressing 10xHis-WhiB7 C45A C48A; AmpR	This Study
pSigA	pColDuet-1 derivative for the expression of strepII-SigAC170; KanR	This Study
pSigAB7	pColDuet-1 derivative for the co-expression of 10xHis-WhiB7 and strepII-SigAC170; KanR	This Study
pSigAB748	Mutant of pCDR43B7 co-expressing strepII-$SigA_{C170}$ and 10xHis-WhiB7 C48A; KanR	This Study
pSigAB74548	Mutant of pCDR43B7 co-expressing strepII-$SigA_{C170}$ and 10xHis-WhiB7 C45A C48A; KanR	This Study
pR4B7	pColDuet-1 derivative for the co-expression of 10xHis-WhiB7 and strepII-SigAC82; KanR	This Study
pFB7KI	pUC19 derivative containing a WhiB7 with a N-terminal 3xFLAG for insertion into *M. smegmatis*; AmpR	This Study
pFB7	pMV261 derivative for constitutive expression of WhiB7 with a N-terminal3xFLAG epitope; KanR	This Study
pFB7AT	pMV261 derivative for constitutive expression of WhiB7 with a N-terminal3xFLAG epitope and lacking the C-terminal AT-hook; KanR	This Study
pFB7d	pMV261 derivative for constitutive expression of WhiB7with a N-terminal 3xFLAG epitope and a WhiB7 E63D mutation; KanR	This Study
pB7fun	pMV261 derivative for constitutive expression of the WhiB7 functional region (WhiB7ΔN19C6); KanR	This Study
pSig515	pYUB854 derivative with mutated SigA (R515H); HygR	This Study
pSig515KI	pSig515 derivative with mutated SigA (R515H) including expanded lower region for insertion into *M. smegmatis*; HygR	This Study
pERM.hyg	Constitutively expressed *ermMT* (*Rv1958*) using HSP60 promoter in the integrative vector pMV361.hyg; HygR	This Study
pORFdelGFP	*egfp* controlled by the *M. smegmatis whiB7* promoter (up to 229 nucleotides upstream) in the promoterless, multi-copy pMycVec1; KanR	This Study
pGEM-3637/8	pGEM-T easy containing *MSMEG_3637/8* and surrounding region; AmpR	This Study
pGEM-3637/8KO	pGEM-3637/8 derivative cotanining a hygromycin insertion from pYUB854 for deletion of *MSMEG_3637* and *MSMEG_3638*; AmpR HygR	This Study
pGEM-3027	pGEM-T easy containing *MSMEG_3027* and surrounding region; AmpR	This Study
pGEM-3027KO	pGEM-3027 derivative containing a hygromycin insertion from pYUB854 for deletion of *MSMEG_3027*; AmpR HygR	This Study
pGEM-4269	pGEM-T easy containing *MSMEG_4269* and surrounding region; AmpR	This Study
pGEM-4269KO	pGEM-4269 derivative containing a hygromycin insertion from pYUB854 for deletion of *MSMEG_4269*; AmpR HygR	This Study
pGEM6099	pGEM-T easy containing *MSMEG_6099* and surrounding region; AmpR	This Study
pGEM6099KO	pGEM-6099 derivative containing a hygromycin insertion from pYUB854 for deletion of *MSMEG_6099*; AmpR HygR	This Study
pGEM-3493/4	pGEM-T easy containing *MSMEG_3493/4* and surrounding region; AmpR	This Study
pGEM-3493KO	pGEM-3493/4 derivative containing a hygromycin insertion from pYUB854 for deletion of *MSMEG_3493*; AmpR HygR	This Study
pGEM-3494KO	pGEM-3493/4 derivative containing a hygromycin insertion from pYUB854 for deletion of *MSMEG_3494*; AmpR HygR	This Study
pGEM-3493/4KO	pGEM-3493/4 derivative containing a hygromycin insertion from pYUB854 for deletion of *MSMEG_3493*/*3494*; AmpR HygR	This Study

Plamids	Description	Reference
p0385OV	pMV261 derivative for constitutive expression of *MSMEG_0385*; KanR	This Study
p0688OV	pMV261 derivative for constitutive expression of *MSMEG_0688*; KanR	This Study
p2691OV	pMV261 derivative for constitutive expression of *MSMEG_2691*; KanR	This Study
p2779OV	pMV261 derivative for constitutive expression of *MSMEG_2779*; KanR	This Study
p3374OV	pMV261 derivative for constitutive expression of *MSMEG_3374*; KanR	This Study
p3637OV	pMV261 derivative for constitutive expression of *MSMEG_3637*; KanR	This Study
p5121OV	pMV261 derivative for constitutive expression of *MSMEG_5121*; KanR	This Study
p5270OV	pMV261 derivative for constitutive expression of *MSMEG_5270*; KanR	This Study
p4060L	pYUB854 derivate with *MSMEG_4060* lower region; HygR	This Study
p4060KO	p4060L derivative with added *MSMEG_4060* upper region for insertion into M. smegmatis; HygR	This Study
p4060OV	pMV261 derivative for constitutive expression of *MSMEG_4060*; KanR	This Study

Resistances are labeled as: CmR = chloramphenicol; KanR = kanamycin; HygR = hygromycin; ApraR = apramycin; AmpR = ampicillin; TetR = tetracycline

Table 14. Summary of oligonucleotides

Name	Sequence
261seq_F	TTACGGGTCTTGTTGTCGTT
261seq_R	CCCGTTGAATATGGCTCATAAC
pBTseq_R	CCAGTTTGCTCAGGCTCTCC
pTRGseq_F	CATTCTGGCTGAACAACTGG
pTRGseq_R	ACGCTCAGTGGAACGAAAAC
pMycVec1seq_F	GGCTTGTCCAAGGGTGTATC
pMycVec1seq_R	GCCTTTTTGCGTTTAATACTG
pMV361lux_seqF1	TTACGGGTCTTGTTGTCGTT
pMV361lux_seqF2	ATTAGGTCGCATCTCTGAGG
pMV361lux_seqF3	ATTAGGTCGCATCTCTGAGG
pMV361lux_seqF4	CGATGCTTTAACAACAGGCTA
pMV361lux_seqF5	GGTGCGAAAAGTGTATTGCT
pMV361lux_seqF6	TAATTGGGCGGTAGAGCAT
pMV361lux_seqF7	GGATGTTGCGGTTGAAATAG
pMV361lux_seqF8	TTTGGTTGGGAAGATTTAGC
pMV361lux_seqF9	TGGGACCAGATAGATTTAATGC
pMV361lux_seqR1	CCCGTTGAATATGGCTCATAAC
pMV361lux_seqR2	TGGGACCAGATAGATTTAATGC
pMV361lux_seqR3	AAATGTTCAAATGACGGTTCA
pMV361lux_seqR4	GCAAAACCAGACGCAATAAT
pMV361lux_seqR5	AAACAAGCTCGCTGATCGTA
pMV361lux_seqR6	CCATCTTTGCCCTACCGTAT
pMV361lux_seqR7	AAGCATGGGGATTTACAGAT
pMV361lux_seqR8	CACGGGATTGATTTCGTAAC
pMV361lux_seqR9	TACCAAGCAAACCAAACTCC
M13R	CAGGAAACAGCTATGACC
prAB47a	TCCATTGCGATGACTGCTC
prAB48	GTTCTCGGCGAACCACAG
uORF_F	CTGGCAACGAGAAGGTAAGG
uORF_R	GTACAACGGAAGGAATGAACC
prAB49	CCAAAAACCATCTGCTGGAG

Name	Sequence
prAB50	AGGTTGCCTTCCTGGATGAG
TBpromF	CGTAAACGTTGGTGTGAGACGTGTGCAGC
TBpromR	CGTTGAATTCTCCTGTTTCACCTGCTTCCTGGTC
eGFP_F	AAGCTTATGGTGAGCAAGGGCGAGG
eGFP_R	TCTAGAGATATCTTACTTGTACAGCTCGTCCATG
smegpromF	CTATCGATAAGTGCCTGCCTACGTGGT
smegpromR	ACAAGCTTAGCAGTCATCGCAATGGA
HSPGFP_F	TATAATGGATCCATGGTGAGCAAGGGCGAGGA
HSPGFP_R	TAATAGAATTCCTTACTTGTACAGCTCGTCCATG
B7comp_F	TAATACTCTAGAATTCGTAAAGATCGTGCCAAAACC
B7comp_R	TAATACAAGCTTGTCATTGCCACCGAACTGGTTC
707apra_F	TACATCAAGCTTGCTGACGCCGTTGGATACACC
707apra_R	TACATCACTAGTGGTTGAGGTAGCCGAAGAGCAGC
enrich_C primer	CCAGTGAGCAGAGTGACGAGCCCCCCCCCCC
TSS_adaptor	CCAGTGAGCAGAGTGACGAG
whiB7_TSS58	GGCGTCTGATGCGGCATG
GFPsub_R	TAATAGAATTCCTTACTTGTACAGCTCGTCCATG
438_F	TAATACAACGTTCTGGCAACGAGAAGGTAAGGG
497_F	TACCATCGATGCAGGTAGAAAATAGGTTGTGCG
483_F	TACCATCGATCGCGGTTGTGCGATTCAGCTGCTAG
GFPsubX_R	ATGCTCTAGACTTACTTGTACAGCTCGTCCATGC
B7smF	TAATAGAATTCGACTGCTCCGACCACGGG
B7smReco	TAATAGAATTCGGGGCGGTCGATCAGGC
B7smR_ATeco	TAATAGAATTCTCACGCGACAATGCTTCCGC
B7midFrag_F	AATTCGCTGACCGCGGCGCTCGAACGGCAGGAACCGTGGGGTGTCTGGGGTGGC GAGATCCTCGACCGCGGAAGCATTGTCGCGTGA
B7midFrag_R	TCGATCACGCGACAATGCTTCCGCGGTCGAGGATCTCGCCACCCCAGACACCCCA CGGTTCCTGCCGTTCGAGCGCCGCGGTCAGCG
B7_EPY_F	GCGCTCGAACGGCAGGAACCGTACGGTGTCTGGGGTGGCGAG
B7_EPY_R	CTCGCCACCCCAGACACCGTACGGTTCCTGCCGTTCGAGCGC
B7_VEY_F	GCGCTCGAACGGCAGGTGGAGTACGGTGTCTGGGGTGGCGAG
B7_VEY_R	CTCGCCACCCCAGACACCGTACTCCACCTGCCGTTCGAGCGC
B7_D_F	GCGCTCGAACGGCAGGACCCGTGGGGTGTCTGGGGTGGCGAG
B7_D_R	CTCGCCACCCCAGACACCCCACGGGTCCTGCCGTTCGAGCGC
B7_71D_F	GGTGTCTGGGGTGGCGACATCCTCGACCGCGGAAGC
B7_71D_R	GCTTCCGCGGTCGAGGATGTCGCCACCCCAGACACC
B7_48_F	CCAAGGCCCTGTGCGCGGGGGCCCCGATCCGTGTGCAGTGCC
B7_48_R	GGCACTGCACACGGATCGGGGCCCCCGCGCACAGGGCCTTGG
B7_4548_F	CCTTGAGCGGGCCAAGGCCCTGGCCGCGGGGGCCCCGATCCGTGTGCAGTGCC
B7_4548_R	GGCACTGCACACGGATCGGGGCCCCCGCGGCCAGGGCCTTGGCCCGCTCAAGG
SigAsmF	TAATAGAATTCTGGCAGCGACAAAGGCAAG
SigAsmR	TAATCACTAGTCTAGTCCAGGTAGTCGCGCAGC
mutR42_F	GTCCAAGACCATGTCGAAGCTGCACCACCCGAGCCGTTCGCAGGTG
mutR42_R	CACCTGCGAACGGCTCGGGTGGTGCAGCTTCGACATGGTCTTGGAC
SRG-15	TGCCCATATGACTGCTCCGACCACGG
SRG-16	AAAGGATCCGATCAGGCGGCGGC
CD_R42SM_F	CATATGGCTAGCTGGAGCCACCCGCAGTTCGAAAAAGGCGCGATGGCCGACCAG GCCC
CD_R42SM_R	GGTACCTTACTAGTCCAGGTAGTCGCGCAGC
CD_R42short_F	CATATGGCTAGCTGGAGCCACCCGCAGTTCGAAAAAGGCGCGGTGGACGCCGTG TCGTTC
pMycB7	TCTCGGCTCGATGATCC
B7+185	ACCAGCGGCGGCGTGAG

Name	Sequence
pB7GFP_6F	TAATACAACGTTCGTAAAGATCGTGCCAAAACC
pB7GFP_7F	TAATACAACGTTCCGACGACGCCGCACTC
R4D_R	TAATATCTGCAGGCGGCGCAATGGCAGC
pMV261F	TTACGGGTCTTGTTGTCGTT
pMV261R	ATTGCGAAGTGATTCCTCC
FB7L_F	TAATAGGTACCAGACGGAGAATTCGTCATCG
FB7L_R	TAATACCATGGCAATGGACATGTGTTTTTCC
FB7R_F	TTAATACCATGGACTACAAGGACCACGATGGCGACTACAAGGACCACGATATCG ACTACAAGGACGATGACGACAAGATGACTGCTCCGACCACG
FB7R_R	TAATTAAGCTTGATCTCCGAATGGATGGAAG
HSP60F	CAGGAGCATTGCCGTTCC
HSP60R_pst	TAATAACTGCAGTGCGAAGTGATTCCTCCG
FlagB7smF	TAATACTGCAGATGGACTACAAGGACCACGATGG
FlagB7smR	TAATCAAGCTTGGGGCGGTCGATCAGGC
FlagB7smR_AT	TAATCAAGCTTTCACGCGACAATGCTTCCGC
SigAflank_F	TAATGTCTAGACAGCCGTTCGCAGGTGCTGC
SigAflank_R	TAATAGGTACCGCTTGTCAGAGTTGCGTTCATGG
SigAsmF	TAATAGAATTCTGGCAGCGACAAAGGCAAG
SigAsmR	TAATCACTAGTCTAGTCCAGGTAGTCGCGCAGC
Rv1988_F	TAATAGAATTCCATATGTCCGCCCTCGGACGGTC
Rv1988_R	TAATTAACGTTGGTGACTGGCAGGGGCGGTAA
ORFdel_F	TAATATATCGATGCAGGTAGAAAATAGGTTGTGCGATTCAGCTGCTAGGCTCTAG CCTCAGAAAGTCAACTCTGGCAACGAGAAGGTAAGGGGGTGTCCAAGCGTCGTC GCACC
P7tag	GTCTCGTGGGCTCGGAGATG
NX_pMMT7_out1	GGGTTGAGTGTTGTTCCAGTTTG
NX_pMMT7_out2	CCTTCTTGACGAGTTCTTCTGAGC
phiP5	AATGATACGGCGACCACCGAGATCTACACGCACGACCTGGGACTTATCAGCCAA CCTGTTA
phiMMT7seq_1	CGCACGACCTGGGACTTATCAGCCAACCTGTTA
3637F	CACGGAGTTGACCTTGGACATGAG
3637R	CTCGTGCAGTCCGAAACAGTTCAG
3637/8CHK	CGTGATCGGTGCGATAGACCATG
HYG_out	ACTGCTCGCCTTCACCTTCCTG
3027F	CTGGTGAAGGAGTACGAAGCCGTC
3027R	GCATGGTCACCGAGAAACCCAC
3027CHK	GCCGAGCCGACCAGTTCCG
HYG_out2	CACCTACAACAAAGCTCTCACCAACC
4269F	GCAGAGCCACCCAGGACAATAGAC
4269R	ATCAGCACGGTCCACAGCCTG
4269CHK	GACGCTGTGCTCGACGAAGATC
6099F	CGAATACGAGCTGACCGTCGAG
6099R	GTCGTCGCCAAACCTTTGACG
6099CHK	AAGGATGCCCACGCCGTTG
3494F	CTCATGCAGTTGCGTCAGGTG
3494R	GGGATCGAAGGGTTTGGTGTC
3494CHK	GTCGAGGTCCAGGTAGTTGATGTCG
261p2691F	TAATACTGCAGGTGCGACGCGCGCGCACCTCAGATG
261p2691R	TAATCAAGCTTGAGGAGTTCTGAGCCGAGAGTCCTACAG
261p2779F	TAATACTGCAGGTGACCTCTGCCGAACCGGCAC
261p2779R	TAATCAAGCTTGGTATCCCCTTGGGTCATCTCTATGCG)
261p3374F	TAATACTGCAGGTGAAGGTCCCTGAACTCACTGG
261p3374R	TAATCAAGCTTACGAATGAAGCAACGTAACAGGAC

Name	Sequence
261p3637F	TAATACCATGGGTGAAGTCGCGATGAGC
261p3637R	TAATCAAGCTTCACCGAACACATCACCCATTGG
261p5121F	TAATACTGCAGATGGTGCGTCAGCGCCGCTC
261p5121R	TAATCAAGCTTGCCTGCTGTTGTCGCTGAGTCTGC
261p5270F	TAATACTGCAGATGCGCATAGCCAGGCACATC
261p5270R	TAATCAAGCTTGGGCAACCTAGTGCCGGTAACC
261p0385F	TAATACCATGGCGAGTTATGGCACCC
261p0385R	TAATCAAGCTTTATAGGTGCATATCCCGATGCC
261p0688F	TAATACCATGGAACGCGTGACTACCCACCAG
261p0688R	TAATCAAGCTTGTGCGAGTGGGAATGCGAATGC
4060LF	TATTATCTAGATATTCCCGCAACTACCGGC
4060LR	TAATAGGTACCAACGGTGAGTTCGATCTCGAC
4060UF	TAATCAAGCTTCGGATTACTTCGCCAACAGCC
4060UR	TAATACCATGGTAGCTGCCGCCCTCGGTG
4060CHK	TACGCCTACTCGCCTTATCGC
261p4060_F	TAATACTGCAGATGCACTCGGCCAGTACAGAGG
261p4060_R	TAATCAAGCTTACTCGTCCTTGTTTCATTCATTCC

6.1.3 MIC determination

M. smegmatis wild type or *whiB7* KO was inoculated into 3 mL of 7H9 and grown for 48-54 hours to a final OD_{600} of 6-8. The culture was diluted to an OD_{600} of 0.005 and 100 μL was added to 100 μL of antibiotic containing 7H9 at twofold serial dilutions across a 96 well plate (Costar 3370). The plate was incubated for 48 hours and 30 μL of sterile 10 mg/100mL (w/v) Rezazurin solution was added and the plate was incubated for an additional 24 hours. Wells which remained blue were deemed to contain an inhibitory concentration of antibiotic.

6.1.4 Disk Assay

M. smegmatis strains were grown in 3 mL 7H9 for two days (i.e., stationary phase). 7H9 agar (no tyloxapol) was prepared with a 15 mL 1.5 % (w/v) base and 7 mL 0.5 % (w/v) top agar. Once the base was solidified, the *M. smegmatis* strains were inoculated, to a final OD_{600} of 0.005, into the 7 mL top agar held at 50 ºC. The suspension was mixed and poured onto the agar base. When the agar solidified blank paper discs (BD 231039) were placed on the top agar and 7.25 μL antibiotic

solution was inoculated onto them. Amounts of spotted antibiotic were: 145 μg spectinomycin, 2.9 μg clarithromycin, 145 μg isoniazid, and 0.7 μg tetracycline. The plates were then incubated in a closed, non-airtight container with a beaker of water at 37 ºC for 48 hours.

6.1.5 mRNA isolation and quantification

M. smegmatis was grown to an OD_{600} of 0.6-0.8 and split into 30-50 mL aliquots. The appropriate amount of antibiotic was added to selected aliquots and the cultures are incubated for 1 hour. Four times culture volume of GTC buffer (5 M guanidine thiocyanate , 17 mM sodium lauroyl sarcosinate, 28.5 mM trisodium citrate, 0.5 % (v/v) Tween 80, 0.7 % (v/v) 2-mercaptoethanol) was added and the samples were incubated for 1 hour at room temperature. Samples were pelleted by centrifugation for 10 minutes, 5000 rpm, 4 ºC and the supernatant discarded. The pellets were suspended in 1mL QIAzol (Qiagen #79306) and transferred to a 2 mL screw cap tube (MBP #3488) containing ~100 μL of 0.1 mm glass beads (BioSpec #11079101). The tubes were beaten three times using a MP FastPrep-24 at 6.0 m/s for 45 s with 3-5 minute ice breaks. The samples were centrifuged for 5 minutes at 13000 rpm, 4 ºC and the supernatants were transferred to phase gel lock tubes (5 Prime #2302830). The tubes were incubated at room temperature for 5 minutes and 0.2 mL of ice cold chloroform was added. The tube contents were mixed by inversion for 15 s, incubated at room temperature for 3 minutes and finally centrifuged for 5 minutes at 13000 rpm, 4 ºC. The upper fraction was transferred to a 1.5 mL Eppendorf containing 550 μL of 30 mM sodium acetate in isopropanol, mixed well, and incubated overnight at -20ºC. The samples were centrifuged for 10 minutes at 13000 rpm, 4 ºC, the supernatant discarded, and the pellets were washed with 1 mL ice cold 75 % (v/v) ethanol. Samples were centrifuged for 5 minutes at 13000 rpm, 4 ºC and the supernatant discarded. The

pellets were dissolved in 90 µL RNase free water by incubation at 65 ºC for 10 minutes. Samples were then treated for 30 minutes at 37 ºC with Turbo DNase (Ambion #AM2239) and finally the RNA was isolated by RNAspin mini columns (GE #25-0500-72) according to manufacturer instructions.

The qScript cDNA synthesis kit (Quanta #95047-100) was used to reverse transcribe a total of 100 ng of RNA per 20 µL reaction as per manufacturer instructions. The cDNA samples were diluted 1/10 and 2.5 µL was used per 25 µL quantitave PCR rection. A mix of PerfeCTa SYBR green supermix (Quanta #95054-050), cDNA and primers (1 µM each) was run on a BioRad Opticon2:

95 ºC for 3 minutes
95 ºC for 30 s
55 ºC for 30 s
72 ºC for 30 s (read)
repeat from step 2, 34 times

A standard curve of genomic DNA was used calculate concentrations, and a non-reverse transcribed control to estimate DNA contamination. Primers used for *whiB7* were prAB47a and prAB48. Primers used for the *uorf* were uORF_F and uORF_R. Concentrations were standardized to an internal control, *mysA,* using primers prAB49 and prAB50. Fold increase of *whiB7* was calculated against a non-treated sample run in parallel.

6.2 Methods relating to chapter 2

6.2.1 Methods relating to 2.3.1

6.2.1.1 Construction of the Lux reporters

A DNA fragment containing nucleotides -2 to -674 upstream of the annotated start codon of *whiB7 (Rv3197a)* was amplified from *Mycobacterium tuberculosis* H37Rv genomic DNA by

PCR using the forward and reverse primers TBpromF and TBpromR. The fragment was digested with AclI and EcoRI and cloned into pMV361 digested with the same enzymes to create pMV361-P_{B7TB}. The EcoRI fragment containing the *luxABCDE* genes was isolated from pAmilux (*124*) and cloned into EcoRI digested pMV361 and pMV361-P_{B7TB} to create the HSP60 promoter driven, constitutively active pLUXon and the antibiotic inducible, *whiB7* promoter driven pTB7lux, respectively.

6.2.1.2 Luminescence time course

M. smegmatis harbouring pTB7lux was inoculated into 3 mL of 7H9 + 30 μg/mL kanamycin and grown for 55-60 hours, followed by an incubation at room temperature for 12-15 hours. The culture was diluted to an OD_{600} of 0.01-0.005 into 3 mL of kanamycin free 7H9 and grown to an OD_{600} of 0.6-0.8, ~20-24 hours. Finally, the culture was diluted to an OD_{600} of 0.2 and 200 μL was distributed into a black, clear bottom 96 well plate (Costar 3631). The appropriate compound was added to the desired concentration and the plate was placed immediately into a VarioskanFlash (Thermo Scientific), and the Luminescence time course program was run using SkanIt RE 2.4.3. Briefly, the program raised the temperature to 37 ºC and without waiting shook the plate for 15 s at 420 rpm, followed by measuring the OD_{600} and finally measuring luminescence for 1000 ms in a kinetic loop every 5 minutes six times. The shaking, OD_{600} reading and kinetic loop was repeat 6 times followed by shaking, OD_{600} reading and a luminescence reading every 30 minutes six times, then every 1 hour two times, and finally, every 3 hours twice. *M. smegmatis* wild type and *whiB7* KO harbouring pLUXon were prepared in identical fashion but diluted to an OD_{600} of 0.2 after the room temperature incubation and the time course run.

6.2.2 Methods relating to 2.3.2

6.2.2.1 Construction of the GFP reporters

A DNA fragment containing the *egfp* gene from pEGFP (Clontech) was amplified by PCR using the forward and reverse primers eGFP_F and eGFP_R. The fragment was cloned, using the polymerase added A overhang, into pGEM-Teasy (Promega) to create pAB2. A DNA fragment containing the first three amino acids of the annotated *whiB7 (MSMEG_1953)* and 689 nucleotides upstream was amplified from the genome of *M. smegmatis* by PCR using the forward and reverse primers smegpromF and smegpromR. The fragment was cloned into pGEM-Teasy to create pAB6. pAB6 was digested with ClaI and HindIII and the *whiB7* promoter containing fragment was cloned into pMycVec1 digested with the same enzymes to create pAB7. pAB2 was digested with HindIII and XbaI and the *egfp* containing DNA fragment was cloned into pAB7 digested with the same enzymes to create antibiotic inducible, *whiB7* promoter driven pMS689GFP.

The *efgp* from pMS689GFP was amplified by PCR using the forward and reverse primers HSPGFP_F and HSPGFP_R. The PCR fragment was digested with BamHI and EcoRI and cloned into pMV261 digested with the same enzymes, to create the HSP60 promoter driven, constitutively active pGFPon.

6.2.2.2 Complementation of *whiB7* KO strain

The *whiB7* gene including its 520 bp upstream and 152 bp downstream regions was amplified by PCR from the *M. smegmatis* genome using primers B7comp_F and B7comp_R. The PCR fragment was cloned into pMV361, replacing the HSP60 promoter, using XbaI and HindIII to

construct p361comp. A 1347 bp region of pAB707 containing the apramycin resistance gene *aac(3)IV* was amplified by PCR using the primers 707apra_F and 707apra_R. The product was cloned into p361comp using HindIII and SpeI to construct p361comp.apra. The integrative p361comp.apra was then used to complement the pMS689GFP containing *M. smegmatis whiB7* KO generating the new strain *whiB7* KOC.

6.2.2.3 Fluorescence time course

M. smegmatis harbouring pMS689GFP was inoculated into 3 mL of 7H9 + 30 μg/mL kanamycin and grown for 48-54 hours until a final OD_{600} of 6-8. The culture was diluted to an OD_{600} of 0.01-0.005 into 3 mL of kanamycin free 7H9 and grown to an OD_{600} of 0.6-0.8, ~20-24 h. Finally, the culture was diluted to an OD_{600} of 0.2 and 200 μL was distributed into a black, clear bottom 96 well plate. The appropriate compound was added to the desired concentration and the plate was covered with Microseal® 'B' Film (BioRad MSB1001), placed immediately into a VarioskanFlash, and the GFP time course program was run. Briefly, the program raised the temperature to 37 ºC and without waiting shook the plate for 15 s at 420 rpm, followed by measuring the OD_{600} and finally measuring fluorescence under default settings by excitation at 488nm and measuring emission at 509 nm. The shaking, OD_{600} measurement and fluorescence measurement was repeated every 30 minutes. *M. smegmatis* wild type and *whiB7* KO harbouring pGFPon was prepared in identical fashion but diluted to an OD_{600} of 0.2 after the 49-54 hour incubation and the time course run.

6.2.3 Methods relating to 2.4.1

6.2.3.1 Transcription start site determination

Transcriptional start site of the antibiotic induced *whiB7* promoter was identified by essentially unmodified Directed Mapping of Transcription Start Site (DMTSS) method developed by Mendoza-Vargas *et al*. (*135*). Briefly, RNA was isolated from retapamulin treated *M. smegmatis* by the method mentioned above. About 1.5 µg total RNA was mixed with 700 pmol of a radom hexamer primer (NNNNNN) and the solution was heated to 70 ºC for 10 minutes followed by incubation on ice for 5 minutes. cDNA was generated using Transcriptor reverse transcriptase (Roche 03 351 317 001) according to manufacturer instruction and isolated by the QIAquick PCR purification kit (Qiagen 28106). A guanine tail was added to the 3' end of the cDNA library using Terminal transferase (Roche 03 333 566 001) according to manufacturer's instruction and the cDNA was once again isolated by the QIAquick PCR purification kit. Linear amplification of the tailed cDNA library was carried out using Dynazyme EXT in combination with the enrich_C primer with the protocol:

94 ºC for 10 minutes
94 ºC for 1 minute
50 ºC for 1 minute
72 ºC for 3 minutes
Repeat from step 2, 34 times
72 ºC for 10 minutes

The cDNA was isolated by the QIAquick PCR purification kit. About 15 ng of the DNA was used per 50 µL PCR reaction using Dynazyme EXT with primers TSS_adaptor and whiB7_TSS58 and the protocol:

94 ºC for 3 minutes
94 ºC for 30 s
60 ºC for 10
72 ºC for 30 s
Repeat from step 2, 34 times

72 ºC for 5.5 minutes)

A single PCR product of about 200 bp was observed by agarose gel electrophoresis. This product was cloned, using the polymerase added A overhang, into pGEM-Teasy and transformed into *E. coli* TOP10. Several white transformants visualized on LB+ampicillin+Xgal+IPTG agar plates were transferred to liquid media, and plasmid DNA was isolated using the QIAprep Spin Miniprep Kit (Qiagen 27106). The plasmids were sent for sequencing at the UBC Vancouver campus NAPS unit (http://naps.msl.ubc.ca/) using the M13R primer.

6.2.4 Methods relating to 2.4.2

6.2.4.1 Sub-cloning the GFP reporter promoter

Shorter fragments of the *whiB7* region were amplified from pMS689GFP. The PCR product of GFPsub_R and 438_F was digested with AclI and cloned into ClaI and EcoRV digested pMycVec1 to create pMS438GFP. The PCR products of 497_F and 483_F in combination with GFPsubX_R were digested with ClaI and XbaI and cloned into ClaI/XbaI digested pMycVec1 to create pMS497GFP and pMS483GFP, respectively.

6.2.5 Methods relating to 2.5.1

6.2.5.1 Construction of bait constructs

whiB7 and a truncated, AT-hookless *whiB7* (ΔC19) were amplified by PCR from the *M. smegmatis* genome using the forward primer B7smF and the reverse primers B7smReco and B7smR_ATeco, respectively. The PCR products were digested by EcoRI and ligated into similarly digested pBT to construct pBTW7 and pBTW7ΔC19. A 26 amino acid fragment of WhiB7, spanning the region downstream of the last cysteine and upstream of the AT hook, was

synthesized; B7midFrag_F and B7midFrag_R. The oligonucleotides were dissolved to a concentration of 10 pmol/ μL and mixed at equal volumes. The mixture was heated to 95 ºC for 5 minutes and let slowly cool to room temperature. The resulting dimers were ligated into EcoRI/ XhoI digested pBT to construct pBTW7mid.

6.2.5.2 Construction of pBT7ΔC19 mutants

The QuickChange Lightning mutagenesis kit was used to mutate pBT7ΔC19 to change the EPW region upstream of the GVWGG turn in WhiB7. The sequence was mutated to the WhiB3 EPY sequence using the primers B7_EPY_F and B7_EPY_R to construct pBTW7epy, and to the WhiB3 VEY sequence using the primers B7_VEY_F and B7_VEY_R to construct pBTW7vey. The glutamate was also mutated to an aspartate the primers B7_D_F and B7_D_R and to construct pBTW7d. A glutamate further downstream (E71) was also mutated using the primers B7_71D_F and B7_71D_R to construct pBTW71d. The fourth cysteine (C-terminal of the CXXC motif) was mutated to an alanine using the primers B7_48_F and B7_48_R to construct pBTW748. Lastly, the CXXC motif cysteines were mutated to alanines using primers B7_4548_F and B7_4548_R to construct pBTW74548.

6.2.5.3 Construction of pTRG170

sigA from *M. smegmatis* (*MSMEG_2758*) was amplified by PCR using the primers SigAsmF and SigAsmR. The PCR product was digested with EcoRI and SpeI, and ligated into similarly digested pTRG to construct pSigASM. pSigASM was digested with EcoRI and NcoI, and self-ligated. This resulted in a 901bp deleted region spanning from immediately downstream of the pTRG BamHI site to the ATG within the NcoI site in *sigA* leading to pTRG170. This expressed

Region 4 of *M. smegmatis* SigA (aa 297-466) which is 100% similar (99.6% identical) to the Region 4 of SigA from *Mtb* (aa 359-528). Previous studies investigating WhiB3/ SigA interaction used aa 369-528 (*70*).

6.2.5.4 Construction of pTRG170.515

The QuickChange Lightning mutagenesis kit (Stratagene) was used to mutate pR42 with the primers mutR42_F and mutR42_R to construct pTRG170.515. This resulted in a MSMEG_2758 G1358A mutation leading to expression of SigA R453H. This corresponds to the *Mtb* SigA R515H.

6.2.5.5 Two-hybrid assay

The bait and target vectors were co-transformed into the BacterioMatch II two-hybrid reporter strain by heat shock. Cells were recovered for 1 hour at 37 ºC in LB broth. After they were washed twice with 1 mL of $M9^+$ His-dropout broth (866 mL Salt Base (55 mM Na_2HPO_4, 25.5 mM KH_2PO_4, 9.9 mM NaCl, 21.6 mM NH_4Cl) , 130 mL Solution I (3.08 % glucose, 1.54 mM adenine, 5.92 g/L -His SO supplement (Clontech #630415)) and 4 mL Solution II (0.25 M $MgSO_4$, 0.25 M thiamine, 2.5 mM $ZnSO_4$, 25 mM $CaCl_2$)). Transformants were incubated an additional hour in $M9^+$ His-dropout broth. Individual co-transformants were grown overnight in 3 mL of Nonselective screening medium (NSM; $M9^+$ His-dropout broth supplemented to 50 μM IPTG). Cultures were diluted and 8 μL was spotted on both NSM and selective screening medium (SSM; NSM supplemented to 5 mM 3-amino-1,2,4-triazole) agar plates and grown for 24 hours at 37 ºC. Plates were then incubated for an additional 24 hours at room temperature.

6.2.5.6 Construction of 10xHis:WhiB7 expression vector

whiB7 was PCR amplified from the *M. smegmatis* genome by the SRG-15 and SRG-16 primers. The PCR product was ligated into the pGEM-T Easy vector to construct pGEMB7sm. *whiB7* was cut from pGEMB7sm was using NdeI and BamHI and ligated into similarly digested pET19b (Novagen) to construct pETB7sm.

6.2.5.7 Construction of 10xHis:WhiB7 expression vector mutants

The QuickChange Lightning mutagenesis kit was used to mutate pETB7sm to change WhiB7's EPW sequence (aa 63-65) immediately upstream of the tryptophan-containing turn. The sequence was mutated to the WhiB3 like EPY using the primers B7_EPY_F and B7_EPY_R to construct pETB7epy, and to the WhiB3 like VEY using the primers B7_VEY_F and B7_VEY_R to construct pETB7vey. The glutamate was also mutated to an aspartate using the primers B7_D_F and B7_D_R to construct pETB7d. The fourth cysteine (C-terminal of the CXXC motif) was mutated to an alanine using the primers B7_48_F and B7_48_R to construct pETB748. Lastly, the CXXC motif cysteines were mutated to alanines using primers B7_4548_F and B7_4548_R to construct pETB74548.

6.2.5.8 Construction of WhiB7 and SigA co-expression vector

Region 4 of *M. smegmatis sigA* was amplified by PCR from pTRG170 using the primers CD_R42SM_F and CD_R42SM_R. This added an N-terminal strepII tag. The product was digested with NdeI and KpnI, and cloned into similarly digested pColaDuet-1 (Novagen) to construct pSigA. 10xHis-tagged *whiB7* was extracted from pETB7sm using NcoI and BamHI and cloned into similarly digested pSigA to construct the co-expression vector pSigAB7.

6.2.5.9 Construction of co-expression vector mutants

Mutant forms of 10xHis-WhiB7 were extracted by NcoI/ BamHI from pETB748, and pETB74548 and cloned into similarly digested pSigAB7 to construct pSigAB748 and pSigAB74548, respectively.

6.2.5.10 WhiB7 and SigA co-expression and pulldown

pSigAB7 (and pSigA as a negative control) was transformed into *E. coli* Rosetta2 (DE3) and plated on LB agar containing kanamycin (kan) and chloramphenicol (cm). A single transformant was inoculated into 3 mL of LB broth supplemented with kan and cm, and grown overnight at 37 ºC, 200 rpm. The culture was diluted 1/ 100 into 100 mL LB supplemented with kan and cm, and grown for 2 h 37 ºC, 200 rpm. A sample was taken and IPTG was then added to a final concentration of 1 mM and the culture incubated for an additional 2 h.

Cells were pelleted by centrifugation (3500 g) and the pellet was suspended in 1 mL lysis buffer. The suspension was then sonicated on ice for 20 s three times with 1 minute breaks. A sample was taken and the lysed suspension was centrifuged at 16,000 g for 10 minutes. A sample of the supernatant was taken before the supernatant was transferred to a 2 mL Eppendorf with 200 µL of Ni-NTA prewashed three times with 5 volumes of wash buffer. The mixture was continuously inverted at 4 ºC for 30 minutes. The tube was centrifuged at 16,000 g for 2 minutes. The supernatant was removed and the Ni-NTA resin was washed with 5 volumes of wash buffer with 50, 75, and finally 100 mM imidazole. 150 µL of elution buffer was then added and the tubes were once again inverted at 4 ºC for 30 minutes. After, the tubes were centrifuged and the supernatant transferred to a fresh tube. The supernatant and previous samples were mixed 1:1

with 4x Sample buffer (0.25 M tris-HCl, 0.28 M sodium dodecyl sulfate, 40 % (v/v) glycerol, 20 % (v/v) 2-mercaptoethanol, 5 drops 1 % (w/v) bromophenol blue, pH 6.8), and the samples were separated using a 10 % Tricine-SDS PAGE gel as described by Schagger (*200*). The gel was then stained using GelCode (Thermo Scientific) as per manufacturer's instruction.

6.2.5.11 UV spectroscopy

A Hitachi U-3010 was used to monitor absorbance between 300 nm and 600 nm with a scan rate of 300 nm/minute. For the diamide treated samples, diamide was added to a final concentration of 7 mM and the spectra were taken a 0, 5, 10, 20 and 30 minutes. Diamide interfered with measurements below ca. 380 nm.

6.2.5.12 Construction of WhiB7 and region 4 of SigA co-expression vector

A similar alignment to that used by Vassylyev *et al.* (*90*) was used to identify the discreet regions of *M. smegmatis* SigA. The primers CD_R42short_F and CD_R42SM_R were used to PCR amplify region 4 of SigA. The product was then digested with NdeI/ KpnI and cloned into similarly digested pSigAB7 to construct the 10xHis-WhiB7 and strepII-SigA(region 4) co-expression vector pR4B7.

6.2.6 Methods relating to 2.5.2

6.2.6.1 *In vitro* run-off templates

Linear templates for *in vitro* transcription were prepared using PCR. The *whiB7* promoter (-103/+185) and AT-rich sequence lacking promoter (-92/+185), the '-' bases corresponding to sequence upstream of the transcription start site, were amplified from pMS497GFP and

pMS483GFP , respectively, using the primers pMycB7 and B7+185. Alternative templates with varied upstream and downstream lengths were amplified from pMS689GFP using the primer combinations pB7GFP_6F/B7+185, pB7GFP_7F/B7+185, pB7GFP_6F/R4D_R, and pB7GFP_7F/R4D_R , yielding -85/+185, -193/+185, -85/+225, and -193/+225 templates. The groEL2 promoter (-140/+184) was amplified from pMV261 using the primers pMV261F and pMV261R. Templates were amplified by Econotaq (Lucigen). Reaction mixtures were as per the manufacturer's instructions supplemented with 1.5 mM $MgCl_2$ and 5% (v/v) DMSO. PCR reactions were amplified as follows:

95 °C for 5 minutes
94 °C for 20
60 °C for 20
72 °C for 20 s
Repeat from step 2, 35 times
72 °C for 5 minutes

PCR products were isolated with GenElute PCR cleanup kit (Sigma) according to manufacturer's instructions with the exception that the DNA was eluted with a solution of 10 mM Tris (pH 8.5) and 30 mM sodium acetate.

6.2.6.2 Purification of RNA polymerase

M. smegmatis was grown in 7H9 to an OD_{600} of ~1. Cells were pelleted by centrifugation at 4000g for 30 minutes. This process was repeated enough times to gain a combined pellet weighing more than 30 g. RNAP was isolated as described previously (*201*) with the exceptions that the cells were sonicated 18 times and active fractions from the DNA-cellulose column were not concentrated. Active fractions were adjusted to a final concentration of 50 % (v/v) glycerol and then stored at -80 °C for direct use.

6.2.6.3 Purification of WhiB7

pETB7sm was transformed, by heat shock, into *Escherichia coli* Rosetta2 (DE3) and plated on LB agar containing ampicillin (amp) and chloramphenicol (cm). A single transformant was inoculated into 3 mL of LB broth supplemented with amp, cm, and 0.2 % (w/v) dextrose (dex) and grown overnight at 37 ºC, 200 rpm. The culture was diluted 1/ 100 into two flasks containing 1 L LB supplemented with amp, cm and dex and grown for 2 h 37 ºC, 200 rpm to an OD_{600} of ca. 0.2. The cultures were transferred to 16 ºC and incubated for 30 minutes at 200 rpm. Finally, isopropyl-beta-D-thiogalactopyranoside (IPTG) was added to a final concentration of 0.3 mM and the culture incubated for an additional 17 h.

Cells were pelleted by centrifugation (3500 g) and the pellet was suspended in 20 mL lysis buffer (50 mM Na_2PO_4, 300 mM NaCl, 10 mM imidazole, 50 µg/mL phenylmethanesulfonylfluoride, 5 mM 2-mercaptoethanol, pH 8). The suspension was flash frozen in liquid nitrogen and thawed on ice. The suspension was split equally (~ 15 mL fractions) into two 50 mL conical flasks and both were sonicated on ice for 30 s twelve times with 1 minute breaks using a CL4 sonicator (Mandel) at setting 3. The lysed cells were pelleted at 3500g for 20 minutes and the supernatants combined (~ 30 mL) and transferred to one ultracentrifuge tube. The supernatant was centrifuged using an Optima L-90k (Beckman) with a Type 70 Ti rotor at 30, 000 rpm for 30 minutes at 4 ºC. The supernatant was then filtered through a 0.45 µm filter (Mandel 229749).

A 10 mL syringe (BD) was used as a column containing 1 mL of Ni-NTA resin (Qiagen) held at 4 ºC. The column was washed with 6 column volumes (CV) of wash buffer (50 mM Na_2PO_4 pH8, 300 mM NaCl, and 10 mM imidazole) and the flow rate adjusted to 1 mL/minute. The filtered supernatant was then passed over the column resulting in the column turning brown.

The column was then washed with six 10 CV loads of wash buffer containing an increasing amount of imidazole (50, 60, 70, 80, 90, and 100 mM). Finally elution buffer (50 mM Na_2PO_4, 300 mM NaCl, 250 mM imidazole, pH 8) was applied to the column. This resulted in a clear, brown eluate. Fractions which were visibly dark brown were pooled together, DTT was added to a final concentration of 2 mM and aliquots were immediately frozen in liquid nitrogen and stored at -80 ºC.

6.2.6.4 *In vitro* run-off assay

DNA templates were pre-incubated for 2 minutes at 37 °C in transcription buffer (10 mM HEPES pH 8, 10 mM magnesium acetate, 80 mM potassium acetate, 0.1 mM DTT, 0.1 mg/mL acetylated BSA). WhiB7 (various concentrations, as indicated) or elution buffer were incubated for 2 minutes at 37 °C. For reactions in which diamide were used, WhiB7 or elution buffer were mixed with diamide before addition to the reaction. Transcriptions were initiated with RNAP and incubated for an additional 2 minutes at 37 °C. Reactions were then challenged with a mixture of NTP and heparin to limit transcription to a single round. All reactions had a final volume of 10 µl and final concentrations were as follows: transcription buffer, 16 nM template, diamide (7 mM, as indicated), 80 nM RNAP, 50 µg heparin ml^{-1}, 400 µM CTP, 400 µM UTP, 400 µM ATP, 5 µM GTP and 111 kBq [α-^{32}P] GTP. Transcripts were elongated for 5 minutes at 37 °C and then terminated by the addition of 5 µl of loading buffer (1.5X transcription buffer with 0.1 % (w/v) bromophenol blue, 0.1 % (w/v) xylene cyanol and 7 M urea). Transcripts were electrophoresed through 8 % denaturing acrylamide gels and imaged using a Storage Phospor screen (Amersham Biosciences), scanned by a Typhoon 9400 (Amersham Biosciences) and quantified using ImageQuant 5.2 software (Amersham Biosciences). Heparin was supplied by Sigma, NTPs were

obtained from Amersham Biosciences and [α-^{32}P]GTP (111 TBq mmol^{-1}) was supplied by PerkinElmer Life Sciences.

6.2.7 Methods relating to 2.5.3

6.2.7.1 Construction of *M. smegmatis* FB7

The upstream region of *whiB7* was amplified from the *M. smegmatis* genome by PCR using the primers FB7L_F and FB7L_R. *whiB7* and its downstream region was amplified using FB7R_F and FB7R_R adding an N- terminal 3xFLAG tag to *whiB7*. The upstream region was digested with KpnI/NcoI, the downstream region with NcoI/HindIII and a three-way ligation was performed with KpnI/HindIII digested pUC19 to created pFB7KI. The 3xFLAG engineered *whiB7* was extracted from pFB7KI by KpnI/HindIII digestion and recombineered (*140*) into *M. smegmatis whiB7* KO. Recombinants were plated on 7H9 agar supplemented 4 μg/mL spectinomycin. Colonies were then checked for the loss of hygromycin (the resistance marker used for *whiB7* deletion) and restoration of resistance to spectinomycin, tetracycline and clarithromycin.

6.2.7.2 Construction of 3xFLAG::*whiB7* constitutively expressing vectors

The *groEL2* promoter (HSP60) was amplified by PCR from pMV261 using the primers HSP60F and HSP60R_pst. 3xFLAG::*whiB7* was amplified by PCR from pFB7KI using the primer FlagB7smF with either FlagB7smR for full length *whiB7* or FlagB7smR_AT for a shortened *whiB7* lacking the C-terminal AT hook (ΔC19). The HSP60 amplicon was digested with XbaI/PstI while the *whiB7* amplicons with PstI/HindIII. The fragments were combined into XbaI/HindIII digested pMV261 to construct the *whiB7* over-expressing pFB7 and AT-hook-less

whiB7 over-expressing pFB7AT. This assured the expression of the constructs without the addition of N-terminal *groEL2* bases still upstream of the usual pMV261 multiple cloning site. The QuickChange Lightning mutagenesis kit (Stratagene) was used to mutate pFB7 to carry WhiB7 E63D using the primers B7_D_F and B7_D_R generating pFB7d. The functional region of WhiB7 (WhiB7ΔN19C6; Figure 2) was amplified from the *M. smegmatis* genome by PCR using the primers B7fun_F and B7fun_R. The amplicon was digested with NcoI and then blunted using NEB's Quick blunting kit. The amplicon was then digested with HindIII. Similarly, pFB7 was digested with PstI and blunted, followed by digestion with HindIII. The vector backbone fragment was ligated with the digested B7fun amplicon to generate the constitutively expressing *whiB7*ΔN19C6 vector pB7fun. The vectors were then used to transform *M. smegmatis whiB7* KO to assay restoration of antibiotic resistance.

6.2.7.3 Construction of *M.smegmatis* Sig515

The mutated Region 4 of *sigA* was extracted from pTRG170.515 using NcoI and HindIII. It was combined with the XhoI/NcoI *sigA* fragment from pSigA and cloned into XhoI/HindII digested pYUB854 to construct pSig515. The downstream region of *sigA* was then PCR amplified from the *M. smegmatis* genome using the primers SigAflank_F and SigAflank_R. The PCR product was digested with XbaI/KpnI and cloned into similarly digested pSig515 to construct pSig515KI. This reversed the orientation of the hygromycin resistance gene so it matched the orientation of *sigA*. pSig515KI was then digested with XhoI/KpnI and the digest was used for mycobacterial recombineering (*140*) to construct *M. smegmatis* Sig515 (Figure 18a). Three randomly picked recombinants were used for all determinations. *sigA* from the mutants was amplified using the primers SigAsmF and SigAsmR. The product was cloned, utilizing the 5' addition of A

overhangs, into pGEM-T easy and sequenced to assure the Arg515His mutation. The presence of *whiB7* in these strains was confirmed by PCR using the primers 497_F and B7smReco.

6.3 Methods relating to chapter 3

6.3.1 Methods relating to 3.3

6.3.1.1 WhiB7 activation assay

M. smegmatis harbouring pMS689GFP was inoculated into 3mL of 7H9 + 30 μg/mL kanamycin and grown for 48-54 hours to a final OD_{600} of 6-8. The inoculum was diluted to an OD_{600} of 0.0125 in 50mL of kanamycin free 7H9 and grown for ~20 hours to an OD_{600} of 0.6-0.8. The culture was diluted to an OD_{600} of 0.2 and dispensed into a black, clear bottom 96 well plate. Wells 1-11 of row A received 300 μL and the rest of the plate received 200 μL, except for wells in column 12 of row G and H which received 200 μL of sterile media. For the wells that received 300 μL of culture, 3 μL of stock 5 mM compounds was added and 100 μL was used to serially dilute down from row A to row H creating a concentration range of 50 μM to 0.02 μM in a final volume 200 μL. The plate was covered with a lid, wrapped in tin foil, and incubated at 37 ºC, 200 rpm for 5 hours. After the incubation the plate was placed in a VarioskanFlask, the OD_{600} and emission at 509 nm after 488 nm excitation were measured following a shaking for 15 s at 420 rpm. The OD_{600} and fluorescence values were corrected by subtracting the average of the values measured in wells 12 of row G and H (sterile media). The fluorescent values were then standardized to the OD_{600} by dividing the fluorescent value of a well by its corresponding OD_{600} value. Finally the fold increase of standardized fluorescence was calculated by dividing values by the average of the untreated wells (wells 12 of row A to F). Because eGFP continued to

fluoresce in cultures whose OD_{600} had been reduced by antibiotic-induced lysis (data not shown), wells with an OD_{600} less than one third of the untreated wells were disregarded. The concentration range for each compound was analysed in three biologically independent runs. A compound was considered a WhiB7 activator if there was at least a greater than fourfold increase in fluorescence versus the untreated control in two out of the three replicates.

6.3.2 Methods relating to 3.4.1

6.3.2.1 Construction of the *ermMT* over-expression strain

Rv1988 (*ermMT)* was amplified from *Mtb* H37Rv genomic DNA by PCR using the forward and reverse primers Rv1988_F and Rv1988_R. The PCR product was digested with EcoRI and HindIII and cloned into pMV361 digested with the same enzymes. The resulting vector was digested with MfeI and ClaI, and the *ermMT*-containing fragment was cloned into pMV361.hyg digested with the same enzymes to create pERM.hyg. *M. smegmatis* was transformed with the plasmid, transformants were selected by hygromycin and an increased resistance to macrolides was checked.

6.3.3 Methods relating to 3.4.3

6.3.3.1 Analysis of mycothiol content

M. smegmatis wild type or *whiB7* KO was grown in 100 mL of NE (glucose 10 g/L, yeast extract 2 g/L, casaminoacids 2 g/L, lab lemco powder 1 g/L) supplemented to 0.05% Tyloxapol at 37 ºC, 200 rpm to an OD_{600} of 2.0. Cultures were then divided into two 50 mL fractions and one fraction received erythromycin to a final concentration of 256 µg/mL. All fractions were further incubated at 37 ºC for 1 hour. Growth was arrested by the addition of an equal volume of pre-

chilled water. The fractions were then divided for centrifugation at 4 ˚C; 10 mL for MSH determination, 30 mL for MSSM determination, and 5 mL for NEM labeling (negative control). Pellets were flash-frozen in liquid nitrogen and stored at -80 ˚C until analysis. HPLC analysis of MSH levels was performed as previously described (*165*).

6.3.3.2 Nicotinamide adenine dinucleotide quantification

M. smegmatis wild type or *whiB7* KO was grown in 50 mL of NE (glucose 10 g/L, yeast extract 2 g/L, casaminoacids 2 g/L, lab lemco powder 1 g/L) supplemented to 0.05% Tyloxapol at 37 ºC, 200 rpm to an OD_{600} of 2.0. Cultures were then divided into two 25 mL fractions and one fraction received erythromycin to a final concentration of 256 μg/mL. All fractions were further incubated at 37 ºC for 1 hour and samples taken. Erythromycin treated samples were left to incubate for an additional 1 hour for the 2 hour time point. Concentrations of reduced (NADH) and oxidized (NAD^+) forms of nicotinamide adenine dinucleotide were analyzed as previously described (*202*). Once samples were extracted the enzymatic reaction was carried out in a black, clear bottom 96 well plate (Costar 3631). Samples and standards were analyzed in triplicate, and only 6 wells were prepared and followed at one time. The Varioskan was set to read the absorbance (570 nm) every 20 s for 5 minutes. Concentrations were calculated from a standard curve ($R^2 = 0.9996$) of NADH (Sigma N6660-15VL) and standardized to dry weight per litre of culture.

6.4 Methods relating to chapter 4

6.4.1 Methods relating to 4.3.1

6.4.1.1 Construction of pORFdelGFP

The *whiB7* promoter (-53/+33) was fused to a shortened GFP reporter containing only the 229 bp upstream *whiB7* region. PCR of pMS689GFP as carried out with the promoter containing primer ORFdel_F paired with the *eGFP* targeting primer GFPsubX_R. The PCR product was digested with ClaI and XbaI and cloned into the vector backbone of similarly digested pMS689GFP to construct pORFdelGFP. The plasmid was then transformed into *M. smegmatis* and fluorescence monitored.

6.4.2 Methods relating to 4.3.2

6.4.2.1 Transposon library preparation

M. smegmatis was mutagenized with ΦMycoMarT7 to generate a library of transposon mutants (> 55, 000 inserts) essentially as described by Siegrist and Rubin (*203*). Briefly, ΦMycoMarT7 genomic DNA was transformed into *M. smegmatis* and resulting plaques were replica plated at 30 ºC and 37 ºC to ensure sensitivity at 37 ºC. Spots that formed plaques at 30 ºC but not 37 ºC were cut from agarose, mixed with MP buffer and filter sterilized. My experience indicated that storing phage at 4 ºC results in rapid drop to plaque forming units; therefore the extract was mixed immediately at 10^{-3}, 10^{-4}, and 10^{-5} to generate five plates per dilution. The dilution with a near-confluent plaque lawn was flooded with 3 mL of MP buffer per plate and gently rocked for 3 hours at 4 ºC to prepare the phage stock. 1 L of *M. smegmatis* was grown in 7H9g to an OD_{600} of 0.6 – 0.8. The culture was pelleted and washed three times with 30 mL of 7H9g (no tyloxapol)

and finally suspended in 50 mL. 4 mL of the suspended *M. smegmatis* were combined with 1 mL of fresh phage stock and incubated at 37 ºC for 3 hours. The transduction mix was inverted once every 45 minutes. Finally, glycerol was added to 18 % (v/v) and aliquots frozen at -80 ºC. Samples were plated to estimate library quantity for final plating. Roughly 55, 000 colonies obtained from 7H9g+kan agar plates were combined in 50 mL with 18% (v/v) glycerol to a final OD_{600} of 100.

6.4.2.2 Transposon library treatment

Alamar blue assays, with varied starting concentration of antibiotics, were used to determine the MICs of *M. smegmatis* and its ΔwhiB7 derivative to several WhiB7-specific antibiotics. The MICs (μg/mL) were found to be 6.3 and 0.4 for roxithromycin, 25 and 3 for chloramphenicol, and 1.9 and 0.8 for tetracycline. To allow for *M. smegmatis* growth, but inhibit mutants with *whiB7* KO like sensitivity, the concentrations chosen as treatments were 2 μg/mL for roxithromycin, 15 μg/mL for chloramphenicol, and 1.25 μg/mL for tetracycline. With *whiB7* pre-induction increasing roxithromycin resistance fourfold, a concentration of 18 μg/mL was chosen to select for mutants with constitutive *whiB7* expression.

200 mL of 7H9g+kan was inoculated with 20 μL of the transposon library (>70X library quantity; OD_{600} 0.01) and grown at 37 ºC for 2 hours at 200 rpm after which antibiotics were added to the previously indicated concentrations. Untreated, spectinomycin and chloramphenicol treated cultures were grown for 48 h and reached a final OD_{600} of 5.6, 6.2, and 5.2, respectively. 2 μg/mL roxithromycin treated cultures was grown for 70 h to a final OD_{600} 6; tetracycline treated culture for 98 h to a final OD_{600} 3.68; and 18 μg/mL roxithromycin treated culture for

120 h to a final OD_{600} 4. Cultures were then centrifuged and genomic DNA extracted. The DNA concentration was measured with the Qubit dsDNA HS assay kit (Invitrogen).

6.4.3 Methods relating to 4.3.3

6.4.3.1 Transposon library mapping and analysis

Most mass transposon mapping protocols have a fragmentation step followed by an addition of a specific primer and PCR. I used Griffin *et al.* (*176*) protocol as inspiration and combined it with Illumina's Nextera 'tagmentation' protocol to universally add primers during the fragmentation step. The Nextera DNA sample preparation kit (Illumina) was used to fragment isolated genomic DNA, with minor modification; 10 ng/μL DNA was used as input for larger fragment generation, and the tagmentation reaction was purified with a Qiagen PCR purification kit with a 57 μL elution. Three 25 μL RT-qPCR reactions were prepared per primer pair per condition with 9 μL of the eluate. Quanta's PerfeCTa® SYBR® Green SuperMix with a final concentration of 0.8 μM per primer was used for the reactions. A primer targeting the P7 tagmentation (P7tag) was paired with primers targeting either end of the ΦMycoMarT7 transposon (Accession: AF411123); NX_pMMT7_out1 and NX_pMMT7_out2. Reactions were run in a CFX96 RT-PCR machine (Bio-Rad) with decreasing annealing temperatures:

94 ºC for 30 s
Annealing for 30 s (60 ºC for 5 cycles, 58 ºC for5 cycles, and then 55 ºC for 35 cycles)
72 ºC for 30 s

The reactions were observed until 6 cycles have passed since the signal increased above background (~23 cycles total). All reactions were then separated on a 2% agarose-TAE gel with the smear between 250-500 bp cut out, the triplicates combined, and DNA purified with the Quiagen Gel purification kit with a 45 μL elution. Eluates were quantified with the Qubit

dsDNA HS assay kit, and the products from the two reactions pooled at equal amounts to a final concentration of ~1.4 ng/μL. Note, if there wasn't enough DNA from both reactions for an equal pool, the more concentrated partner was added at higher amounts to get the desired final concentration. The Nextera sample preparation kit protocol was then continued. The PCR was set up with 24 μL of pooled DNA as suggested, but with 1 μL at 20 μM of a custom P5 primer (phiP5) and 10 cycles. The Nextera indexing kit P7 primers were used to barcode the individual conditions. Samples were combined and sequenced using the MiSeq reagent kit v2 (Illumina) with 50 bp reads using the custom P5 primer phiMMT7seq_1. Around 3 million reads were obtained per condition with about 1 million for the 18 μg/mL roxithromycin treatment. The ESSENTIALS software developed by Zomer *et al*. (*181*) was used to map sequencing read frequency to annotated *M. smegmatis* genes. Candidate genes were then analyzed using UGENE (*182*) to determine the number of transposon insertions.

6.4.4 Methods relating to 4.3.4

6.4.4.1 Construction of gene knock-outs

In all cases mycobacterial recombineering (*140*) was used to generate gene knock-outs in *M. smegmatis* mc^2155. The hygromycin resistance marker (HygR), flanked by resolvase sites, was extracted from pYUB854 using AgeI and NheI, and the product blunted with the NEB Quick Blunting kit to be used as a selectable marker.

MSMEG_3637/8 – The genomic region containing *MSMEG_3637* and *MSMEG_3638* was amplified by PCR using the primers 3637F and 3637R. The gene product was cloned, using the polymerase added 3' A overhangs, into pGEM-T easy to construct pGEM-3637/8. pGEM-3637/8 was then digested with BamHI, the product blunted with the NEB Quick Blunting kit,

and combined with the blunted HygR (which inserted in the same orientation as the two genes) to generate pGEM-3637/8KO. pGEM-3637/8KO was then digested with NotI and the products used for recombineering to generate *M. smegmatis* 3637/8KO. The correct placement of the insertion was verified by PCR using the primers 3637/8CHK and HYG_out .

MSMEG_3027 – The genomic region containing *MSMEG_3027* was amplified by PCR using the primers 3027F and 3027R. The gene product was cloned, using the polymerase added 3' A overhangs, into pGEM-T easy to construct pGEM-3027. HygR was inserted into the 5' proximal NruI in the inverse orientation to construct pGEM-3027KO. pGEM-3027KO was then digested with PvuII and the products used for recombineering to generate *M. smegmatis* 3027KO. The correct placement of the insertion was verified by PCR using the primers 3027CHK and HYG_out2.

MSMEG_4269 – The genomic region containing *MSMEG_4249* was amplified by PCR using the primers 4269F and 4269R. The gene product was cloned, using the polymerase added 3' A overhangs, into pGEM-T easy to construct pGEM-4269. pGEM4269 was then digested with SmaI and AfeI, and HygR inserted in the inverse orientation to construct pGEM-4269KO. pGEM-4269KO was then digested with NcoI and NdeI, and the prodcuts used for recombineering to generate *M. smegmatis* 4269KO. The correct placement of the insertion was verified by PCR using the primers 4269CHK and HYG_out2.

MSMEG_6099 – The genomic region containing *MSMEG_6099* was amplified by PCR using the primers 6099F and 6099R. The gene product was cloned, using the polymerase added 3' A overhangs, into pGEM-T easy to construct pGEM-6099. pGEM6099 was then digested with NarI, blunted with the NEB Quick Blunting kit, and HygR was inserted in the inverse orientation to construct pGEM-6099KO. Sequencing showed HygR inserted between the third

and seventh NarI site. pGEM-6099KO was then digested with NcoI and NdeI, and the products used for recombineering to generate *M. smegmatis* 6099KO. The correct placement of the insertion was verified by PCR using the primers 6099CHK and HYG_out2.

MSMEG_3493/4 – The genomic region containing *MSMEG_3493* and *MSMEG_3493* was amplified by PCR using the primers 3494F and 3494R. The gene product was cloned, using the polymerase added 3' A overhangs, into pGEM-T easy to construct pGEM-3493/4. To generate a *MSMEG_3493* KO, pGEM3493/4 was digested with HindIII, blunted with the NEB Quick Blunting kit, and HygR inserted in the inverse orientation to generate pGEM-3493KO. pGEM-3493KO was then digested with NcoI and NdeI, and the products used for recombineering to generate *M. smegmatis* 3493KO. It is worth noting that *MSMEG_3493* and *MSMEG_3494* are only separated by 41 bp and therefore the *MSMEG_3493* KO may also be disrupting *MSMEG_3494* expression. To generate a *MSMEG_3494* KO, pGEM-3493/4 was digested with EcoRV and AfeI, and HygR inserted in the inverse orientation to generate pGEM-3494KO. pGEM-3494KO was then digested with NcoI and NdeI, and the products used for recombineering to generate *M. smegmatis* 3494KO. To generate a *MSMEG_3493* and *MSMEG_3494* double KO, pGEM-3493/4 was digested with HindIII and AfeI, blunted with the NEB Quick Blunting kit, and HygR inserted in the inverse orientation to generate pGEM-3493/4KO. pGEM-3493/4KO was then digested with NcoI and NdeI, and the products used for recombineering to generate *M. smegmatis* 3493/4KO. In all instances the correct placement of the insertion was verified by PCR using the primers 3494CHK and HYG_out2.

6.4.4.2 Constructions of constitutive expression strains

PCR was used to amplify *MSMEG_2691* using the primers 261p2691F and 261p2691R; *MSMEG_2779* using the primers 261p2779F and 261p2779R; *MSMEG_3374* using the primers 261p3374F and 261p3374R; *MSMEG_3637* using the primers 261p3637F and 261p3637R; *MSMEG_5121* using the primers 261p5121F and 261p5121R; *MSMEG_5270* using the primers (261p5270F and 261p5270R. The PCR products were digested with PstI and HindIII, and cloned into similarly digested pFB7 (*204*) to construct p2691OV, p2779OV, p3374OV, p3637OV, p5121OV, and p5270OV. These plasmids were sequence verified and used to transform *M. smegmatis* mc^2155 to generate their respective constitutive expression strains. p2691OV and p5121OV were also used to transform *M. smegmatis whiB7* KO.

PCR was used to amplify *MSMEG_0385* using the primers 261p0385F 261p0385R, and *MSMEG_0688* using the primers 261p0688F and 261p0688R. The PCR products were digested with NcoI, blunted, and then digested with HindIII. These were then cloned into pFB7 (NAR ref) which was digested with PstI, blunted and then digested with HindIII to generate p0385OV and p0688OV. The vectors were sequence verified and transformed into *M. smegmatis* mc^2155.

6.4.5 Methods relating to 4.3.5

6.4.5.1 Construction of a MSMEG_4060 knock-out and constitutive expression strain

Genomic sequencing indicates *MSMEG_4060* as a 1207 bp psedogene. Within the sequence is a stop codon after 933 bp. Based on blastp results of the translation product, this truncated gene resembles an aminotransferase up to 777 bp of the coding sequence. The transposon screen indicated hyper-insertions in the TATA region (1001-1004 bp) falling downstream of the truncation. Subsequent work showed, with the results from three independent

PCRs, that our strain of *M. smegmatis* contained a deletion of the G at base 779. This resulted in a frame shift which removed the internal stop and allowed for the translation of a longer MSMEG_4060 (1206 bp).

A disruption of the TATA region (1001-1004 bp) region was designed to mimic the transposon insertion. The lower region of *MSMEG_4060* was amplified by PCR with the primers 4060LF and 4060LR. The product was digested with XbaI and KpnI and cloned into similarly digested pYUB854 (*140*) to construct p4060L. The upper region of *MSMEG_4060* was amplified by PCR with the primers 4060UF and 4060UR. The product was digested with HindIII and NcoI and cloned into similarly digested p4060L to construct p4060KO. p4060KO was then digested with HindIII and KpnI with the products used for mycobacterial recombineering (ref). This resulted in an insertion of a hygromycin resistance gene, in the inverse orientation to MSMEG_4060, and the deletion of the TATA region to generate the strain *M. smegmatis* 4060KO. The correct location of the insertion was verified by PCR on genomic DNA using the primers 4060CHK and Hyg_out.

The 1206 bp *MSMEG_4060* gene variant (containing the 779 G deletion) was cloned for constitutive expression. *MSMEG_4060* was amplified by PCR using the primers 261p4060_F and 261p4060_R. The product was digested with PstI and HindIII, and cloned into the backbone of similarly digested pFB7 (*204*) to construct p4060OV. The vector was then used to transform *M. smegmatis* to generate.

Bibliography

1. Embley, T. M., and Stackebrandt, E. (1994) The molecular phylogeny and systematics of the actinomycetes, *Annu Rev Microbiol 48*, 257-289.

2. Olsen, G. J., Woese, C. R., and Overbeek, R. (1994) The winds of (evolutionary) change: breathing new life into microbiology, *J Bacteriol 176*, 1-6.

3. Roller, C., Ludwig, W., and Schleifer, K. H. (1992) Gram-positive bacteria with a high DNA G+C content are characterized by a common insertion within their 23S rRNA genes, *J Gen Microbiol 138*, 1167-1175.

4. Newton, G. L., Arnold, K., Price, M. S., Sherrill, C., Delcardayre, S. B., Aharonowitz, Y., Cohen, G., Davies, J., Fahey, R. C., and Davis, C. (1996) Distribution of thiols in microorganisms: mycothiol is a major thiol in most actinomycetes, *J Bacteriol 178*, 1990-1995.

5. Gao, B., Paramanathan, R., and Gupta, R. S. (2006) Signature proteins that are distinctive characteristics of Actinobacteria and their subgroups, *Antonie Van Leeuwenhoek 90*, 69-91.

6. Martinkova, L., Uhnakova, B., Patek, M., Nesvera, J., and Kren, V. (2009) Biodegradation potential of the genus Rhodococcus, *Environ Int 35*, 162-177.

7. Miao, V., and Davies, J. (2010) Actinobacteria: the good, the bad, and the ugly, *Antonie Van Leeuwenhoek 98*, 143-150.

8. Baltz, R. H. (2011) Strain improvement in actinomycetes in the postgenomic era, *J Ind Microbiol Biotechnol 38*, 657-666.

9. Murakami, T., Burian, J., Yanai, K., Bibb, M. J., and Thompson, C. J. (2011) A system for the targeted amplification of bacterial gene clusters multiplies antibiotic yield in Streptomyces coelicolor, *Proc Natl Acad Sci U S A 108*, 16020-16025.

10. Lambert, P. A. (2002) Cellular impermeability and uptake of biocides and antibiotics in Gram-positive bacteria and mycobacteria, *Journal of applied microbiology 92 Suppl*, 46S-54S.

11. Ryll, R., Kumazawa, Y., and Yano, I. (2001) Immunological properties of trehalose dimycolate (cord factor) and other mycolic acid-containing glycolipids--a review, *Microbiology and immunology 45*, 801-811.

12. Ventura, M., Canchaya, C., Tauch, A., Chandra, G., Fitzgerald, G. F., Chater, K. F., and van Sinderen, D. (2007) Genomics of Actinobacteria: tracing the evolutionary history of an ancient phylum, *Microbiol Mol Biol Rev 71*, 495-548.

13. Paulson, T. (2013) Epidemiology: A mortal foe, *Nature 502*, S2-3.

14. Daniel, T. M. (2006) The history of tuberculosis, *Respir Med 100*, 1862-1870.

15. Kaufmann, S. H. (2005) Robert Koch, the Nobel Prize, and the ongoing threat of tuberculosis, *N Engl J Med 353*, 2423-2426.

16. Gutierrez, M. C., Brisse, S., Brosch, R., Fabre, M., Omais, B., Marmiesse, M., Supply, P., and Vincent, V. (2005) Ancient origin and gene mosaicism of the progenitor of Mycobacterium tuberculosis, *PLoS Pathog 1*, e5.

17. Jarlier, V., and Nikaido, H. (1994) Mycobacterial cell wall: structure and role in natural resistance to antibiotics, *FEMS Microbiol Lett 123*, 11-18.

18. Myers, J. A. (1963) Can tuberculosis be eradicated?, *Dis Chest 43*, 327-329.

19. Sudre, P., Dam, G. t., Chan, C., and Kochi, A. (1990) *Tuberculosis in the present time: a global overview of the tuberculosis situation*, World Health Organization, Geneva, Switzerland.

20. World Health Organization. (2009) *Global tuberculosis control : epidemiology, strategy, financing : WHO report 2009*, World Health Organization, Geneva.

21. Walsh, D. S., Portaels, F., and Meyers, W. M. (2010) Recent advances in leprosy and Buruli ulcer (Mycobacterium ulcerans infection), *Curr Opin Infect Dis 23*, 445-455.

22. Cole, S. T., Eiglmeier, K., Parkhill, J., James, K. D., Thomson, N. R., Wheeler, P. R., Honore, N., Garnier, T., Churcher, C., Harris, D., Mungall, K., Basham, D., Brown, D., Chillingworth, T., Connor, R., Davies, R. M., Devlin, K., Duthoy, S., Feltwell, T., Fraser, A., Hamlin, N., Holroyd, S., Hornsby, T., Jagels, K., Lacroix, C., Maclean, J., Moule, S., Murphy, L., Oliver, K., Quail, M. A., Rajandream, M. A., Rutherford, K. M., Rutter, S., Seeger, K., Simon, S., Simmonds, M., Skelton, J., Squares, R., Squares, S., Stevens, K., Taylor, K., Whitehead, S., Woodward, J. R., and Barrell, B. G. (2001) Massive gene decay in the leprosy bacillus, *Nature 409*, 1007-1011.

23. Gomez-Valero, L., Rocha, E. P., Latorre, A., and Silva, F. J. (2007) Reconstructing the ancestor of Mycobacterium leprae: the dynamics of gene loss and genome reduction, *Genome Res 17*, 1178-1185.

24. Scollard, D. M., Adams, L. B., Gillis, T. P., Krahenbuhl, J. L., Truman, R. W., and Williams, D. L. (2006) The continuing challenges of leprosy, *Clinical microbiology reviews 19*, 338-381.

25. Kar, H. K., and Gupta, R. (2015) Treatment of leprosy, *Clinics in dermatology 33*, 55-65.

26. Sizaire, V., Nackers, F., Comte, E., and Portaels, F. (2006) Mycobacterium ulcerans infection: control, diagnosis, and treatment, *Lancet Infect Dis 6*, 288-296.

27. Karakousis, P. C., Moore, R. D., and Chaisson, R. E. (2004) Mycobacterium avium complex in patients with HIV infection in the era of highly active antiretroviral therapy, *Lancet Infect Dis 4*, 557-565.

28. Nishino, K., Nikaido, E., and Yamaguchi, A. (2009) Regulation and physiological function of multidrug efflux pumps in Escherichia coli and Salmonella, *Biochim Biophys Acta 1794*, 834-843.

29. Cole, S. T., Brosch, R., Parkhill, J., Garnier, T., Churcher, C., Harris, D., Gordon, S. V., Eiglmeier, K., Gas, S., Barry, C. E., 3rd, Tekaia, F., Badcock, K., Basham, D., Brown, D., Chillingworth, T., Connor, R., Davies, R., Devlin, K., Feltwell, T., Gentles, S., Hamlin, N., Holroyd, S., Hornsby, T., Jagels, K., Krogh, A., McLean, J., Moule, S., Murphy, L., Oliver, K., Osborne, J., Quail, M. A., Rajandream, M. A., Rogers, J., Rutter, S., Seeger, K., Skelton, J., Squares, R., Squares, S., Sulston, J. E., Taylor, K., Whitehead, S., and Barrell, B. G. (1998) Deciphering the biology of Mycobacterium tuberculosis from the complete genome sequence, *Nature 393*, 537-544.

30. Nguyen, L., and Pieters, J. (2009) Mycobacterial subversion of chemotherapeutic reagents and host defense tactics: challenges in tuberculosis drug development, *Annu Rev Pharmacol Toxicol 49*, 427-453.

31. Nguyen, L., and Thompson, C. J. (2006) Foundations of antibiotic resistance in bacterial physiology: the mycobacterial paradigm, *Trends Microbiol 14*, 304-312.

32. Ainsa, J. A., Blokpoel, M. C., Otal, I., Young, D. B., De Smet, K. A., and Martin, C. (1998) Molecular cloning and characterization of Tap, a putative multidrug efflux pump present in Mycobacterium fortuitum and Mycobacterium tuberculosis, *J Bacteriol 180*, 5836-5843.

33. Ramon-Garcia, S., Martin, C., Thompson, C. J., and Ainsa, J. A. (2009) The role of the Mycobacterium tuberculosis P55 efflux pump in intrinsic drug resistance, oxidative stress responses and growth, *Antimicrob Agents Chemother*.

34. Doucet-Populaire, F., Buriankova, K., Weiser, J., and Pernodet, J. L. (2002) Natural and acquired macrolide resistance in mycobacteria, *Curr Drug Targets Infect Disord 2*, 355-370.

35. Colijn, C., Cohen, T., Ganesh, A., and Murray, M. (2011) Spontaneous emergence of multiple drug resistance in tuberculosis before and during therapy, *PLoS One 6*, e18327.

36. Wright, A., Zignol, M., and WHO/IUATLD Global Project on Anti-tuberculosis Drug Resistance Surveillance. (2008) *Anti-tuberculosis drug resistance in the world : fourth global report : the World Health Organization/International Union Against Tuberculosis and Lung Disease (WHO/UNION) Global Project on Anti-Tuberculosis Drug Resistance Surveillance, 2002-2007*, World Health Organization, Geneva, Switzerland.

37. Walsh, C. (2000) Molecular mechanisms that confer antibacterial drug resistance, *Nature 406*, 775-781.

38. Goh, E. B., Yim, G., Tsui, W., McClure, J., Surette, M. G., and Davies, J. (2002) Transcriptional modulation of bacterial gene expression by subinhibitory concentrations of antibiotics, *Proc Natl Acad Sci U S A 99*, 17025-17030.

39. Holmes, D. J., Caso, J. L., and Thompson, C. J. (1993) Autogenous transcriptional activation of a thiostrepton-induced gene in Streptomyces lividans, *The EMBO journal 12*, 3183-3191.

40. Novotna, J., Vohradsky, J., Berndt, P., Gramajo, H., Langen, H., Li, X. M., Minas, W., Orsaria, L., Roeder, D., and Thompson, C. J. (2003) Proteomic studies of diauxic lag in the differentiating prokaryote Streptomyces coelicolor reveal a regulatory network of stress-induced proteins and central metabolic enzymes, *Mol Microbiol 48*, 1289-1303.

41. Ren, H., and Liu, J. (2006) AsnB is involved in natural resistance of Mycobacterium smegmatis to multiple drugs, *Antimicrob Agents Chemother 50*, 250-255.

42. Vohradsky, J., Li, X. M., Dale, G., Folcher, M., Nguyen, L., Viollier, P. H., and Thompson, C. J. (2000) Developmental control of stress stimulons in Streptomyces coelicolor revealed by statistical analyses of global gene expression patterns, *J Bacteriol 182*, 4979-4986.

43. VanBogelen, R. A., and Neidhardt, F. C. (1990) Ribosomes as sensors of heat and cold shock in Escherichia coli, *Proc Natl Acad Sci U S A 87*, 5589-5593.

44. Girgis, H. S., Hottes, A. K., and Tavazoie, S. (2009) Genetic architecture of intrinsic antibiotic susceptibility, *PLoS One 4*, e5629.

45. Fajardo, A., Martinez-Martin, N., Mercadillo, M., Galan, J. C., Ghysels, B., Matthijs, S., Cornelis, P., Wiehlmann, L., Tummler, B., Baquero, F., and Martinez, J. L. (2008) The neglected intrinsic resistome of bacterial pathogens, *PLoS One 3*, e1619.

46. Gallagher, L. A., Shendure, J., and Manoil, C. (2011) Genome-scale identification of resistance functions in Pseudomonas aeruginosa using Tn-seq, *mBio 2*, e00315-00310.

47. Gomez, M. J., and Neyfakh, A. A. (2006) Genes involved in intrinsic antibiotic resistance of Acinetobacter baylyi, *Antimicrob Agents Chemother 50*, 3562-3567.

48. Nguyen, L., Chinnapapagari, S., and Thompson, C. J. (2005) FbpA-Dependent biosynthesis of trehalose dimycolate is required for the intrinsic multidrug resistance, cell wall structure, and colonial morphology of Mycobacterium smegmatis, *J Bacteriol 187*, 6603-6611.

49. Philalay, J. S., Palermo, C. O., Hauge, K. A., Rustad, T. R., and Cangelosi, G. A. (2004) Genes required for intrinsic multidrug resistance in Mycobacterium avium, *Antimicrob Agents Chemother 48*, 3412-3418.

50. Shatalin, K., Shatalina, E., Mironov, A., and Nudler, E. (2011) H2S: a universal defense against antibiotics in bacteria, *Science 334*, 986-990.

51. Vega, N. M., and Gore, J. (2014) Collective antibiotic resistance: mechanisms and implications, *Curr Opin Microbiol 21C*, 28-34.

52. Yamaguchi, Y., Park, J. H., and Inouye, M. (2011) Toxin-antitoxin systems in bacteria and archaea, *Annual review of genetics 45*, 61-79.

53. Barlow, M. (2009) What antimicrobial resistance has taught us about horizontal gene transfer, *Methods Mol Biol 532*, 397-411.

54. Rosas-Magallanes, V., Deschavanne, P., Quintana-Murci, L., Brosch, R., Gicquel, B., and Neyrolles, O. (2006) Horizontal transfer of a virulence operon to the ancestor of Mycobacterium tuberculosis, *Mol Biol Evol 23*, 1129-1135.

55. Morris, R. P., Nguyen, L., Gatfield, J., Visconti, K., Nguyen, K., Schnappinger, D., Ehrt, S., Liu, Y., Heifets, L., Pieters, J., Schoolnik, G., and Thompson, C. J. (2005) Ancestral antibiotic resistance in Mycobacterium tuberculosis, *Proc Natl Acad Sci U S A 102*, 12200-12205.

56. Soliveri, J. A., Gomez, J., Bishai, W. R., and Chater, K. F. (2000) Multiple paralogous genes related to the Streptomyces coelicolor developmental regulatory gene whiB are present in Streptomyces and other actinomycetes, *Microbiology 146 (Pt 2)*, 333-343.

57. Hopwood, D. A., Wildermuth, H., and Palmer, H. M. (1970) Mutants of Streptomyces coelicolor defective in sporulation, *J Gen Microbiol 61*, 397-408.

58. Chater, K. F. (1972) A morphological and genetic mapping study of white colony mutants of Streptomyces coelicolor, *J Gen Microbiol 72*, 9-28.

59. Davis, N. K., and Chater, K. F. (1992) The Streptomyces coelicolor whiB gene encodes a small transcription factor-like protein dispensable for growth but essential for sporulation, *Mol Gen Genet 232*, 351-358.

60. Soliveri, J., Vijgenboom, E., Granozzi, C., Plaskitt, K. A., and Chater, K. F. (1993) Functional and evolutionary implications of a survey of various actinomycetes for homologues of two Streptomyces coelicolor sporulation genes, *J Gen Microbiol 139*, 2569-2578.

61. Alam, M. S., Garg, S. K., and Agrawal, P. (2009) Studies on structural and functional divergence among seven WhiB proteins of Mycobacterium tuberculosis H37Rv, *FEBS J 276*, 76-93.

62. Smith, L. J., Stapleton, M. R., Fullstone, G. J., Crack, J. C., Thomson, A. J., Le Brun, N. E., Hunt, D. M., Harvey, E., Adinolfi, S., Buxton, R. S., and Green, J. (2010) Mycobacterium tuberculosis WhiB1 is an essential DNA-binding protein with a nitric oxide-sensitive iron-sulfur cluster, *Biochem J 432*, 417-427.

63. Stapleton, M., Haq, I., Hunt, D. M., Arnvig, K. B., Artymiuk, P. J., Buxton, R. S., and Green, J. (2010) Mycobacterium tuberculosis cAMP receptor protein (Rv3676) differs

from the Escherichia coli paradigm in its cAMP binding and DNA binding properties and transcription activation properties, *J Biol Chem 285*, 7016-7027.

64. Rickman, L., Scott, C., Hunt, D. M., Hutchinson, T., Menendez, M. C., Whalan, R., Hinds, J., Colston, M. J., Green, J., and Buxton, R. S. (2005) A member of the cAMP receptor protein family of transcription regulators in Mycobacterium tuberculosis is required for virulence in mice and controls transcription of the rpfA gene coding for a resuscitation promoting factor, *Mol Microbiol 56*, 1274-1286.

65. Agarwal, N., Lamichhane, G., Gupta, R., Nolan, S., and Bishai, W. R. (2009) Cyclic AMP intoxication of macrophages by a Mycobacterium tuberculosis adenylate cyclase, *Nature 460*, 98-102.

66. Gomez, J. E., and Bishai, W. R. (2000) whmD is an essential mycobacterial gene required for proper septation and cell division, *Proc Natl Acad Sci U S A 97*, 8554-8559.

67. Raghunand, T. R., and Bishai, W. R. (2006) Mapping essential domains of Mycobacterium smegmatis WhmD: insights into WhiB structure and function, *J Bacteriol 188*, 6966-6976.

68. Rybniker, J., Nowag, A., van Gumpel, E., Nissen, N., Robinson, N., Plum, G., and Hartmann, P. (2010) Insights into the function of the WhiB-like protein of mycobacteriophage TM4--a transcriptional inhibitor of WhiB2, *Mol Microbiol 77*, 642-657.

69. Geiman, D. E., Raghunand, T. R., Agarwal, N., and Bishai, W. R. (2006) Differential gene expression in response to exposure to antimycobacterial agents and other stress conditions among seven Mycobacterium tuberculosis whiB-like genes, *Antimicrob Agents Chemother 50*, 2836-2841.

70. Steyn, A. J., Collins, D. M., Hondalus, M. K., Jacobs, W. R., Jr., Kawakami, R. P., and Bloom, B. R. (2002) Mycobacterium tuberculosis WhiB3 interacts with RpoV to affect host survival but is dispensable for in vivo growth, *Proc Natl Acad Sci U S A 99*, 3147-3152.

71. Singh, A., Crossman, D. K., Mai, D., Guidry, L., Voskuil, M. I., Renfrow, M. B., and Steyn, A. J. (2009) Mycobacterium tuberculosis WhiB3 maintains redox homeostasis by regulating virulence lipid anabolism to modulate macrophage response, *PLoS Pathog 5*, e1000545.

72. Singh, A., Guidry, L., Narasimhulu, K. V., Mai, D., Trombley, J., Redding, K. E., Giles, G. I., Lancaster, J. R., Jr., and Steyn, A. J. (2007) Mycobacterium tuberculosis WhiB3 responds to O2 and nitric oxide via its [4Fe-4S] cluster and is essential for nutrient starvation survival, *Proc Natl Acad Sci U S A 104*, 11562-11567.

73. Guo, M., Feng, H., Zhang, J., Wang, W., Wang, Y., Li, Y., Gao, C., Chen, H., Feng, Y., and He, Z. G. (2009) Dissecting transcription regulatory pathways through a new bacterial one-hybrid reporter system, *Genome Res 19*, 1301-1308.

74. Chawla, M., Parikh, P., Saxena, A., Munshi, M., Mehta, M., Mai, D., Srivastava, A. K., Narasimhulu, K. V., Redding, K. E., Vashi, N., Kumar, D., Steyn, A. J., and Singh, A. (2012) Mycobacterium tuberculosis WhiB4 regulates oxidative stress response to modulate survival and dissemination in vivo, *Mol Microbiol 85*, 1148-1165.

75. Casonato, S., Cervantes Sanchez, A., Haruki, H., Rengifo Gonzalez, M., Provvedi, R., Dainese, E., Jaouen, T., Gola, S., Bini, E., Vicente, M., Johnsson, K., Ghisotti, D., Palu, G., Hernandez-Pando, R., and Manganelli, R. (2012) WhiB5: a transcriptional regulator contributing to Mycobacterium tuberculosis virulence and reactivation, *Infect Immun 80*, 3132-3144.

76. Humpel, A., Gebhard, S., Cook, G. M., and Berney, M. (2010) The SigF regulon in Mycobacterium smegmatis reveals roles in adaptation to stationary phase, heat, and oxidative stress, *J Bacteriol 192*, 2491-2502.

77. Das, C., Ghosh, T. S., and Mande, S. S. (2011) Computational analysis of the ESX-1 region of Mycobacterium tuberculosis: insights into the mechanism of type VII secretion system, *PLoS One 6*, e27980.

78. Homolka, S., Niemann, S., Russell, D. G., and Rohde, K. H. (2010) Functional genetic diversity among Mycobacterium tuberculosis complex clinical isolates: delineation of conserved core and lineage-specific transcriptomes during intracellular survival, *PLoS Pathog 6*, e1000988.

79. Larsson, C., Luna, B., Ammerman, N. C., Maiga, M., Agarwal, N., and Bishai, W. R. (2012) Gene Expression of Mycobacterium tuberculosis Putative Transcription Factors whiB1-7 in Redox Environments, *PLoS One 7*, e37516.

80. Rohde, K. H., Veiga, D. F., Caldwell, S., Balazsi, G., and Russell, D. G. (2012) Linking the transcriptional profiles and the physiological states of Mycobacterium tuberculosis during an extended intracellular infection, *PLoS Pathog 8*, e1002769.

81. Johnson, D. C., Dean, D. R., Smith, A. D., and Johnson, M. K. (2005) Structure, function, and formation of biological iron-sulfur clusters, *Annu Rev Biochem 74*, 247-281.

82. Kiley, P. J., and Beinert, H. (2003) The role of Fe-S proteins in sensing and regulation in bacteria, *Curr Opin Microbiol 6*, 181-185.

83. Ding, H., Hidalgo, E., and Demple, B. (1996) The redox state of the [2Fe-2S] clusters in SoxR protein regulates its activity as a transcription factor, *J Biol Chem 271*, 33173-33175.

84. Constantinidou, C., Hobman, J. L., Griffiths, L., Patel, M. D., Penn, C. W., Cole, J. A., and Overton, T. W. (2006) A reassessment of the FNR regulon and transcriptomic analysis of the effects of nitrate, nitrite, NarXL, and NarQP as Escherichia coli K12 adapts from aerobic to anaerobic growth, *J Biol Chem 281*, 4802-4815.

85. Khoroshilova, N., Popescu, C., Munck, E., Beinert, H., and Kiley, P. J. (1997) Iron-sulfur cluster disassembly in the FNR protein of Escherichia coli by O2: [4Fe-4S] to [2Fe-2S] conversion with loss of biological activity, *Proc Natl Acad Sci U S A 94*, 6087-6092.

86. Schwartz, C. J., Giel, J. L., Patschkowski, T., Luther, C., Ruzicka, F. J., Beinert, H., and Kiley, P. J. (2001) IscR, an Fe-S cluster-containing transcription factor, represses expression of Escherichia coli genes encoding Fe-S cluster assembly proteins, *Proc Natl Acad Sci U S A 98*, 14895-14900.

87. Jakimowicz, P., Cheesman, M. R., Bishai, W. R., Chater, K. F., Thomson, A. J., and Buttner, M. J. (2005) Evidence that the Streptomyces developmental protein WhiD, a member of the WhiB family, binds a [4Fe-4S] cluster, *J Biol Chem 280*, 8309-8315.

88. Stapleton, M. R., Smith, L. J., Hunt, D. M., Buxton, R. S., and Green, J. (2012) Mycobacterium tuberculosis WhiB1 represses transcription of the essential chaperonin GroEL2, *Tuberculosis (Edinb) 92*, 328-332.

89. Raghunand, T. R., and Bishai, W. R. (2006) Mycobacterium smegmatis whmD and its homologue Mycobacterium tuberculosis whiB2 are functionally equivalent, *Microbiology 152*, 2735-2747.

90. Vassylyev, D. G., Sekine, S., Laptenko, O., Lee, J., Vassylyeva, M. N., Borukhov, S., and Yokoyama, S. (2002) Crystal structure of a bacterial RNA polymerase holoenzyme at 2.6 A resolution, *Nature 417*, 712-719.

91. Dove, S. L., Darst, S. A., and Hochschild, A. (2003) Region 4 of sigma as a target for transcription regulation, *Mol Microbiol 48*, 863-874.

92. van Hijum, S. A., Medema, M. H., and Kuipers, O. P. (2009) Mechanisms and evolution of control logic in prokaryotic transcriptional regulation, *Microbiol Mol Biol Rev 73*, 481-509, Table of Contents.

93. Collins, D. M., Kawakami, R. P., de Lisle, G. W., Pascopella, L., Bloom, B. R., and Jacobs, W. R., Jr. (1995) Mutation of the principal sigma factor causes loss of virulence in a strain of the Mycobacterium tuberculosis complex, *Proc Natl Acad Sci U S A 92*, 8036-8040.

94. Garg, S., Alam, M. S., Bajpai, R., Kishan, K. R., and Agrawal, P. (2009) Redox biology of Mycobacterium tuberculosis H37Rv: protein-protein interaction between GlgB and WhiB1 involves exchange of thiol-disulfide, *BMC Biochem 10*, 1.

95. Suhail Alam, M., and Agrawal, P. (2008) Matrix-assisted refolding and redox properties of WhiB3/Rv3416 of Mycobacterium tuberculosis H37Rv, *Protein Expr Purif 61*, 83-91.

96. Alam, M. S., Garg, S. K., and Agrawal, P. (2007) Molecular function of WhiB4/Rv3681c of Mycobacterium tuberculosis H37Rv: a [4Fe-4S] cluster co-ordinating protein disulphide reductase, *Mol Microbiol 63*, 1414-1431.

97. Konar, M., Alam, M., Arora, C., and Agrawal, P. (2012) WhiB2/Rv3260c, a cell division-associated protein of Mycobacterium tuberculosis H37Rv, has properties of a chaperone, *FEBS J 279*, 2781-2792.

98. Newton, G. L., Bewley, C. A., Dwyer, T. J., Horn, R., Aharonowitz, Y., Cohen, G., Davies, J., Faulkner, D. J., and Fahey, R. C. (1995) The structure of U17 isolated from Streptomyces clavuligerus and its properties as an antioxidant thiol, *European journal of biochemistry / FEBS 230*, 821-825.

99. Patel, M., and Blanchard, J. (1998) Synthesis of Des-myo-Inositol Mycothiol and Demonstration of a Mycobacterial Specific, *J Am Chem Soc 120*, 11538 - 11539.

100. den Hengst, C. D., and Buttner, M. J. (2008) Redox control in actinobacteria, *Biochim Biophys Acta 1780*, 1201-1216.

101. Chandra, G., and Chater, K. F. (2014) Developmental biology of Streptomyces from the perspective of 100 actinobacterial genome sequences, *FEMS Microbiol Rev 38*, 345-379.

102. Rawat, M., Newton, G. L., Ko, M., Martinez, G. J., Fahey, R. C., and Av-Gay, Y. (2002) Mycothiol-deficient Mycobacterium smegmatis mutants are hypersensitive to alkylating agents, free radicals, and antibiotics, *Antimicrob Agents Chemother 46*, 3348-3355.

103. Buchmeier, N. A., Newton, G. L., and Fahey, R. C. (2006) A mycothiol synthase mutant of Mycobacterium tuberculosis has an altered thiol-disulfide content and limited tolerance to stress, *J Bacteriol 188*, 6245-6252.

104. Buchmeier, N. A., Newton, G. L., Koledin, T., and Fahey, R. C. (2003) Association of mycothiol with protection of Mycobacterium tuberculosis from toxic oxidants and antibiotics, *Mol Microbiol 47*, 1723-1732.

105. Dosanjh, M., Newton, G. L., and Davies, J. (2008) Characterization of a mycothiol ligase mutant of Rhodococcus jostii RHA1, *Research in microbiology 159*, 643-650.

106. Liu, Y. B., Long, M. X., Yin, Y. J., Si, M. R., Zhang, L., Lu, Z. Q., Wang, Y., and Shen, X. H. (2013) Physiological roles of mycothiol in detoxification and tolerance to multiple poisonous chemicals in Corynebacterium glutamicum, *Archives of microbiology 195*, 419-429.

107. Ramon-Garcia, S., Ng, C., Jensen, P. R., Dosanjh, M., Burian, J., Morris, R. P., Folcher, M., Eltis, L. D., Grzesiek, S., Nguyen, L., and Thompson, C. J. (2013) WhiB7, an Fe-S-dependent transcription factor that activates species-specific repertoires of drug resistance determinants in actinobacteria, *J Biol Chem 288*, 34514-34528.

108. Reeves, R., and Nissen, M. S. (1990) The A.T-DNA-binding domain of mammalian high mobility group I chromosomal proteins. A novel peptide motif for recognizing DNA structure, *J Biol Chem 265*, 8573-8582.

109. Ramon-Garcia, S., Ng, C., Anderson, H., Chao, J. D., Zheng, X., Pfeifer, T., Av-Gay, Y., Roberge, M., and Thompson, C. J. (2011) Synergistic drug combinations for tuberculosis therapy identified by a novel high-throughput screen, *Antimicrob Agents Chemother 55*, 3861-3869.

110. Wei, J., Dahl, J. L., Moulder, J. W., Roberts, E. A., O'Gaora, P., Young, D. B., and Friedman, R. L. (2000) Identification of a Mycobacterium tuberculosis gene that enhances mycobacterial survival in macrophages, *J Bacteriol 182*, 377-384.

111. Kim, K. H., An, D. R., Song, J., Yoon, J. Y., Kim, H. S., Yoon, H. J., Im, H. N., Kim, J., Kim, D. J., Lee, S. J., Lee, H. M., Kim, H. J., Jo, E. K., Lee, J. Y., and Suh, S. W. (2012) Mycobacterium tuberculosis Eis protein initiates suppression of host immune responses by acetylation of DUSP16/MKP-7, *Proc Natl Acad Sci U S A*.

112. Chen, W., Biswas, T., Porter, V. R., Tsodikov, O. V., and Garneau-Tsodikova, S. (2011) Unusual regioversatility of acetyltransferase Eis, a cause of drug resistance in XDR-TB, *Proc Natl Acad Sci U S A 108*, 9804-9808.

113. Roberts, E. A., Clark, A., McBeth, S., and Friedman, R. L. (2004) Molecular characterization of the eis promoter of Mycobacterium tuberculosis, *J Bacteriol 186*, 5410-5417.

114. Zaunbrecher, M. A., Sikes, R. D., Jr., Metchock, B., Shinnick, T. M., and Posey, J. E. (2009) Overexpression of the chromosomally encoded aminoglycoside acetyltransferase eis confers kanamycin resistance in Mycobacterium tuberculosis, *Proc Natl Acad Sci U S A 106*, 20004-20009.

115. Wu, S., Barnes, P. F., Samten, B., Pang, X., Rodrigue, S., Ghanny, S., Soteropoulos, P., Gaudreau, L., and Howard, S. T. (2009) Activation of the eis gene in a W-Beijing strain of Mycobacterium tuberculosis correlates with increased SigA levels and enhanced intracellular growth, *Microbiology 155*, 1272-1281.

116. Ramon-Garcia, S., Martin, C., Ainsa, J. A., and De Rossi, E. (2006) Characterization of tetracycline resistance mediated by the efflux pump Tap from Mycobacterium fortuitum, *J Antimicrob Chemother 57*, 252-259.

117. Ramon-Garcia, S., Mick, V., Dainese, E., Martin, C., Thompson, C. J., De Rossi, E., Manganelli, R., and Ainsa, J. A. (2012) Functional and genetic characterization of the tap efflux pump in Mycobacterium bovis BCG, *Antimicrob Agents Chemother 56*, 2074-2083.

118. Adams, K. N., Takaki, K., Connolly, L. E., Wiedenhoft, H., Winglee, K., Humbert, O., Edelstein, P. H., Cosma, C. L., and Ramakrishnan, L. (2011) Drug tolerance in replicating mycobacteria mediated by a macrophage-induced efflux mechanism, *Cell 145*, 39-53.

119. da Silva, P. E., Von Groll, A., Martin, A., and Palomino, J. C. (2011) Efflux as a mechanism for drug resistance in Mycobacterium tuberculosis, *FEMS immunology and medical microbiology 63*, 1-9.

120. Louw, G. E., Warren, R. M., Gey van Pittius, N. C., Leon, R., Jimenez, A., Hernandez-Pando, R., McEvoy, C. R., Grobbelaar, M., Murray, M., van Helden, P. D., and Victor, T. C. (2011) Rifampicin Reduces Susceptibility to Ofloxacin in Rifampicin-resistant Mycobacterium tuberculosis through Efflux, *Am J Respir Crit Care Med 184*, 269-276.

121. Buriankova, K., Doucet-Populaire, F., Dorson, O., Gondran, A., Ghnassia, J. C., Weiser, J., and Pernodet, J. L. (2004) Molecular basis of intrinsic macrolide resistance in the Mycobacterium tuberculosis complex, *Antimicrob Agents Chemother 48*, 143-150.

122. Nash, K. A. (2003) Intrinsic macrolide resistance in Mycobacterium smegmatis is conferred by a novel erm gene, erm(38), *Antimicrob Agents Chemother 47*, 3053-3060.

123. Jiang, T., Xing, B., and Rao, J. (2008) Recent developments of biological reporter technology for detecting gene expression, *Biotechnology & genetic engineering reviews 25*, 41-75.

124. Mesak, L. R., Yim, G., and Davies, J. (2009) Improved lux reporters for use in Staphylococcus aureus, *Plasmid 61*, 182-187.

125. Cormack, B. P., Valdivia, R. H., and Falkow, S. (1996) FACS-optimized mutants of the green fluorescent protein (GFP), *Gene 173*, 33-38.

126. Meighen, E. A. (1991) Molecular biology of bacterial bioluminescence, *Microbiol Rev 55*, 123-142.

127. Andrew, P. W., and Roberts, I. S. (1993) Construction of a bioluminescent mycobacterium and its use for assay of antimycobacterial agents, *J Clin Microbiol 31*, 2251-2254.

128. Gordon, S., Parish, T., Roberts, I. S., and Andrew, P. W. (1994) The application of luciferase as a reporter of environmental regulation of gene expression in mycobacteria, *Lett Appl Microbiol 19*, 336-340.

129. Roberts, E. A., Clark, A., and Friedman, R. L. (2005) Bacterial luciferase is naturally destabilized in Mycobacterium tuberculosis and can be used to monitor changes in gene expression, *FEMS Microbiol Lett 243*, 243-249.

130. Chalfie, M., Tu, Y., Euskirchen, G., Ward, W. W., and Prasher, D. C. (1994) Green fluorescent protein as a marker for gene expression, *Science 263*, 802-805.

131. Patterson, G. H., Knobel, S. M., Sharif, W. D., Kain, S. R., and Piston, D. W. (1997) Use of the green fluorescent protein and its mutants in quantitative fluorescence microscopy, *Biophys J 73*, 2782-2790.

132. Cubitt, A. B., Heim, R., Adams, S. R., Boyd, A. E., Gross, L. A., and Tsien, R. Y. (1995) Understanding, improving and using green fluorescent proteins, *Trends Biochem Sci 20*, 448-455.

133. Pierce, J. W., Schoenleber, R., Jesmok, G., Best, J., Moore, S. A., Collins, T., and Gerritsen, M. E. (1997) Novel inhibitors of cytokine-induced IkappaBalpha phosphorylation and endothelial cell adhesion molecule expression show anti-inflammatory effects in vivo, *J Biol Chem 272*, 21096-21103.

134. Frohman, M. A., Dush, M. K., and Martin, G. R. (1988) Rapid production of full-length cDNAs from rare transcripts: amplification using a single gene-specific oligonucleotide primer, *Proc Natl Acad Sci U S A 85*, 8998-9002.

135. Mendoza-Vargas, A., Olvera, L., Olvera, M., Grande, R., Vega-Alvarado, L., Taboada, B., Jimenez-Jacinto, V., Salgado, H., Juarez, K., Contreras-Moreira, B., Huerta, A. M., Collado-Vides, J., and Morett, E. (2009) Genome-wide identification of transcription start sites, promoters and transcription factor binding sites in E. coli, *PLoS One 4*, e7526.

136. Cortes, T., Schubert, O. T., Rose, G., Arnvig, K. B., Comas, I., Aebersold, R., and Young, D. B. (2013) Genome-wide mapping of transcriptional start sites defines an extensive leaderless transcriptome in Mycobacterium tuberculosis, *Cell reports 5*, 1121-1131.

137. Burian, J., Ramon-Garcia, S., Sweet, G., Gomez-Velasco, A., Av-Gay, Y., and Thompson, C. J. (2012) The Mycobacterial Transcriptional Regulator whiB7 Gene Links Redox Homeostasis and Intrinsic Antibiotic Resistance, *J Biol Chem 287*, 299-310.

138. Sweeney, W. V., and Rabinowitz, J. C. (1980) Proteins containing 4Fe-4S clusters: an overview, *Annu Rev Biochem 49*, 139-161.

139. Smith, L. J., Stapleton, M. R., Buxton, R. S., and Green, J. (2012) Structure-Function Relationships of the Mycobacterium tuberculosis Transcription Factor WhiB1, *PLoS One 7*, e40407.

140. van Kessel, J. C., and Hatfull, G. F. (2008) Mycobacterial recombineering, *Methods Mol Biol 435*, 203-215.

141. Crack, J. C., Green, J., Thomson, A. J., and Le Brun, N. E. (2012) Iron-sulfur cluster sensor-regulators, *Current opinion in chemical biology 16*, 35-44.

142. Kim, D. E., Chivian, D., and Baker, D. (2004) Protein structure prediction and analysis using the Robetta server, *Nucleic Acids Res 32*, W526-531.

143. Punta, M., Coggill, P. C., Eberhardt, R. Y., Mistry, J., Tate, J., Boursnell, C., Pang, N., Forslund, K., Ceric, G., Clements, J., Heger, A., Holm, L., Sonnhammer, E. L., Eddy, S. R., Bateman, A., and Finn, R. D. (2012) The Pfam protein families database, *Nucleic Acids Res 40*, D290-301.

144. Eswar, N., Webb, B., Marti-Renom, M. A., Madhusudhan, M. S., Eramian, D., Shen, M. Y., Pieper, U., and Sali, A. (2007) Comparative protein structure modeling using MODELLER, *Current protocols in protein science / editorial board, John E. Coligan ... [et al.] Chapter 2*, Unit 2 9.

145. Murakami, K. S. (2013) X-ray Crystal Structure of Escherichia coli RNA Polymerase sigma70 Holoenzyme, *J Biol Chem 288*, 9126-9134.

146. Kozakov, D., Hall, D. R., Beglov, D., Brenke, R., Comeau, S. R., Shen, Y., Li, K., Zheng, J., Vakili, P., Paschalidis, I., and Vajda, S. (2010) Achieving reliability and high accuracy in automated protein docking: ClusPro, PIPER, SDU, and stability analysis in CAPRI rounds 13-19, *Proteins 78*, 3124-3130.

147. Murakami, K. S., Masuda, S., Campbell, E. A., Muzzin, O., and Darst, S. A. (2002) Structural basis of transcription initiation: an RNA polymerase holoenzyme-DNA complex, *Science 296*, 1285-1290.

148. Sachdeva, P., Misra, R., Tyagi, A. K., and Singh, Y. (2009) The sigma factors of Mycobacterium tuberculosis: regulation of the regulators, *FEBS J 277*, 605-626.

149. Aravind, L., and Landsman, D. (1998) AT-hook motifs identified in a wide variety of DNA-binding proteins, *Nucleic Acids Res 26*, 4413-4421.

150. Typas, A., Becker, G., and Hengge, R. (2007) The molecular basis of selective promoter activation by the sigmaS subunit of RNA polymerase, *Mol Microbiol 63*, 1296-1306.

151. Saini, V., Farhana, A., Glasgow, J. N., and Steyn, A. J. (2012) Iron sulfur cluster proteins and microbial regulation: implications for understanding tuberculosis, *Current opinion in chemical biology 16*, 45-53.

152. Chater, K. F., and Chandra, G. (2006) The evolution of development in Streptomyces analysed by genome comparisons, *FEMS Microbiol Rev 30*, 651-672.

153. Bentley, S. D., Brown, S., Murphy, L. D., Harris, D. E., Quail, M. A., Parkhill, J., Barrell, B. G., McCormick, J. R., Santamaria, R. I., Losick, R., Yamasaki, M., Kinashi, H., Chen, C. W., Chandra, G., Jakimowicz, D., Kieser, H. M., Kieser, T., and Chater, K. F. (2004) SCP1, a 356,023 bp linear plasmid adapted to the ecology and developmental biology of its host, Streptomyces coelicolor A3(2), *Mol Microbiol 51*, 1615-1628.

154. Brazas, M. D., and Hancock, R. E. (2005) Using microarray gene signatures to elucidate mechanisms of antibiotic action and resistance, *Drug Discov Today 10*, 1245-1252.

155. Bajorath, J. (2001) Selected concepts and investigations in compound classification, molecular descriptor analysis, and virtual screening, *J Chem Inf Comput Sci 41*, 233-245.

156. Poehlsgaard, J., and Douthwaite, S. (2005) The bacterial ribosome as a target for antibiotics, *Nat Rev Microbiol 3*, 870-881.

157. Blondeau, J. M. (2004) Fluoroquinolones: mechanism of action, classification, and development of resistance, *Surv Ophthalmol 49 Suppl 2*, S73-78.

158. Kopka, M. L., Yoon, C., Goodsell, D., Pjura, P., and Dickerson, R. E. (1985) The molecular origin of DNA-drug specificity in netropsin and distamycin, *Proc Natl Acad Sci U S A 82*, 1376-1380.

159. Robinson, H., Yang, D., and Wang, A. H. (1994) Structure and dynamics of the antitumor drugs nogalamycin and disnogalamycin complexed to d(CGTACG)2: comparison of crystal and solution structures, *Gene 149*, 179-188.

160. Wu, W., Vanderwall, D. E., Turner, C. J., Hoehn, S., Chen, J., Kozarich, J. W., and Stubbe, J. (2002) Solution structure of the hydroperoxide of Co(III) phleomycin complexed with d(CCAGGCCTGG)2: evidence for binding by partial intercalation, *Nucleic Acids Res 30*, 4881-4891.

161. Alatossava, T., Jutte, H., Kuhn, A., and Kellenberger, E. (1985) Manipulation of intracellular magnesium content in polymyxin B nonapeptide-sensitized Escherichia coli by ionophore A23187, *J Bacteriol 162*, 413-419.

162. Gutierrez-Lugo, M. T., Baker, H., Shiloach, J., Boshoff, H., and Bewley, C. A. (2009) Dequalinium, a new inhibitor of Mycobacterium tuberculosis mycothiol ligase identified by high-throughput screening, *J Biomol Screen 14*, 643-652.

163. Smulski, D. R., Huang, L. L., McCluskey, M. P., Reeve, M. J., Vollmer, A. C., Van Dyk, T. K., and LaRossa, R. A. (2001) Combined, functional genomic-biochemical approach to intermediary metabolism: interaction of acivicin, a glutamine amidotransferase inhibitor, with Escherichia coli K-12, *J Bacteriol 183*, 3353-3364.

164. Wang, Q., and Xu, L. (2012) Beauvericin, a bioactive compound produced by fungi: a short review, *Molecules 17*, 2367-2377.

165. Ung, K. S., and Av-Gay, Y. (2006) Mycothiol-dependent mycobacterial response to oxidative stress, *FEBS Lett 580*, 2712-2716.

166. Boshoff, H. I., Myers, T. G., Copp, B. R., McNeil, M. R., Wilson, M. A., and Barry, C. E., 3rd. (2004) The transcriptional responses of Mycobacterium tuberculosis to inhibitors of metabolism: novel insights into drug mechanisms of action, *J Biol Chem 279*, 40174-40184.

167. Wecke, T., and Mascher, T. (2011) Antibiotic research in the age of omics: from expression profiles to interspecies communication, *J Antimicrob Chemother 66*, 2689-2704.

168. Boshoff, H. I., Xu, X., Tahlan, K., Dowd, C. S., Pethe, K., Camacho, L. R., Park, T. H., Yun, C. S., Schnappinger, D., Ehrt, S., Williams, K. J., and Barry, C. E., 3rd. (2008) Biosynthesis and recycling of nicotinamide cofactors in mycobacterium tuberculosis. An essential role for NAD in nonreplicating bacilli, *J Biol Chem 283*, 19329-19341.

169. Venketaraman, V., Dayaram, Y. K., Talaue, M. T., and Connell, N. D. (2005) Glutathione and nitrosoglutathione in macrophage defense against Mycobacterium tuberculosis, *Infect Immun 73*, 1886-1889.

170. Green, J., and Paget, M. S. (2004) Bacterial redox sensors, *Nat Rev Microbiol 2*, 954-966.

171. Dinan, A. M., Tong, P., Lohan, A. J., Conlon, K. M., Miranda-CasoLuengo, A. A., Malone, K. M., Gordon, S. V., and Loftus, B. J. (2014) Relaxed selection drives a noisy noncoding transcriptome in members of the Mycobacterium tuberculosis complex, *mBio 5*, e01169-01114.

172. Reeves, A. Z., Campbell, P. J., Sultana, R., Malik, S., Murray, M., Plikaytis, B. B., Shinnick, T. M., and Posey, J. E. (2013) Aminoglycoside Cross-Resistance in Mycobacterium tuberculosis Due to Mutations in the 5' Untranslated Region of whiB7, *Antimicrob Agents Chemother 57*, 1857-1865.

173. Barquist, L., Boinett, C. J., and Cain, A. K. (2013) Approaches to querying bacterial genomes with transposon-insertion sequencing, *RNA biology 10*, 1161-1169.

174. van Opijnen, T., and Camilli, A. (2013) Transposon insertion sequencing: a new tool for systems-level analysis of microorganisms, *Nat Rev Microbiol 11*, 435-442.

175. Christen, B., Abeliuk, E., Collier, J. M., Kalogeraki, V. S., Passarelli, B., Coller, J. A., Fero, M. J., McAdams, H. H., and Shapiro, L. (2011) The essential genome of a bacterium, *Molecular systems biology 7*, 528.

176. Griffin, J. E., Gawronski, J. D., Dejesus, M. A., Ioerger, T. R., Akerley, B. J., and Sassetti, C. M. (2011) High-resolution phenotypic profiling defines genes essential for mycobacterial growth and cholesterol catabolism, *PLoS Pathog 7*, e1002251.

177. Gawronski, J. D., Wong, S. M., Giannoukos, G., Ward, D. V., and Akerley, B. J. (2009) Tracking insertion mutants within libraries by deep sequencing and a genome-wide screen for Haemophilus genes required in the lung, *Proc Natl Acad Sci U S A 106*, 16422-16427.

178. Langridge, G. C., Phan, M. D., Turner, D. J., Perkins, T. T., Parts, L., Haase, J., Charles, I., Maskell, D. J., Peters, S. E., Dougan, G., Wain, J., Parkhill, J., and Turner, A. K. (2009) Simultaneous assay of every Salmonella Typhi gene using one million transposon mutants, *Genome Res 19*, 2308-2316.

179. Dong, T. G., Ho, B. T., Yoder-Himes, D. R., and Mekalanos, J. J. (2013) Identification of T6SS-dependent effector and immunity proteins by Tn-seq in Vibrio cholerae, *Proc Natl Acad Sci U S A 110*, 2623-2628.

180. Sassetti, C. M., Boyd, D. H., and Rubin, E. J. (2001) Comprehensive identification of conditionally essential genes in mycobacteria, *Proc Natl Acad Sci U S A 98*, 12712-12717.

181. Zomer, A., Burghout, P., Bootsma, H. J., Hermans, P. W., and van Hijum, S. A. (2012) ESSENTIALS: software for rapid analysis of high throughput transposon insertion sequencing data, *PLoS One 7*, e43012.

182. Okonechnikov, K., Golosova, O., and Fursov, M. (2012) Unipro UGENE: a unified bioinformatics toolkit, *Bioinformatics 28*, 1166-1167.

183. Aird, D., Ross, M. G., Chen, W. S., Danielsson, M., Fennell, T., Russ, C., Jaffe, D. B., Nusbaum, C., and Gnirke, A. (2011) Analyzing and minimizing PCR amplification bias in Illumina sequencing libraries, *Genome biology 12*, R18.

184. Mavrici, D., Marakalala, M. J., Holton, J. M., Prigozhin, D. M., Gee, C. L., Zhang, Y. J., Rubin, E. J., and Alber, T. (2014) Mycobacterium tuberculosis FtsX extracellular domain activates the peptidoglycan hydrolase, RipC, *Proc Natl Acad Sci U S A 111*, 8037-8042.

185. Campagna, D., Albiero, A., Bilardi, A., Caniato, E., Forcato, C., Manavski, S., Vitulo, N., and Valle, G. (2009) PASS: a program to align short sequences, *Bioinformatics 25*, 967-968.

186. Langmead, B., Trapnell, C., Pop, M., and Salzberg, S. L. (2009) Ultrafast and memory-efficient alignment of short DNA sequences to the human genome, *Genome biology 10*, R25.

187. Stephan, J., Mailaender, C., Etienne, G., Daffe, M., and Niederweis, M. (2004) Multidrug resistance of a porin deletion mutant of Mycobacterium smegmatis, *Antimicrob Agents Chemother 48*, 4163-4170.

188. Ramu, H., Mankin, A., and Vazquez-Laslop, N. (2009) Programmed drug-dependent ribosome stalling, *Mol Microbiol 71*, 811-824.

189. Gupta, P., Kannan, K., Mankin, A. S., and Vazquez-Laslop, N. (2013) Regulation of gene expression by macrolide-induced ribosomal frameshifting, *Molecular cell 52*, 629-642.

190. Yanofsky, C. (2000) Transcription attenuation: once viewed as a novel regulatory strategy, *J Bacteriol 182*, 1-8.

191. Zukher, I., Novikova, M., Tikhonov, A., Nesterchuk, M. V., Osterman, I. A., Djordjevic, M., Sergiev, P. V., Sharma, C. M., and Severinov, K. (2014) Ribosome-controlled transcription termination is essential for the production of antibiotic microcin C, *Nucleic Acids Res 42*, 11891-11902.

192. Cashel, M., Gentry, D. R., Hernandez, V. J., and Vinella, D. (1996) *The stringent response*, Vol. 1, 2 ed., ASM press, Washington, D.C.

193. Nguyen, D., Joshi-Datar, A., Lepine, F., Bauerle, E., Olakanmi, O., Beer, K., McKay, G., Siehnel, R., Schafhauser, J., Wang, Y., Britigan, B. E., and Singh, P. K. (2011) Active starvation responses mediate antibiotic tolerance in biofilms and nutrient-limited bacteria, *Science 334*, 982-986.

194. Dahl, J. L., Kraus, C. N., Boshoff, H. I., Doan, B., Foley, K., Avarbock, D., Kaplan, G., Mizrahi, V., Rubin, H., and Barry, C. E., 3rd. (2003) The role of RelMtb-mediated adaptation to stationary phase in long-term persistence of Mycobacterium tuberculosis in mice, *Proc Natl Acad Sci U S A 100*, 10026-10031.

195. Schenk, H., Klein, M., Erdbrugger, W., Droge, W., and Schulze-Osthoff, K. (1994) Distinct effects of thioredoxin and antioxidants on the activation of transcription factors NF-kappa B and AP-1, *Proc Natl Acad Sci U S A 91*, 1672-1676.

196. Lee, N., Yuen, K. Y., and Kumana, C. R. (2003) Clinical role of beta-lactam/beta-lactamase inhibitor combinations, *Drugs 63*, 1511-1524.

197. Snapper, S. B., Melton, R. E., Mustafa, S., Kieser, T., and Jacobs, W. R., Jr. (1990) Isolation and characterization of efficient plasmid transformation mutants of Mycobacterium smegmatis, *Mol Microbiol 4*, 1911-1919.

198. Stover, C. K., de la Cruz, V. F., Fuerst, T. R., Burlein, J. E., Benson, L. A., Bennett, L. T., Bansal, G. P., Young, J. F., Lee, M. H., Hatfull, G. F., and et al. (1991) New use of BCG for recombinant vaccines, *Nature 351*, 456-460.

199. Kaps, I., Ehrt, S., Seeber, S., Schnappinger, D., Martin, C., Riley, L. W., and Niederweis, M. (2001) Energy transfer between fluorescent proteins using a co-expression system in Mycobacterium smegmatis, *Gene 278*, 115-124.

200. Schagger, H. (2006) Tricine-SDS-PAGE, *Nature protocols 1*, 16-22.

201. Seredick, S. D., and Spiegelman, G. B. (2007) Bacillus subtilis RNA polymerase recruits the transcription factor Spo0A approximately P to stabilize a closed complex during transcription initiation, *J Mol Biol 366*, 19-35.

202. San, K. Y., Bennett, G. N., Berrios-Rivera, S. J., Vadali, R. V., Yang, Y. T., Horton, E., Rudolph, F. B., Sariyar, B., and Blackwood, K. (2002) Metabolic engineering through cofactor manipulation and its effects on metabolic flux redistribution in Escherichia coli, *Metab Eng 4*, 182-192.

203. Siegrist, M. S., and Rubin, E. J. (2009) Phage transposon mutagenesis, *Methods Mol Biol 465*, 311-323.

204. Burian, J., Yim, G., Hsing, M., Axerio-Cilies, P., Cherkasov, A., Spiegelman, G. B., and Thompson, C. J. (2013) The mycobacterial antibiotic resistance determinant WhiB7 acts as a transcriptional activator by binding the primary sigma factor SigA (RpoV), *Nucleic Acids Res 41*, 10062-10076.

Appendix

Appendix A: Supporting Figures

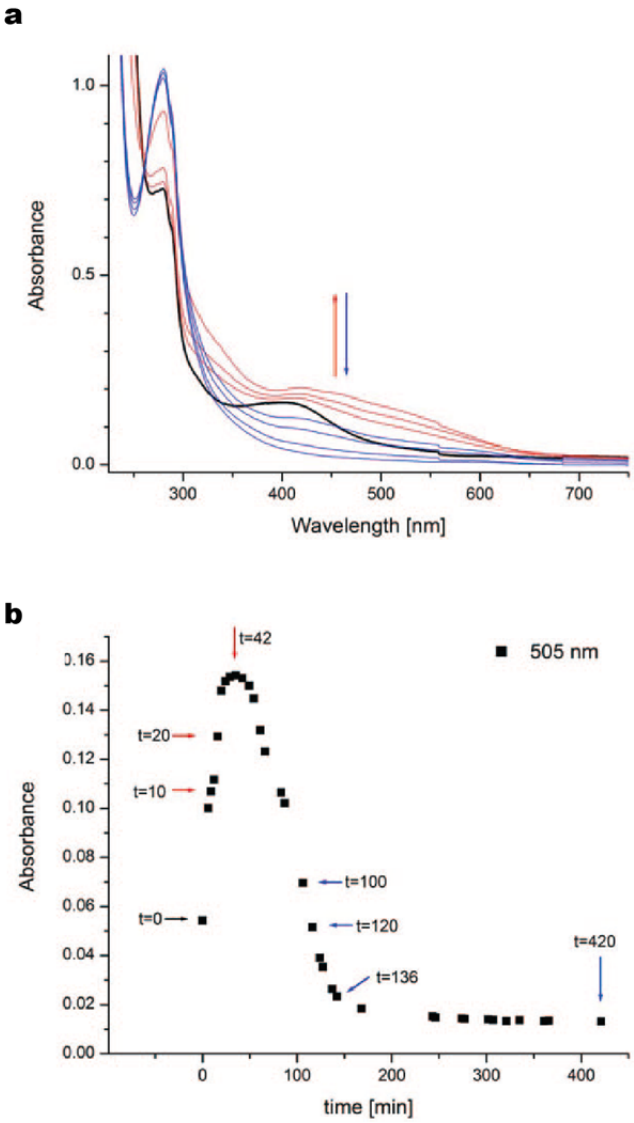

Figure S1. O_2-induced transformation and degradation of FeS clusters in WhiD. **(a)**, absorption spectra of the anaerobically reconstituted protein containing a [4Fe-4S] cluster before (black line) and after exposure to air (2–42 minutes (conversion to [2Fe-2S]), red lines; 47–420 minutes (conversion to apo form), blue lines; the exact time points are indicated by the arrows in panel 'b'). **(b)**, absorption of WhiD at 505 nm versus time after exposure to air at time 0. WhiD (20 M) in 20 mM Tris-HCl, pH 8.0, 150 mM NaCl, 1 mM DTT. This research was originally published in the Journal of Biological Chemistry. Jakimowicz, P., Cheesman, M. R., Bishai, W. R., Chater, K. F., Thomson, A. J., and Buttner, M. J. Evidence that the Streptomyces developmental protein WhiD, a member of the WhiB family, binds a [4Fe-4S] cluster. 2005. *J Biol Chem* 280, 8309-8315. © the American Society for Biochemistry and Molecular Biology.